V. Post Cold Drop Disassembly

The cold drop disassembly was performed in accordance with Section 5.5 of JSP-7953-01[1] with one exception.[1]

Section 5.5.2 of JSP-7953-01 states the following:

> *With the NS30 #1 test article in a vertical (top end up) orientation, disassemble the removable lid canister by utilizing an abrasive cutting wheel to circumferentially sever the canister body from the body flange near the original circumferential girth weld. Remove the removable lid canister lid assembly and body flange to permit inspection of the top end cap assembly to body interface. Similarly, cut three equally spaced viewing windows out of the removable lid canister body near the body flat head original circumferential girth weld.*

Upon discussion with the Washington TRU Solutions test engineer, it was decided that following this course of action would induce sand like particles into the test article due to the breakdown of the abrasive cutting wheel and potentially alter the released fine sand particulate assessment. As this was undesirable and the canister lid appeared to be undamaged, it was determined that an alternative procedure of attempting to mechanically remove the lid as designed and perform inspection of the contents was preferred.

The canister lid assembly lock pins were unlocked and the lid assembly was rotated to the unlocked position. This was no more difficult than the installation of the lid assembly suggesting that no damage to the interlock mechanism had occurred. Once in the unlocked position, the lid assembly was removed. The canister lid assembly came out cleanly. There was no sand present on the canister lid or body flange surfaces.

Internally, the first observation noted was that the CDX Grade plywood spacer was deformed as it had been forced up into the canister lid assembly pocket (the space created between the canister lid flange and the lid plate) by impact with the shield insert top end cap during the end drop (Figure 37 - Figure 39). The plywood was splintered and some of the splintered wood had broken off. Deformation of the plywood, as documented in Appendix E, was insufficient to allow the axial gap between components to disengage either end cap from the body pipe.

The plywood was removed and the top surface of the NS30 top end cap was inspected. While there were plywood pieces and dust, there was no evidence of sand or deformation on the outer surface of the top end cap (Figure 40). Inspection of the interface between the shield insert top end cap and body pipe indicated no gaps or separation as the end cap was fully seated with the body pipe.

The top end cap was then slowly removed from the body pipe and in the process the seated gasket fell away from the top end cap as it was found to have a tear in the gasket (Figure 41). No sand was visible on any surface, inside or out, of the top end cap. The top payload drum was then visible with the top end cap removed (Figure 42). The lock ring for the lid of that payload drum was released; the top lip of the drum and lid had definite deformation and in a few places had been punctured due to the impact against the heads of the self tapping screws that held the gasket ring onto the top end cap. No sand was visible on the top surface of the top payload drum (Figure 42).

Next a viewing window was cut into the bottom of the canister body using a hole cutting bit and a reciprocating saw (so as not to induce abrasive cutting material into the inside of the canister). There were pieces of plywood visible at the bottom of the canister flat head that had broken off of the plywood spacer and fallen down between the exterior of the shield insert assembly (end caps and body pipe) and the canister shell. There were metal shavings that had come from the metal removal process but there was no evidence of sand present near the bottom of the canister, at the bottom end cap to body pipe interface, or exterior to the shield insert assembly (Figure 43).

After finding no evidence of sand release beyond the shield insert assembly, cautious removal of the payload drums from the body pipe was performed. The drum handling bags were in an impaired condition and had been partially sheared at the interface between drums in the end drop. The payload drums experienced closure ring and lid deformations (Figure 44, Figure 45, Figure 46).

With the payload drums (1, 2 and 3) removed from the NS30 #1, the remaining components were removed. The twine shown was used to thread a rope through the D-Ring of the bottom end cap (Figure 47). The bottom end cap and the body pipe were removed together (Figure 48). Initially they were lifted up a few inches to inspect through the viewing window in the bottom of the canister to confirm the absence of released sand from the shield insert assembly (Figure 49).

The bottom end cap and body pipe were then removed fully and disassembled for inspection of the individual components. It was noted that upon disassembly the gasket attached to the bottom end cap assembly did show signs of shear damage, but there was no evidence that the seal was broken between the bottom end cap and the body pipe (Figure 50, Figure 51).

In addition to inspecting for released contents, a primary objective of the cold drop testing was to confirm the ductile performance of the EHMW-HDPE components at –20 F. A severe defect was routed across the top end cap at the location of maximum tensile bending stresses during the end drop and about the midline circumference of the pipe body at the location of maximum tensile bending stresses during the side drop. The routed defects were inspected to confirm no propagation of the flaw or brittle cracking (Figure 52, Figure 53).

All of the EHMW-HDPE plastic parts were inspected for gouges, dents, cuts and scratches due to interaction of the HDPE with the surrounding canister structure or the internal payload (Figure 54, Figure 55). The deepest one for each are documented in Appendix E, but none of them are deeper than the 1/4" V-groove that bounded the worst-case condition in the top end cap and the body pipe. There were no indications of material cracking or failure in any of the v-notch cuts, scratches, dents or gouges - machined or otherwise.

The measured accelerations due to impact were recorded and are provided in Appendix I. Sensors indicated some clipping of the signal due to excessive electrical input to the 500 g accelerometers. Filtering of the data utilizing a low-pass Butterworth 10-pole filter with a 75 Hz cut-off frequency provides a conservative minimum acceleration peak, on average from the two sensors, of approximately 375 g's for the cold end drop and 136 g's for the cold side drop.

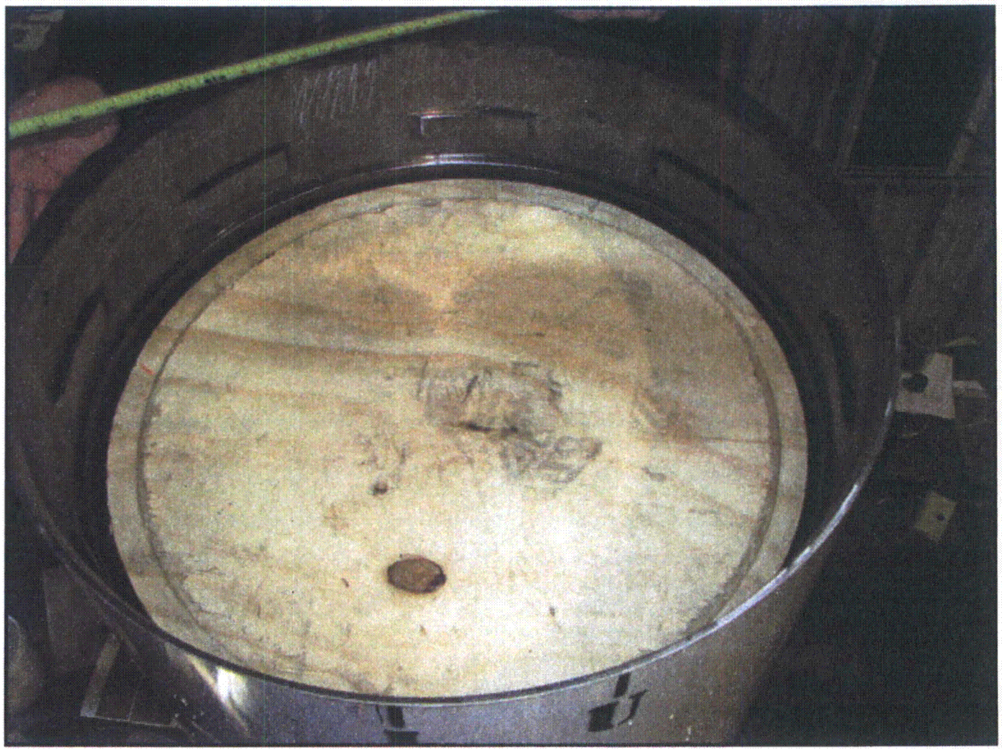

Figure 37 – Inspection of Plywood Spacer in NS30 #1 after Cold End and Side Drop Tests

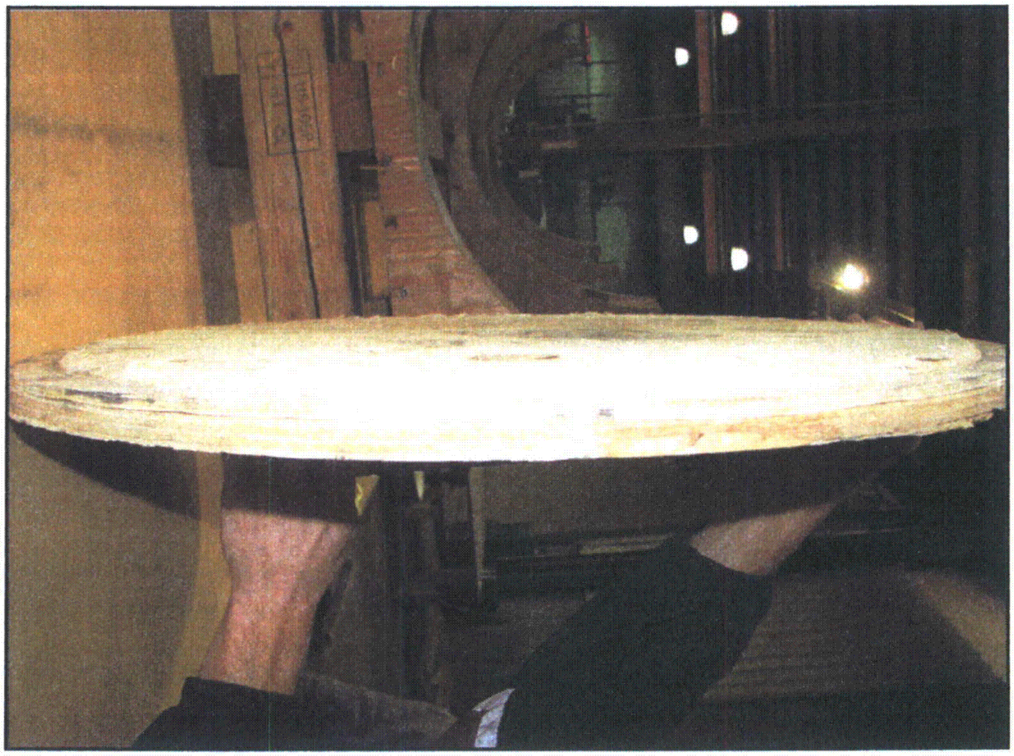

Figure 38 – Deformation of NS30 #1 Plywood Spacer (canister lid interface side)

Figure 39 – Deformation of NS30 #1 Plywood Spacer (shield top end cap interface side)

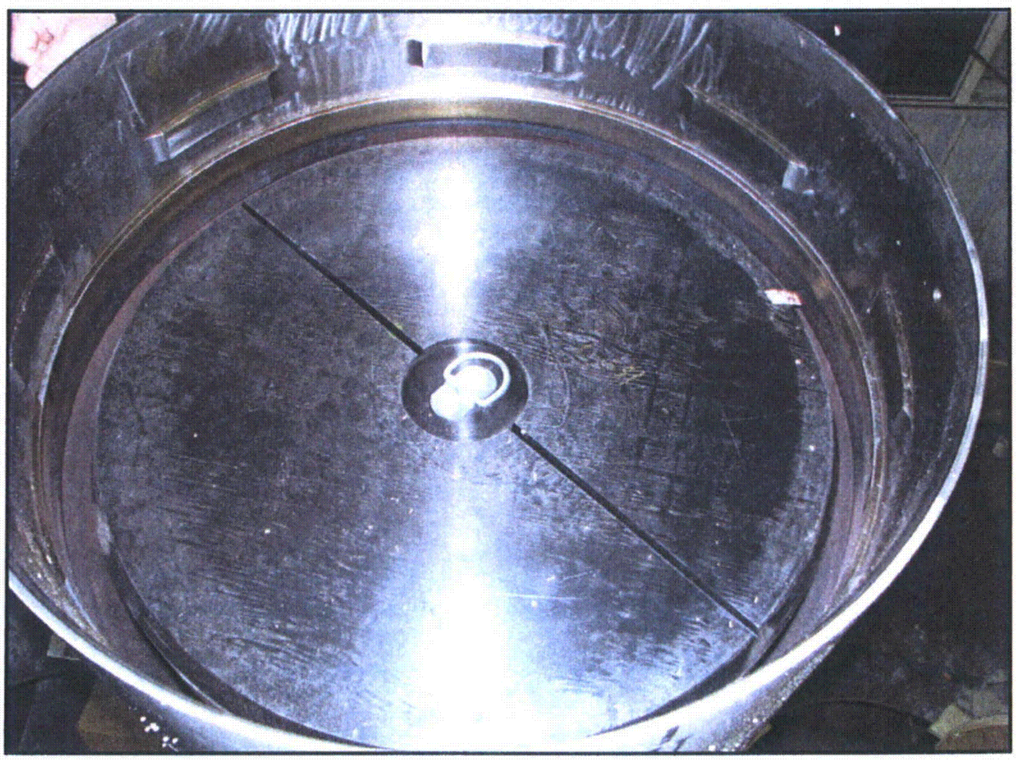

Figure 40 – Undamaged NS30 #1 Top End Cap (containing routed ¼" deep v-groove defect)

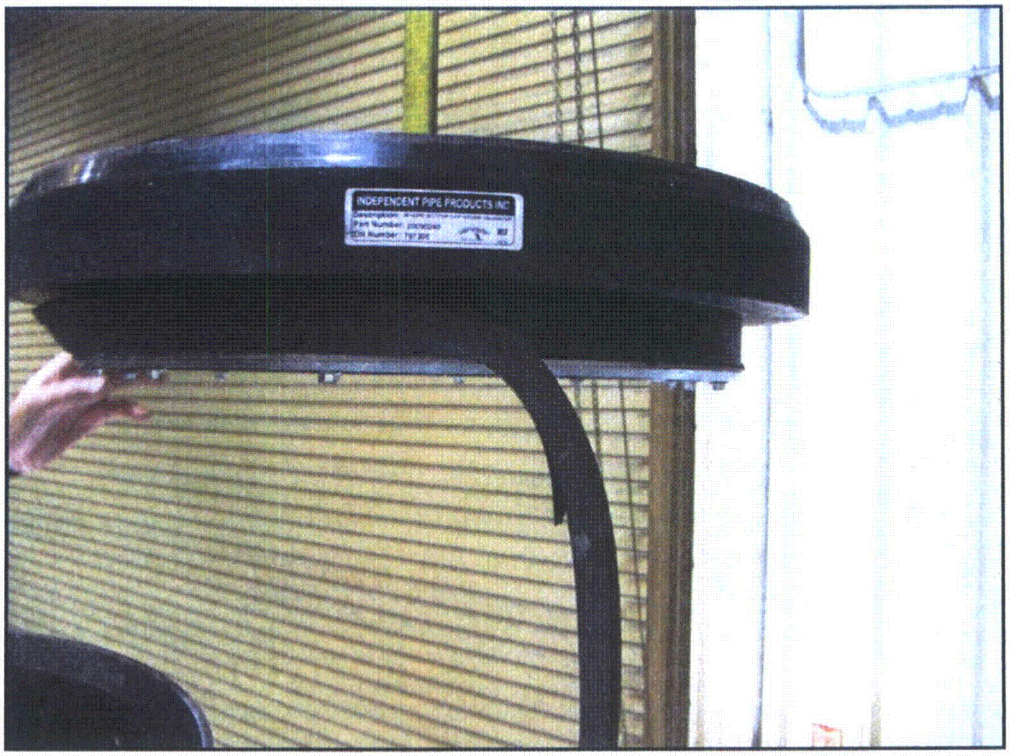

Figure 41 – Removal of NS30 #1 Top End Cap Revealing (gasket tear)

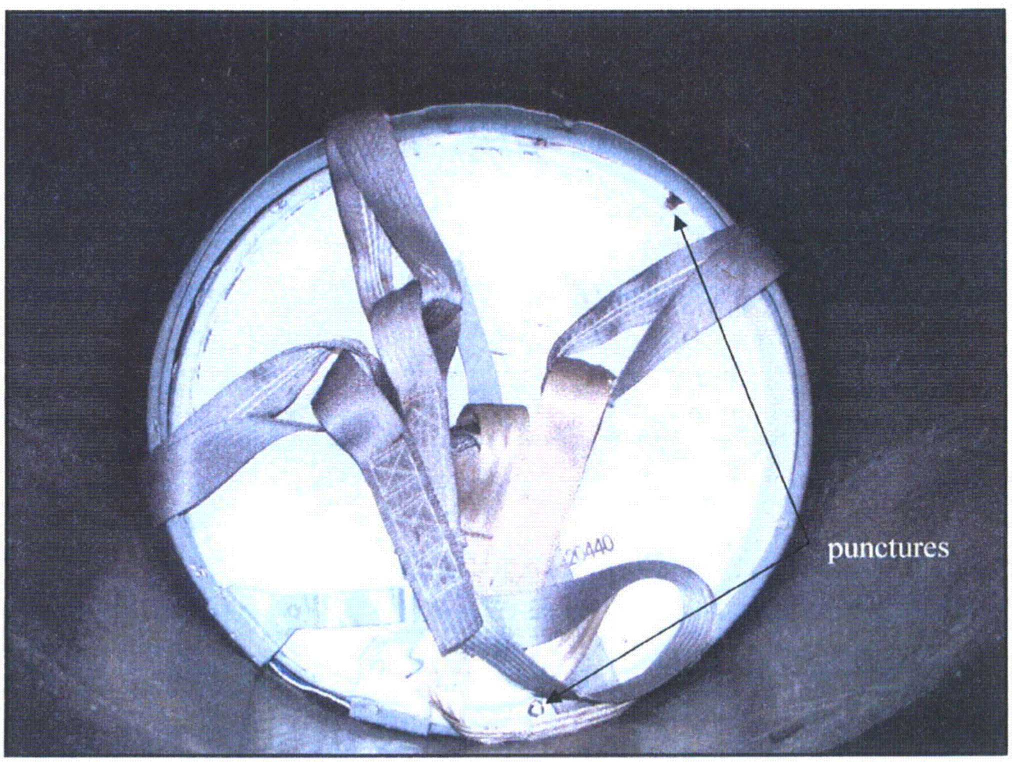

Figure 42 – NS30 #1 Top Payload Drum Inside Shield Body (punctured lid due to interaction with End Cap gasket retainer screws)

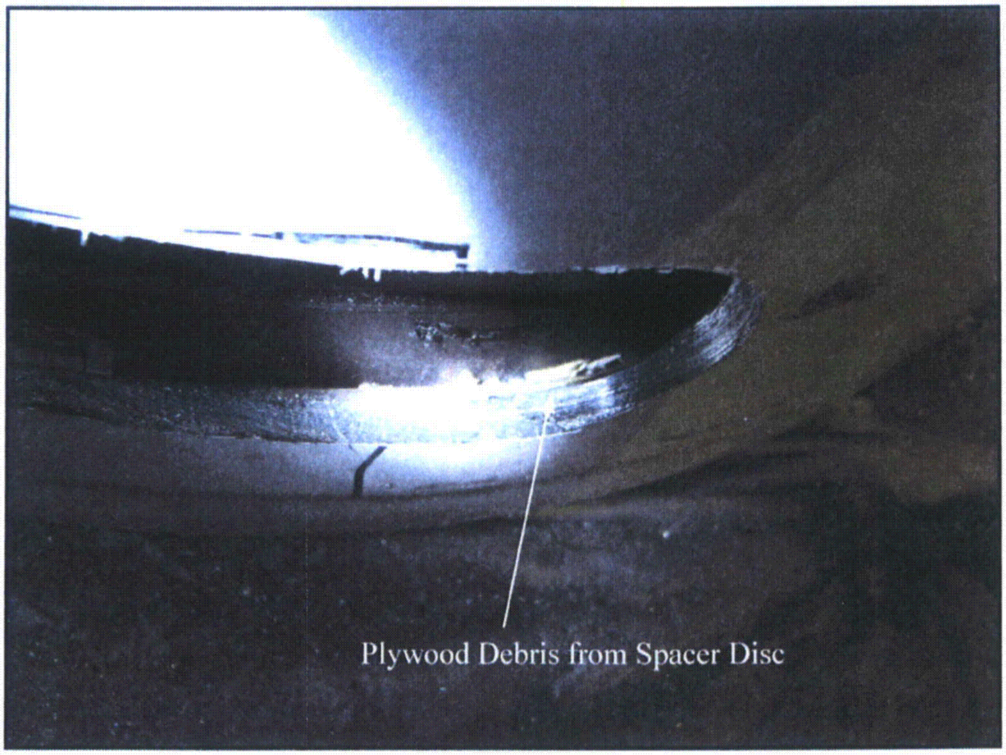

Figure 43 – NS30 #1 Cut-out from Lower Canister Shell to Inspect Engagement of Bottom End Cap

Figure 44 –Top Payload Drum #3

Figure 45 – Middle Payload Drum #2

Figure 46 – Bottom Payload Drum #1

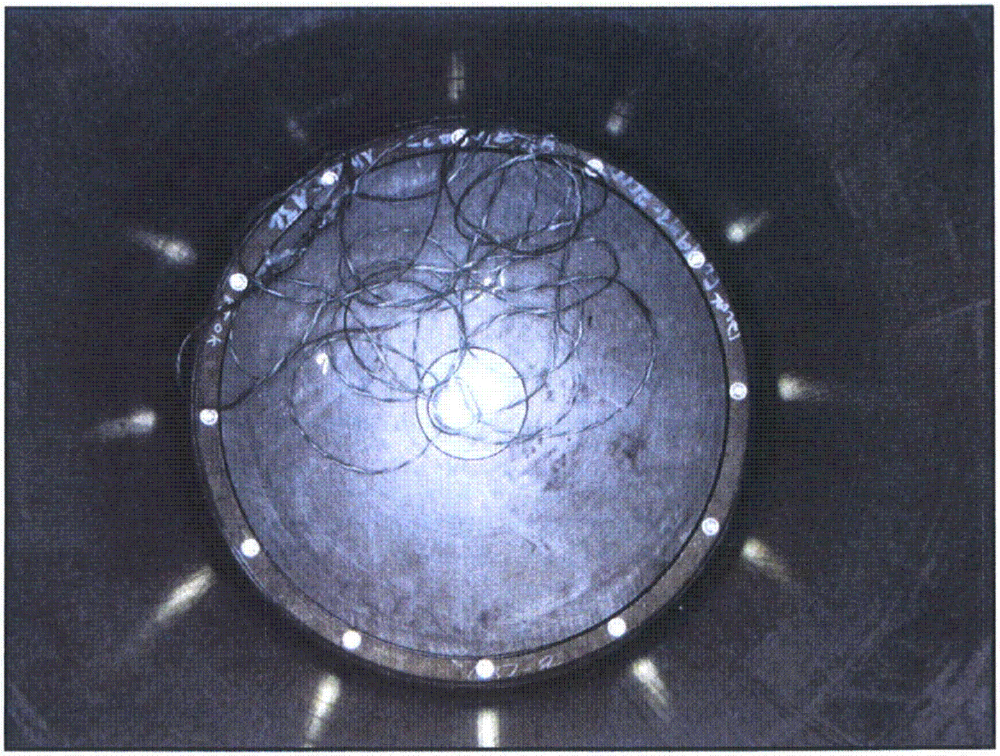

Figure 47 – View of NS30 #1 Bottom End Cap from the Lid End of the Shield Body Pipe

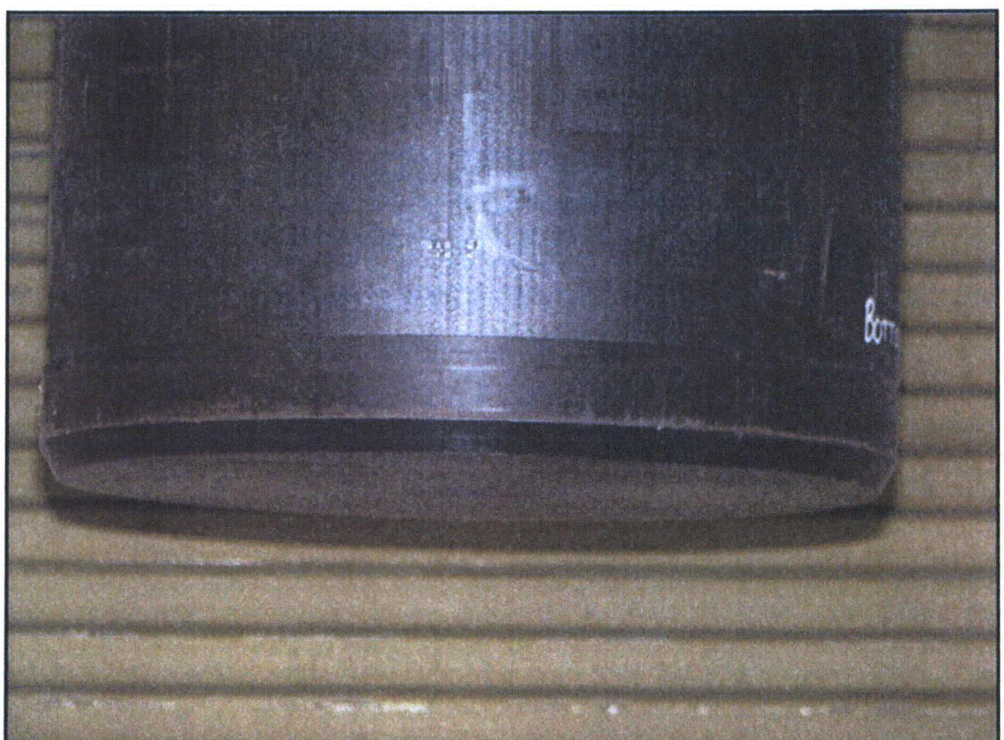

Figure 48 – View of Bottom End Cap and Pipe Body During Removal from Canister

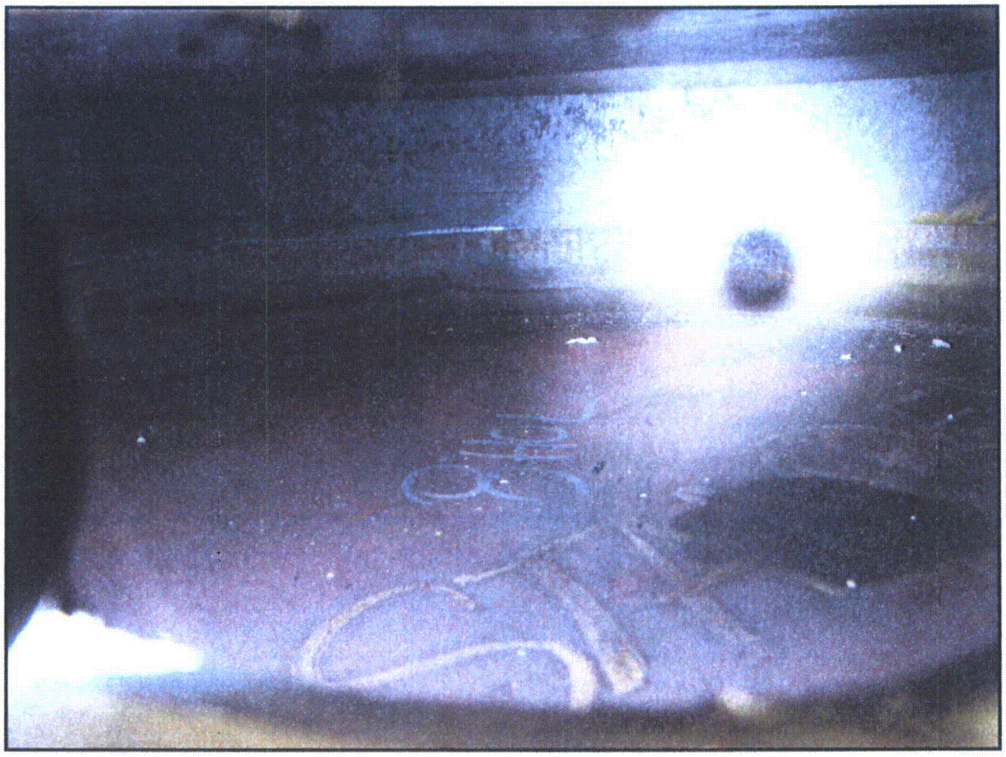

Figure 49 – NS30 #1 Canister Bottom Plate After Removal of Shield Insert Components through Viewing Port (no presence of releasable source term, i.e., sand)

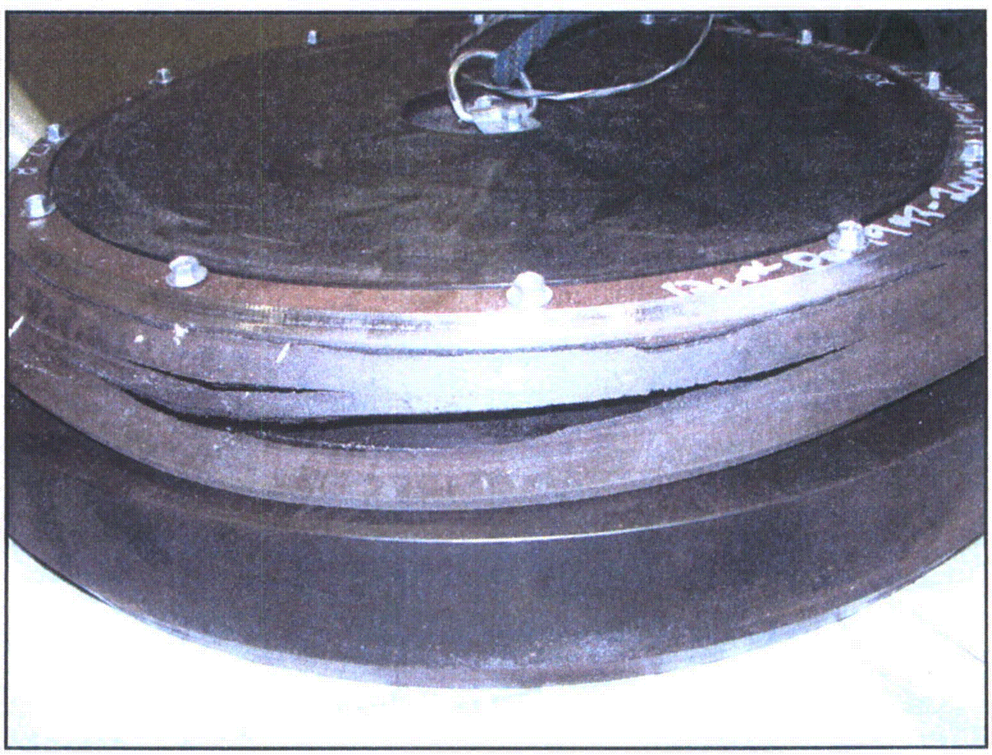

Figure 50 – Bottom End Cap Gasket (with circumferential tear)

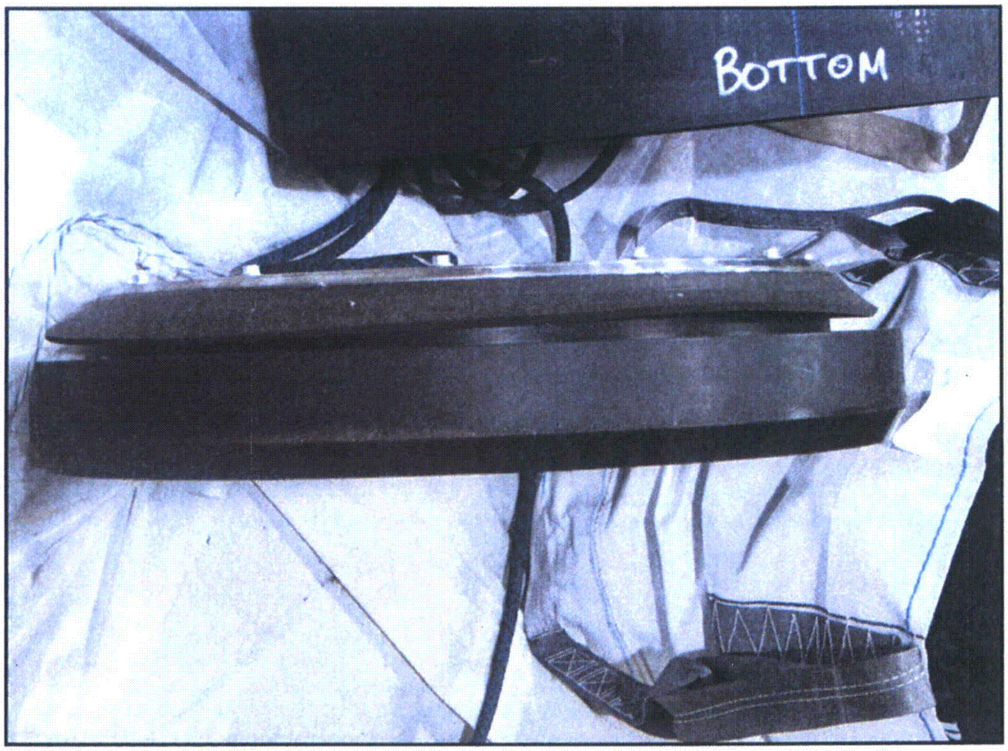

Figure 51 – Bottom End Cap Gasket (opposite side, no thru-thickness damage)

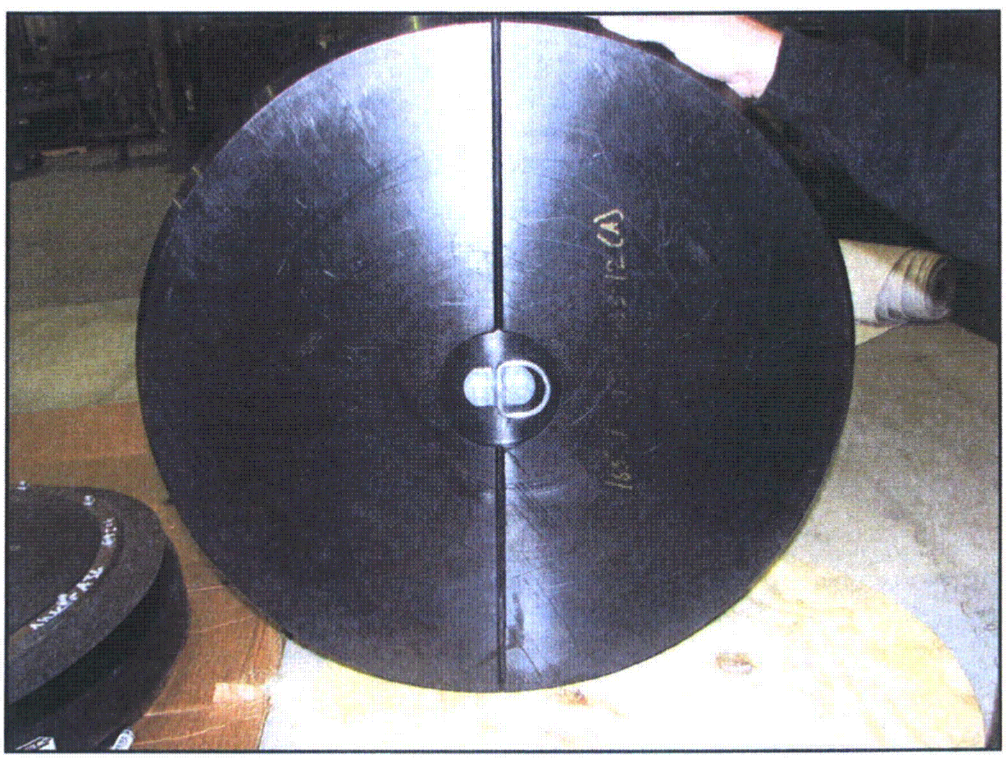

Figure 52 – NS30 #1 Top End Cap Exterior with No Propagation of V-groove Defect

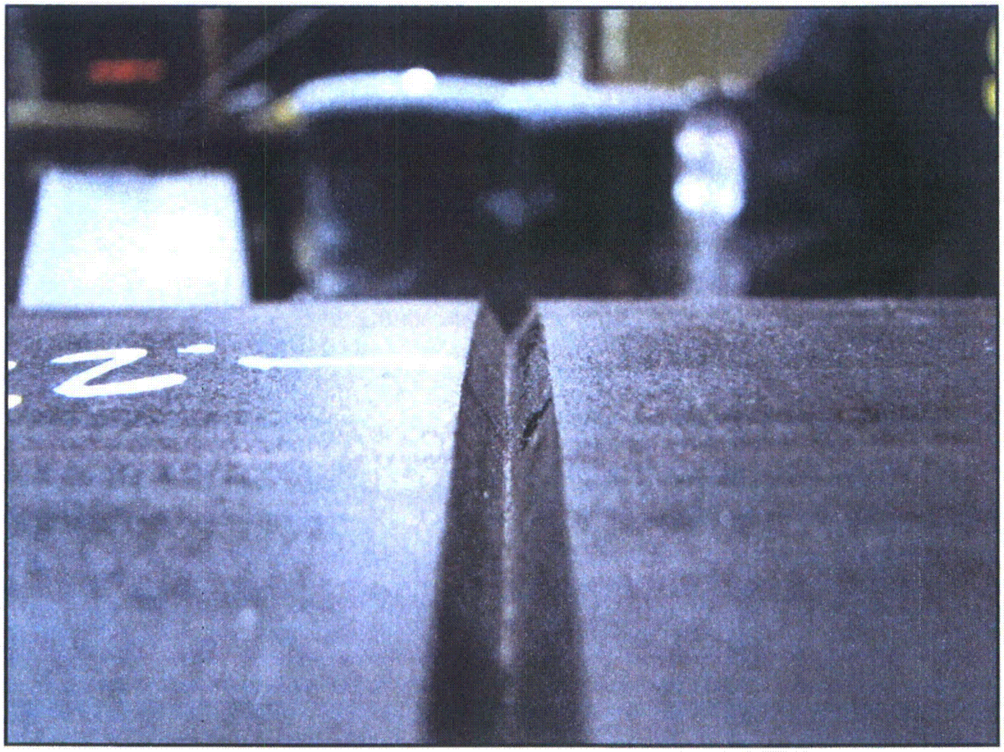

Figure 53 – NS30 #1 Body Pipe Exterior with No Propagation of V-groove Defect

Figure 54 – NS30 #1 Body Pipe Scuff/Dent Due to Interaction with Canister Shell at Upper Test Fixture Centering Ring Location during Cold Side Drop

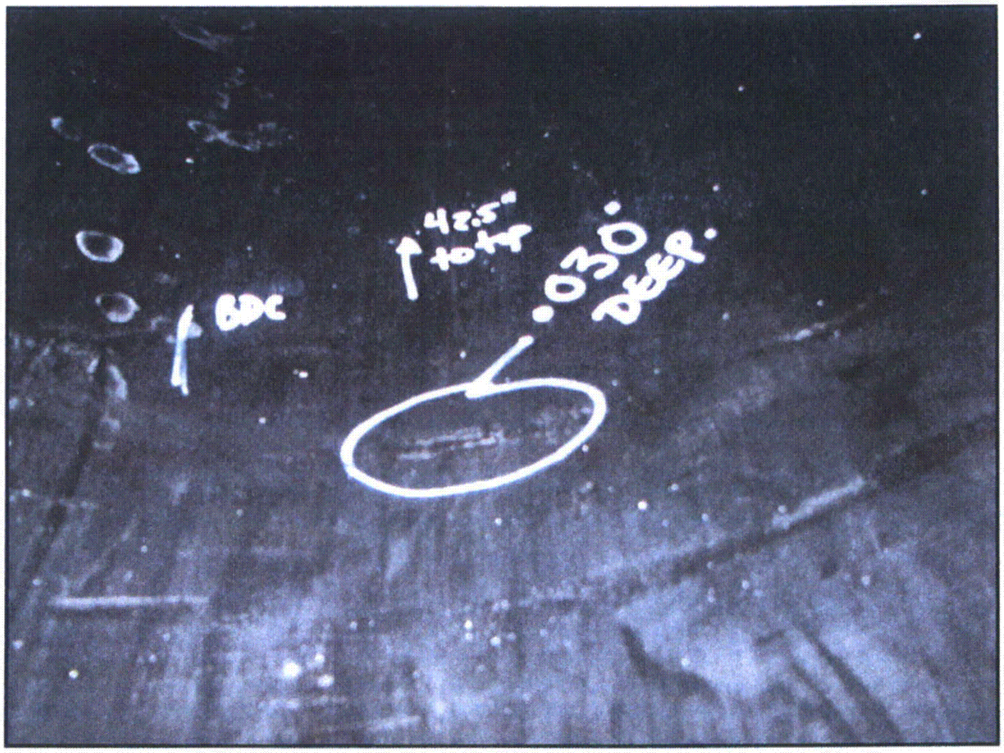

Figure 55 – NS30 #1 Body Pipe Interior Deformation Resulting from Interaction with Drum Ring

VI. Hot End Drop

To establish the hot temperature conditioning unit set-point and confirm that the temperature of the shield components would be at or above the required test temperature of 150 °F at the time of the drop test, the hot cycle temperature conditioning was first run with the set-point of 158.0 °F per Section 4.6 of JSP-7953-01.[1] As detailed in Appendix F, the shield insert body pipe temperature at the start of the "X" hour dwell period was 159.9 °F and fell below 150 °F at the end of 1 hour to 143.2 °F. As a result, the temperature set-point was raised to 176 °F, and the second iteration test was performed. As detailed in Appendix F, the shield insert body pipe temperature during the 2nd iteration at the start of the "X" hour dwell period was 170.5 °F and remained above 150 °F at the end of 1 hour at 150.8 °F.

The hot end drop sequence was performed in accordance with Section 5.6 and 5.7 of JSP-7953-01.[1] As soon as the hot cycle conditioning test requirement was met, the lid of the temperature conditioning chamber was placed back on the base and the conditioning unit was again turned on and the temperature was brought up to 171.7 °F on the internal (shield insert pipe body) thermocouple (see Appendix F).

Once the temperature set-point was achieved, the "X" hour clock was started, the temperature conditioning unit was turned off, and the NS30 #2 canister was removed from its horizontal orientation in the temperature conditioning chamber and lowered vertically into the test fixture. The test fixture was rotated 90° and the test fixture end impact limiter #2 was installed. The assembled test fixture was then rotated an additional 90° (a total of 180° from the original installation orientation) such that the canister was in a top-down orientation. Simultaneously, data cables for the accelerometers were installed on the two accelerometer mounting bases located on the test fixture outer shell near the drop impact location and in-line with the drop orientation. The test fixture was then transported to the drop test pad, rigged, hoisted, and then dropped after data acquisition had been initiated (Figure 56 - Figure 58). The total elapsed time for the Hot End Drop Test was 44 minutes. The hot end drop ran much the same as the cold end drop. Pictorially it looks the same and so only a photograph of the post drop condition is included in this report.

Deformation to the End Impact Limiter #2 was observed, measured, and recorded (see Appendix F). The end plate of the impact limiter experienced an out-of-plane bending plastic deformation of approximately 1/2" (Figure 59). The end impact limiter experienced axial crushing, as indicated by the residual deformation of the limiter shells at the weld location, of approximately 5/8" (Figure 60). Upon removal of the NS30 #1 Test Article from the Test Fixture, no visible damage to the exterior surfaces of the canister were observed (Figure 61).

Figure 56 – NS30 #2 Hot End Drop After Impact

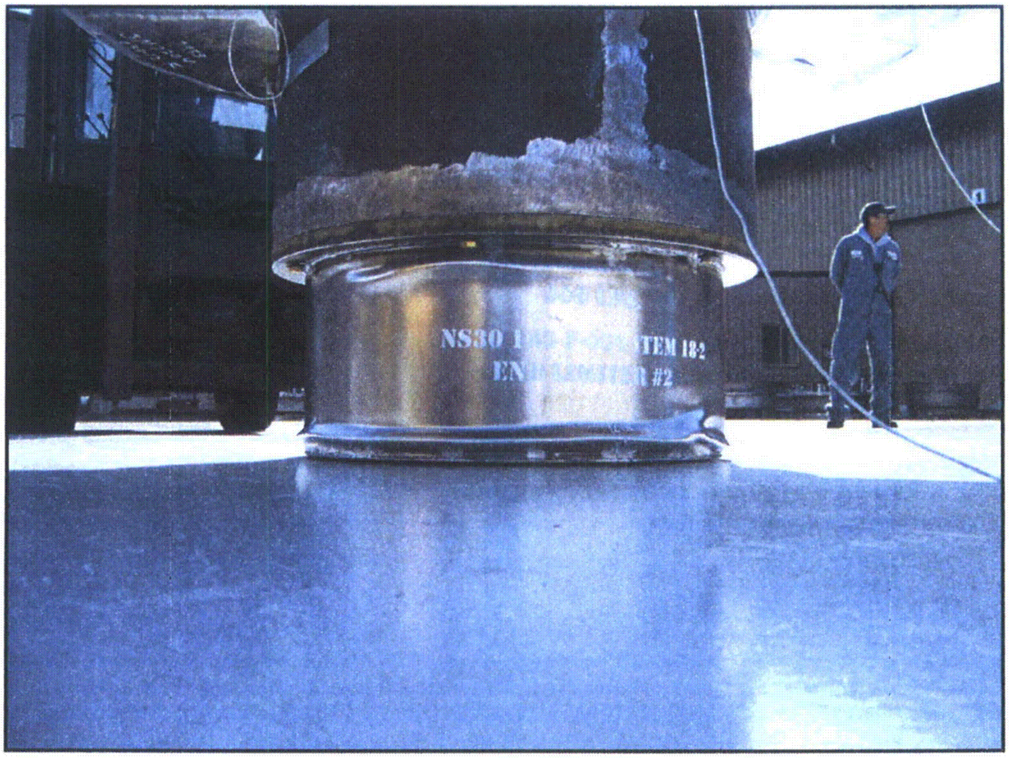

Figure 57 – NS30 #2 Hot End Drop After Impact (close-up of end impact limiter)

Figure 58 – NS30 #2 Hot End Drop After Impact (close-up #2 of end impact limiter)

Figure 59 – Measurement of Plastic Deformation of Base Plate on End Impact Limiter #2

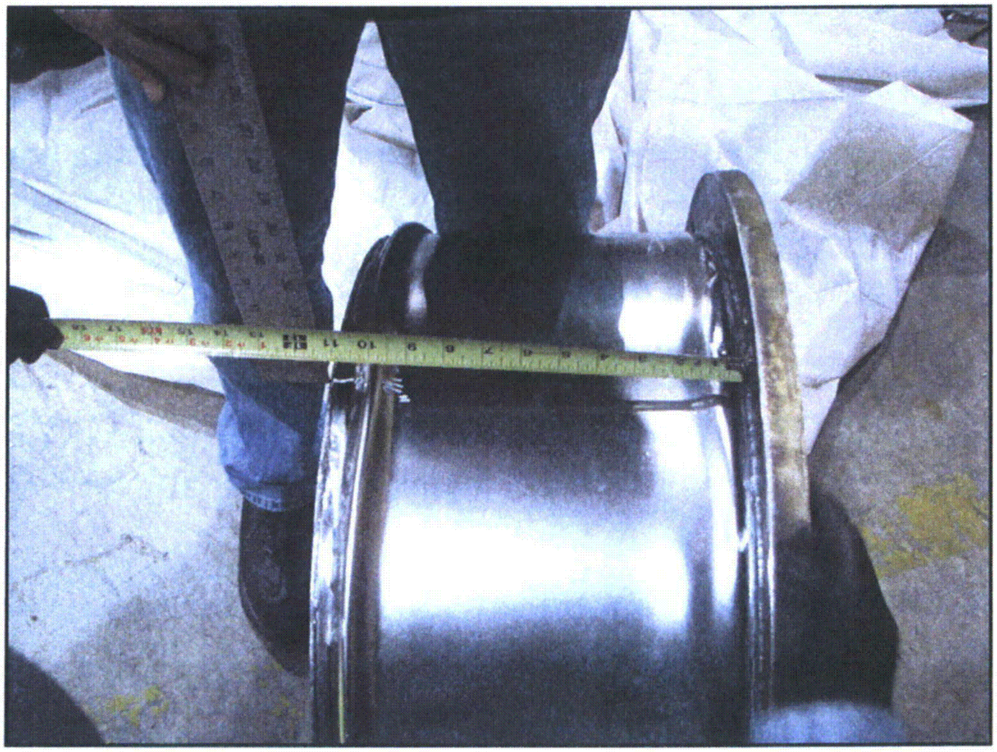

Figure 60 – Foam Crush and Skin Deformation Inspection of End Impact Limiter #2

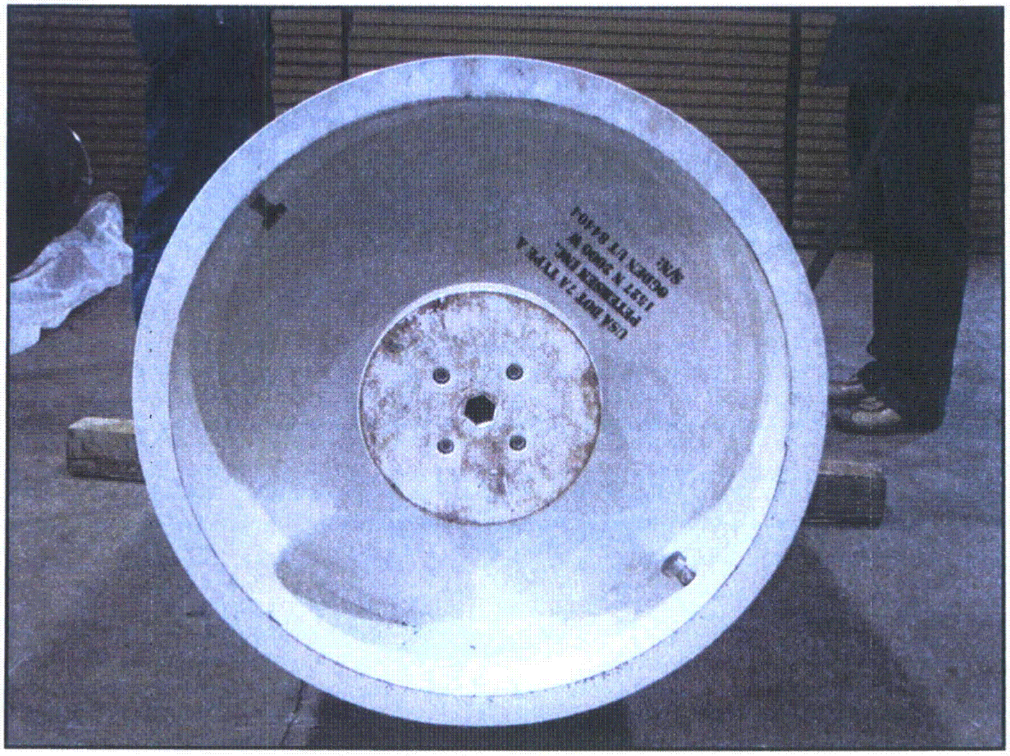

Figure 61 – NS30 #2 Canister After Removal from End Drop Test Fixture

VII. Hot Side Drop

The hot side drop sequence was performed in accordance with Section 5.8 and 5.9 of JSP-7953-01.[1] After completion of the hot end drop test, the NS30 #2 test article again placed in the temperature conditioning chamber and the conditioning unit was activated with the previously established temperature set-point and the temperature was brought down to 172.7 °F on the internal (shield insert pipe body) thermocouple (see Appendix G).

Once the temperature set-point was achieved, the "X" hour clock was started, the temperature conditioning unit was turned off, and the NS30 #2 canister was removed from its horizontal orientation in the temperature conditioning chamber and lowered vertically into the test fixture. The test fixture was rotated 90° such that the canister was in a horizontal orientation and the test fixture end plate was installed. Simultaneously, data cables for the accelerometers were installed on the two accelerometer mounting bases located on the test fixture outer shell near the drop impact location and in-line with the drop orientation. The test fixture was then transported to the drop test pad, rigged, hoisted, and then dropped after data acquisition had been initiated (Figure 62 - Figure 64). The total elapsed time for the Cold Side Drop Test was 36 minutes. Note that the test fixture was oriented such that the previous damage to the side impact limiters from the cold side drop was oriented 180° from the hot side drop impact location. The hot side drop ran much the same as the cold side drop. Pictorially it looks the same and so only a photograph of the post drop condition is included in this report.

Deformation to the Side Impact Limiters was observed, measured, and recorded (see Appendix G). The side impact limiters experienced permanent plastic deformation of approximately 1-5/8" and chord-length contact, as indicated by paint transfer from the drop test pad, of 25-5/8" (Figure 65 - Figure 66). There was no other visible damage to the test fixture. There was indication that the NS30 #2 experienced a slight rotation inside the test fixture (Figure 67).

Upon removal of the NS30 #2 Test Article from the Test Fixture, visible damage to the exterior surfaces of the canister was observed at interface locations with the text fixture upper and lower centering rings (Figure 68). The permanent deformation of approximately 7/8" on the lower and 7/16" on the upper ring interface was located along the lower 1/3 of the canister shell where it aligned to the bottom dead center impact location of the side drop (Figure 69, Figure 70). No other damage or deformation was seen on the exterior of the NS30 #2 Test Article.

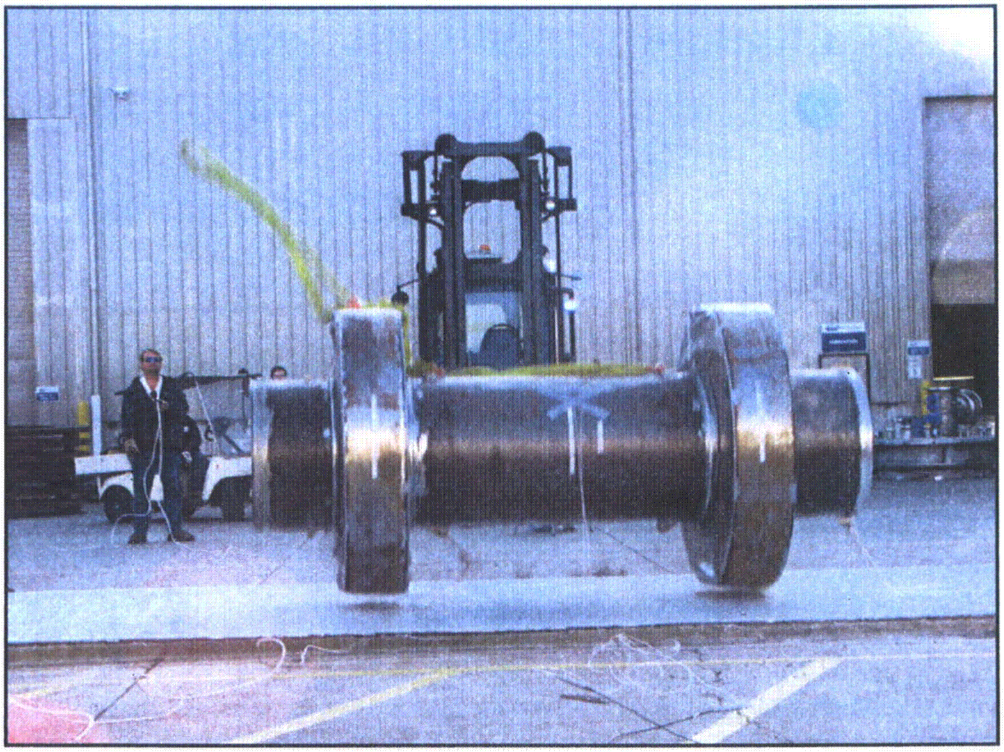

Figure 62 – NS30 #2 Hot Side Drop Just After Impact (during rebound)

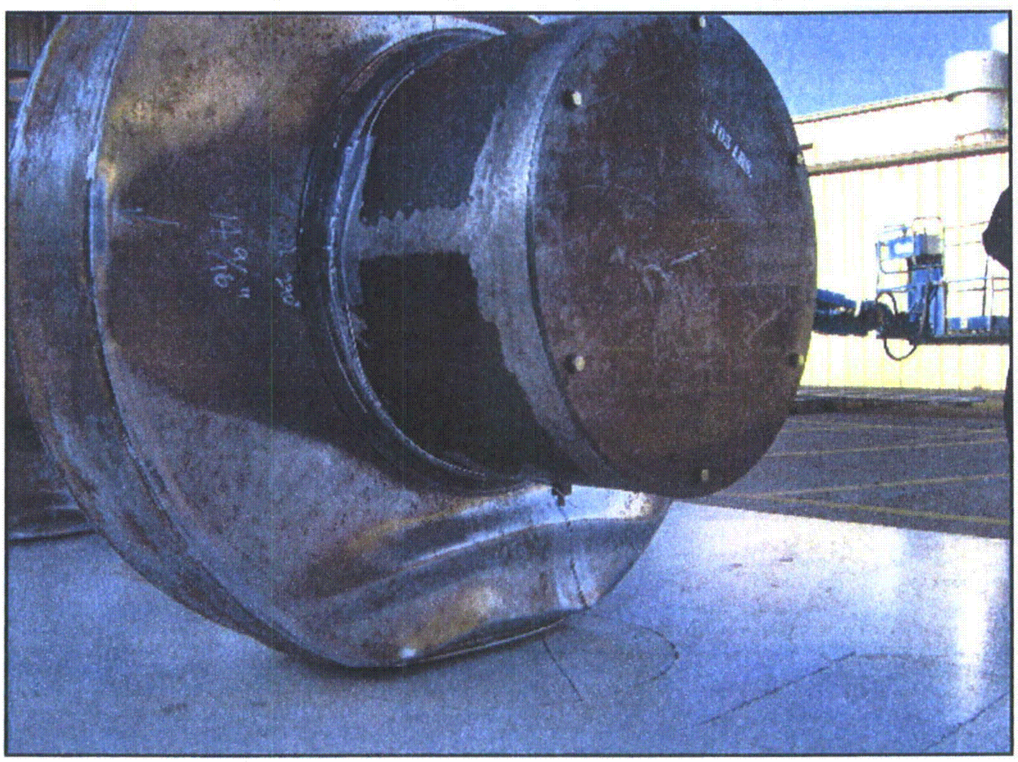

Figure 63 – Right Side (associated with top end of NS30 #2) Impact Limiter Deformation

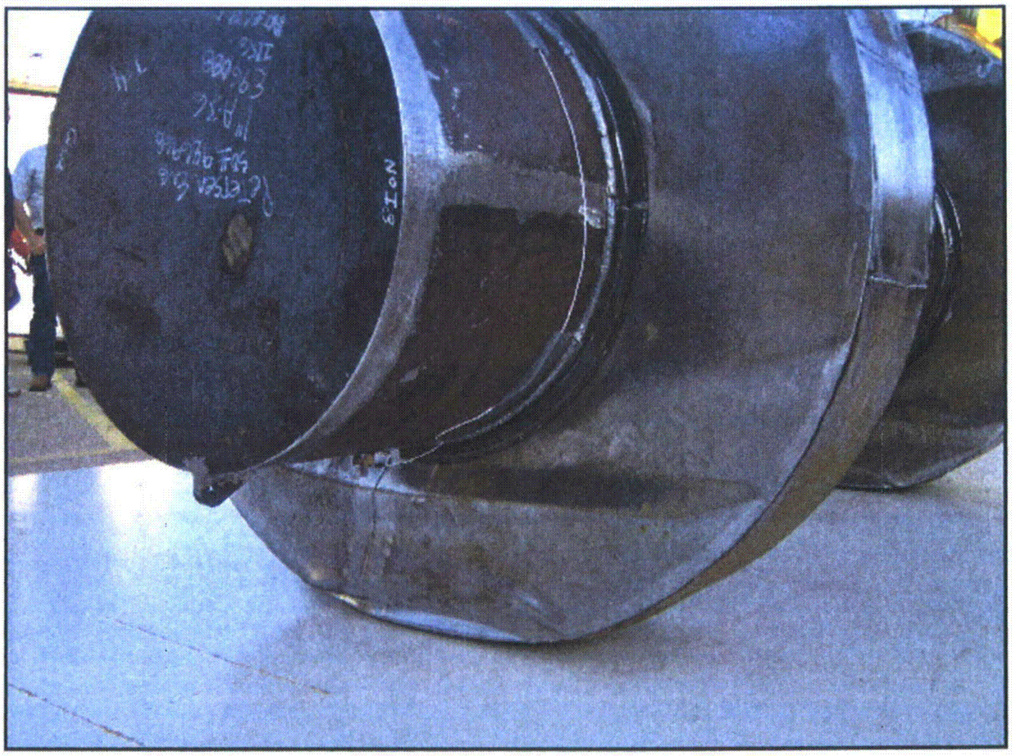

Figure 64 – Left Side (associated with bottom end of NS30 #2) Impact Limiter Deformation

Figure 65 – Measurement of Hot Side Drop Impact Limiter Deformation

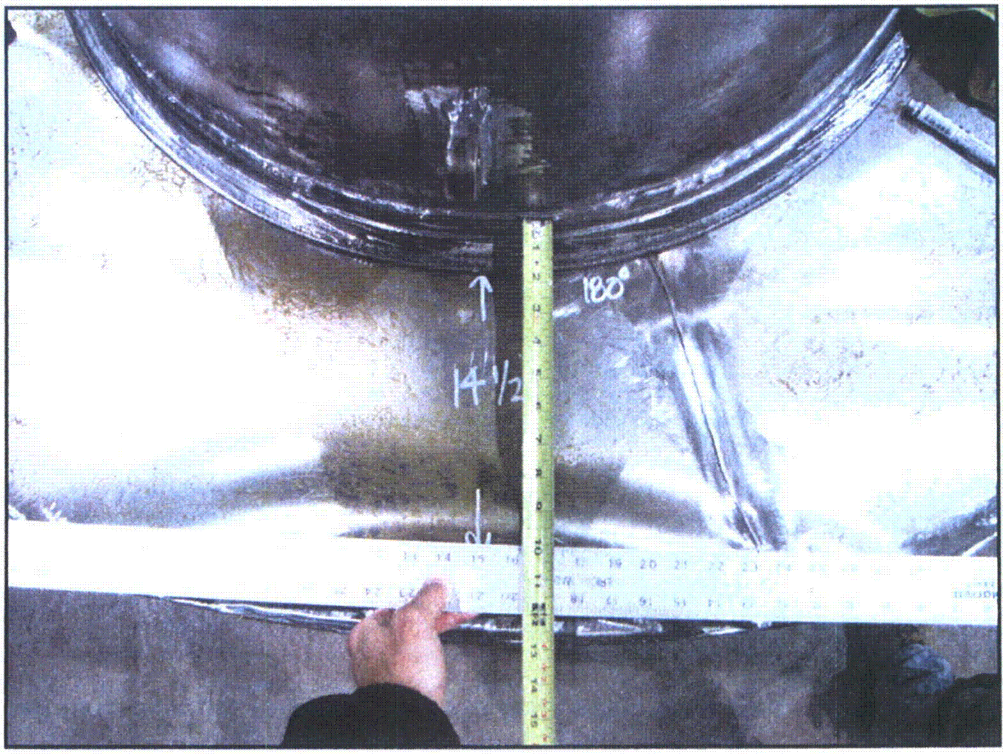

Figure 66 – Measurement of Hot Side Drop Extent of Paint Transfer from Test Pad

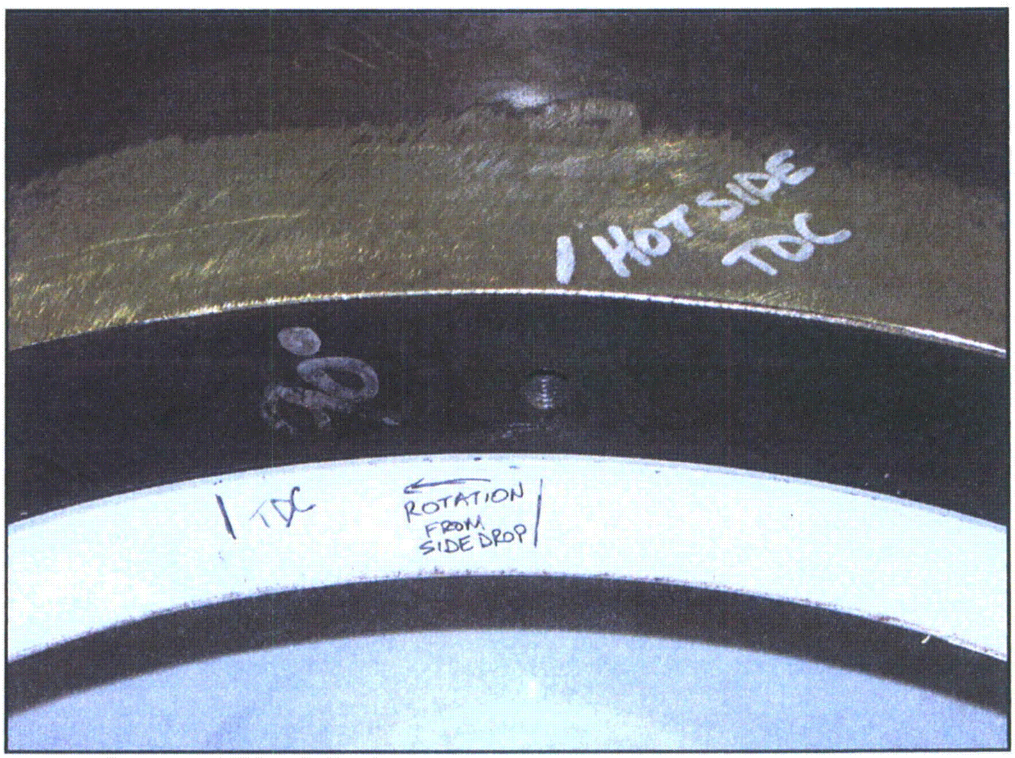

Figure 67 – NS30 #2 Rotation in Test Fixture due to Hot Side Drop

Figure 68 – Removal of NS30 #2 from Test Fixture Following Hot Side Drop Test

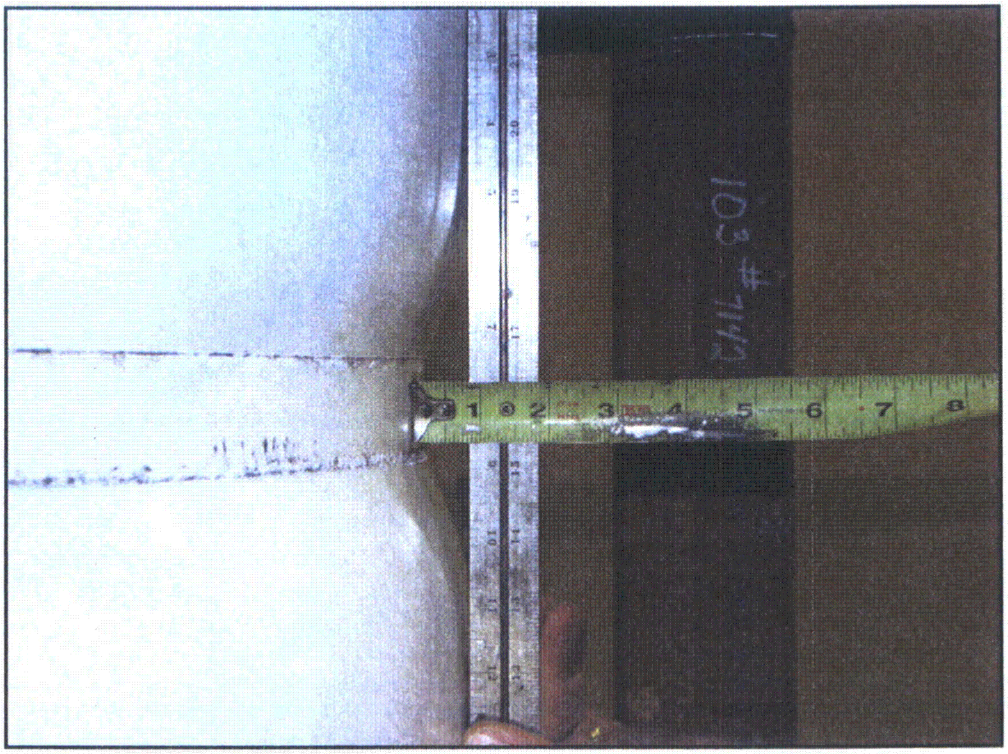

Figure 69 – Permanent Deformation of NS30 #2 Canister Shell due to Interaction with Lower Test Fixture Centering Ring during Hot Side Drop

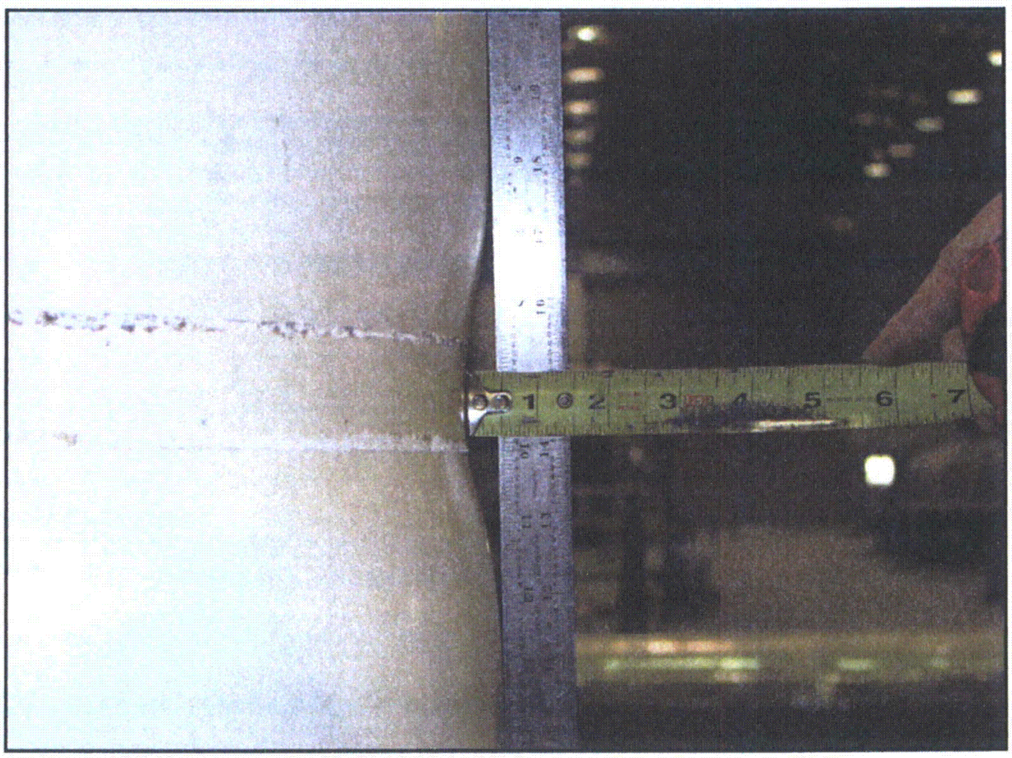

Figure 70 - Permanent Deformation of NS30 #2 Canister Shell due to Interaction with Upper Test Fixture Centering Ring during Hot Side Drop

VIII. Post Hot Drop Disassembly

The hot drop disassembly was performed in accordance with Section 5.10 of JSP-7953-01 following a similar exception as followed for the cold disassembly in not abrasively cutting the canister lid from the body.[1]

The canister lid assembly lock pins were unlocked and the lid assembly was rotated to the unlocked position. The lid was able to rotate to the unlocked position as designed. Upon lifting the canister lid assembly up and out of the canister body, evidence of sand was found along with dirt. As shown in Figure 71 and Figure 72, the sand was stuck to the canister lid assembly and the canister body flange. During normal assembly of the canister lid assembly to body assembly, an optional assembly aid allows for lubrication of the gasket with a silicone spray or light coating of silicone grease. Additionally, a thin coating of petroleum jelly was placed on all lid assembly mating surfaces below the spring plunger for anti-corrosion and as a lubricant during the initial assembly. The sand, dirt, and debris adhered to these lubricants and stayed in place to make the evidence clear. Although there was evidence of sand outside of the shield insert components, there was no evidence of sand outside of the canister confinement boundary as all contents were contained by the canister gasket. The canister lid was fully removed and placed on a clean sheet of plastic and the sand was brushed and scraped off and collected for weight.

The CDX Grade plywood spacer was again deformed as it had been forced up into the canister lid assembly pocket (the space created between the canister lid flange and the lid plate) by impact with the shield insert top end cap during the end drop (Figure 72). The plywood was splintered and some of the splintered wood had broken off. Deformation of the plywood, as documented in Appendix H, was insufficient to allow the axial gap between components to disengage either end cap from the body pipe. The plywood spacer was removed carefully and the sand was brushed off and collected.

The plywood was removed and the top surface of the NS30 top end cap was inspected. There was evidence of plywood pieces, dust, and sand (Figure 73). Inspection of the interface between the shield insert top end cap and body pipe indicated no gaps or separation as the end cap was fully seated with the body pipe.

The top end cap was then slowly removed from the body pipe and at the outer circumference of the top end cap near the bottom dead center side drop orientation, additional evidence of sand adhered/embedded in the plastic was observed (Figure 74). The top end cap was removed, taking special care not to jostle or shake it so as to be able to account for all sand exterior to the shield insert end cap gasket to body pipe interface. Once the top end cap was hoisted above the canister, photographs were taken for documentation and then plastic was wrapped from bottom to top to ensure that no sand was lost. Visual inspection of the top end cap gasket showed a crack adjacent to the gasket retaining ring, but no through-thickness split or tear in the gasket was observed. Indentations due to impact from the drum closure ring in the top down end drop were also observed along with no other significant damage to the top end cap (Figure 75).

A piece of plastic was then cut and taped to the inside wall of the canister just below the body flange to cover the opening of the NS30 #2 shield insert cavity. The sand and dirt that was stuck to the inside wall of the canister body flange was brushed off onto the plastic sheet for collection. Once the sand had been collected and the plastic and tape removed, a new piece of clean plastic was draped from the canister body flange to the inside wall of the NS30 #2 body pipe (Figure 76). It was taped to the inside wall of the NS30 #2 body pipe (creating a funnel) to ensure that any sand or debris that may break free from the payload drums during removal would not inadvertently mix with any sand or debris that was exterior to the shield insert assembly.

A cautious removal of the payload drums from the body pipe was performed. The drum handling bags were in an impaired condition and had been partially sheared at the interface between drums in the end drop. The payload drums experienced closure ring and lid deformations (Figure 77, Figure 78, Figure 79).

With the payload drums (4, 5, and 6) removed from the NS30 #2, the interior surfaces and the inside of the bottom end cap were inspected from the top of the canister. Because of the lighting and distance to the bottom end cap, a video camera was lowered in to give a closer inspection of this gasket prior to removal. It was observed that the bottom end cap gasket was damaged in a manner similar to the top end cap gasket for NS30 #1 (Figure 80, Figure 81). Because of the fact that sand had been found outside of the NS30 #2 shield insert assembly, it was decided that the body pipe and bottom end cap would be removed and inspected rather than viewed further through a window cut out of the base of the canister (and introducing more foreign material into the canister cavity)..

The bottom end cap and the body pipe were removed together in a vertical orientation then placed upon a clean sheet of plastic in a vertical rack to facilitate inspection. This was done so that the joint between the body pipe and the end cap could be analyzed and also so that all debris located on the outside diameter of the body pipe and all other surfaces external to the bottom end cap gasket to body pipe interface could be brushed down and collected for weighing. Three ¼" shims were used to block up the body pipe and remove any debris from between the body pipe and the bottom end cap (any material that bypassed the gasket) Figure 82. This material was collected and weighed along with the other sand and debris.

The bottom end cap and body pipe were then disassembled for inspection of the individual components. All of the EHMW-HDPE plastic parts were inspected for gouges, dents, cuts and scratches due to interaction of the HDPE with the surrounding canister structure or the internal payload (Figure 83). Internal to the body pipe, dents were observed due to interaction with the payload drums (Figure 84). External to the body pipe, deformations were observed due to interaction with the canister shell at the location of the test fixture centering rings (Figure 85). Measurements were taken and a UT inspection was added to determine the minimum body pipe wall thickness in the most deformed areas. The measurements were used to verify that the deformation on the outside wall (from the test fixture centering ring) and the deformation on the inside wall (from the payload drum) did not directly line up, thus providing the true minimum wall thickness. A summary of observed deformation is documented in Appendix H. Scratches, dents, gouges, and deformations were also measured on the top and bottom end caps. There were no indications of material cracking or failure in any of the scratches, dents or gouges.

The canister body was finally laid down on its side and the sand and debris was brushed in a top to bottom, body flange to base direction. The contents were collected for weight measurement.

The collection of this sand and other debris present was performed using new 2" wide paint brushes, a new shop hand broom and clean rags. In the case where sand and debris was being removed from lubricated surfaces, a brush or rag was weighed prior to use, used to capture the sand/lubricant mixture, and then weighed after use to ensure any change in weight was also accounted for.

Due to the lack of immaculate pre-drop test cleaning of the interior canister metallic components and/or the HDPE shield insert components, the weight of "released" materials outside of the shield insert boundary is considered conservative as preexisting dirt and debris was likely also accounted for in the measurement.

The total weight of "released" materials was determined as shown in Table 1, and represents (0.035/15) = 0.23% the weight of the 5 lbs of releasable sand in each of the payload drums.

Table 1 – Summary of Debris Weights

Equipment	Starting Weight	Ending Weight	Delta (lbs of Sand)
Brush	0.055 lbs.	0.06 lbs.	0.005 lbs.
Hand Broom	0.525 lbs.	0.525 lbs.	0 lbs.
Cup	0.085 lbs.	0.105 lbs.	0.02 lbs.
Rag	0.135 lbs.	0.145 lbs.	0.01 lbs.
		Total	0.035 lbs.

The measured accelerations due to impact were recorded and are provided in Appendix I. Sensors indicated some clipping of the signal due to excessive electrical input to the 500 g accelerometers. Filtering of the data utilizing a low-pass Butterworth 10-pole filter with a 75 Hz cut-off frequency provides a conservative minimum acceleration peak, on average from the two sensors, of approximately 382 g's for the hot end drop and 204 g's for the hot side drop.

Figure 71 – NS30 #2 Canister Lid with Sand Particles Adhered to Lubricant

Figure 72 – NS30 #2 Canister Body Flange with Sand Particles Adhered to Lubricant

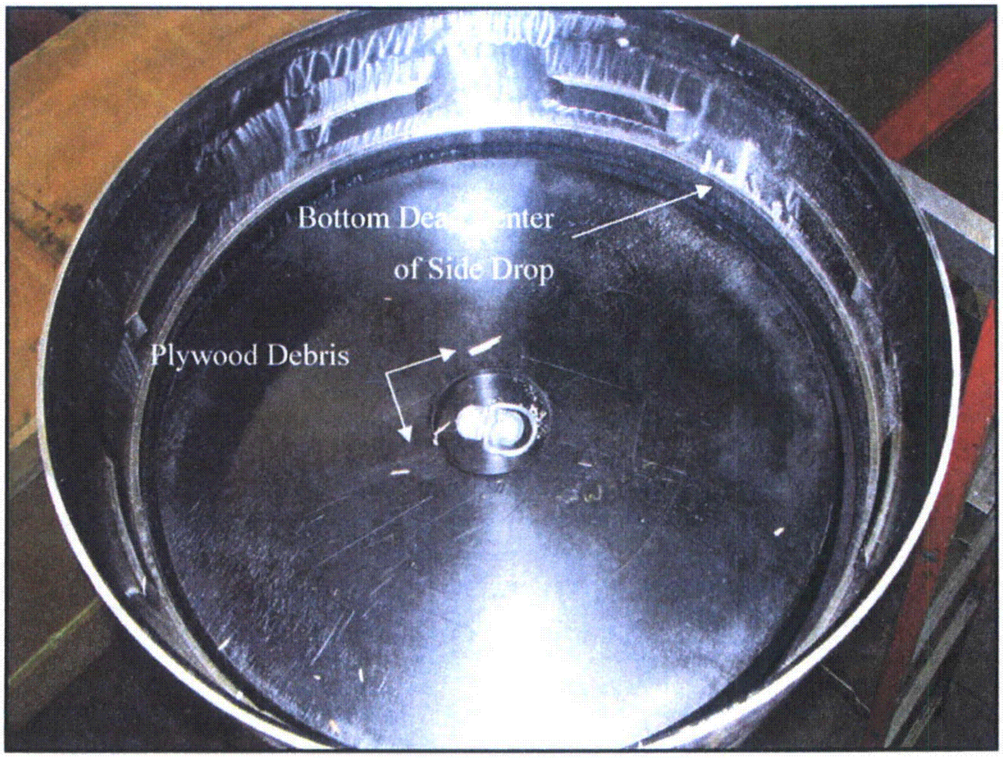

Figure 73 – NS30 #2 Top End Cap with Sand Adhered to Body Flange at Bottom Dead Center from Side Drop Orientation

Figure 74 – NS30 #2 Top End Cap with Sand Adhered or Embedded to Outside Diameter

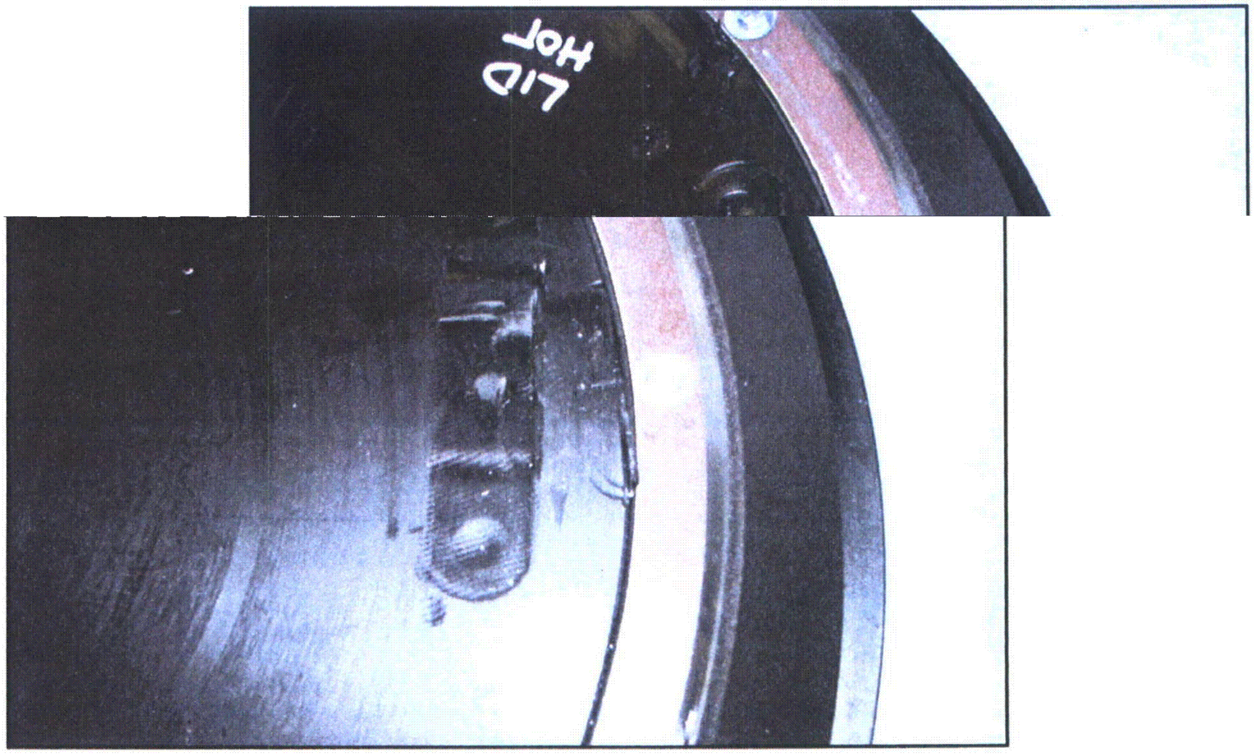

igure 75 – NS30 #2 Top End Cap Inner Surface with Indentations due to Impact by Payload Drum Closure
ing in End Drop Orientation

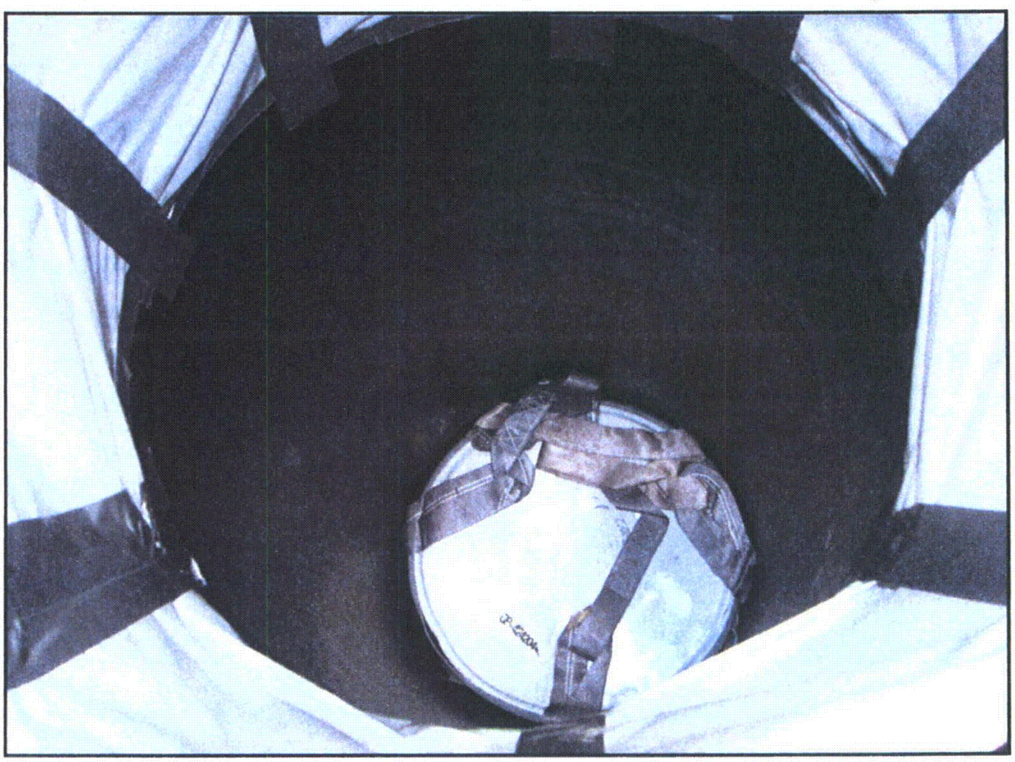

igure 76 – Temporary Plastic Funnel Installed to Facilitate Removal of NS30 #2 Payload Drums by
recluding Spillage of Contents outside of Shield Body Pipe

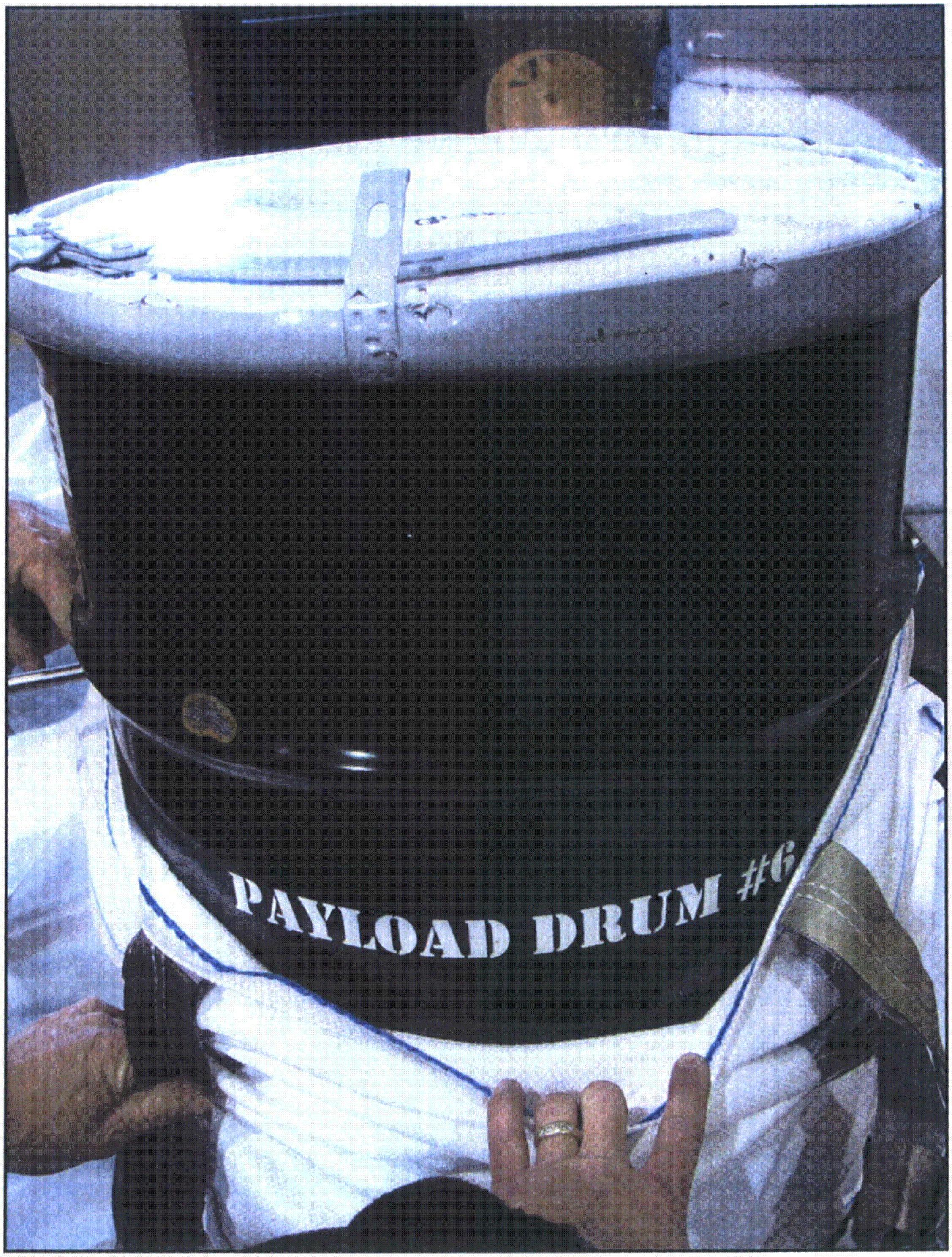

Figure 77 – Top Payload Drum #6

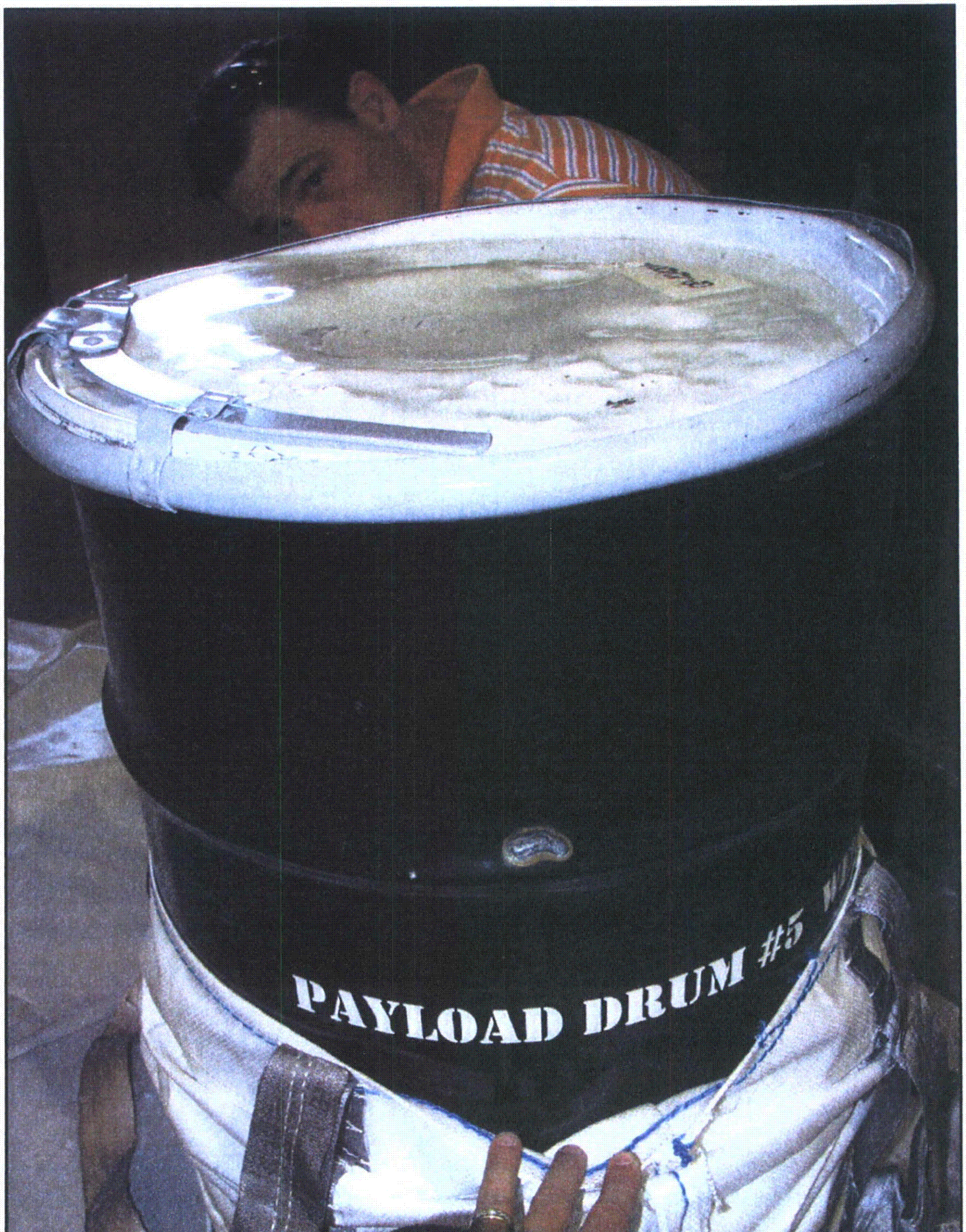

Figure 78 – Middle Payload Drum #5

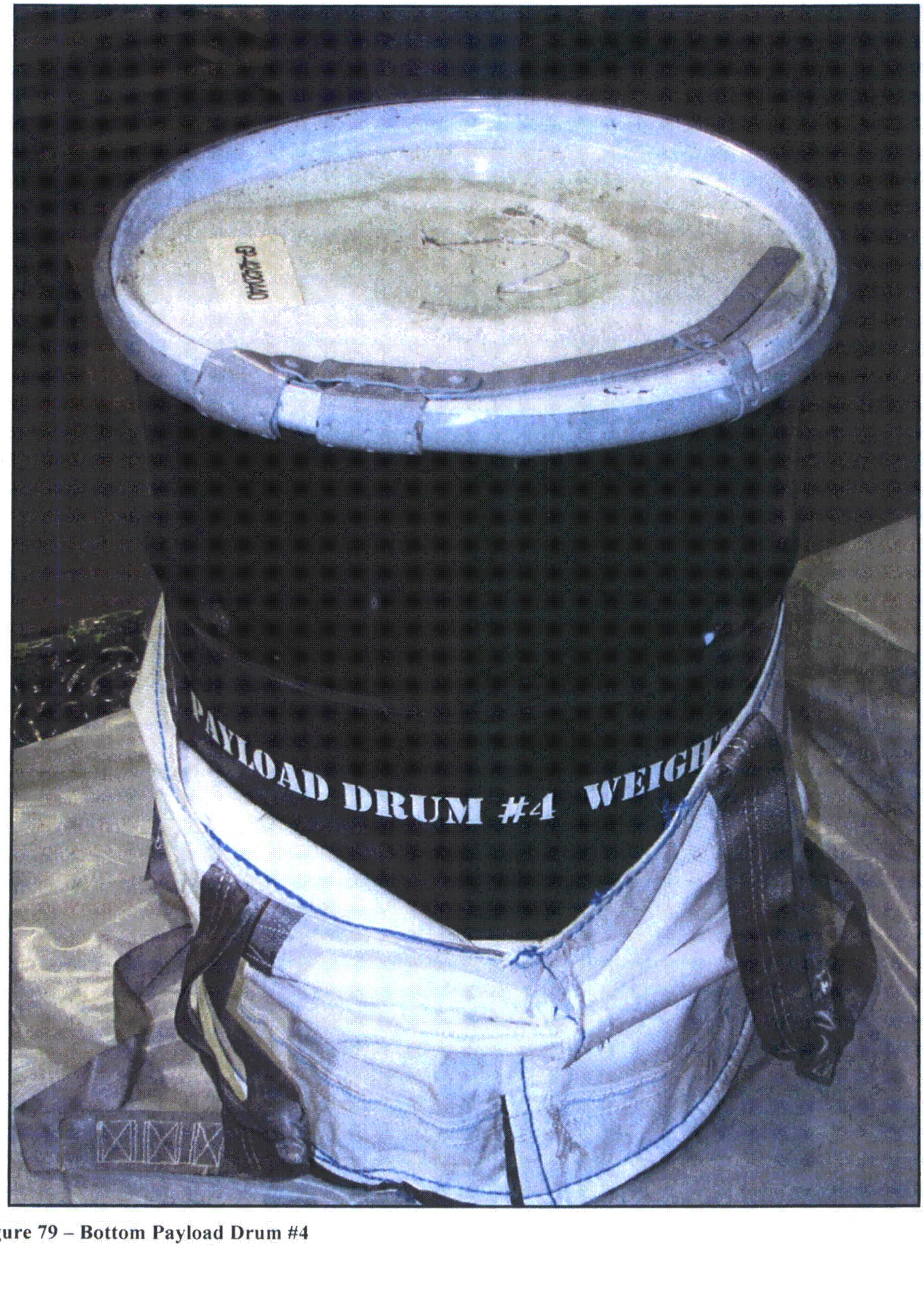

Figure 79 – Bottom Payload Drum #4

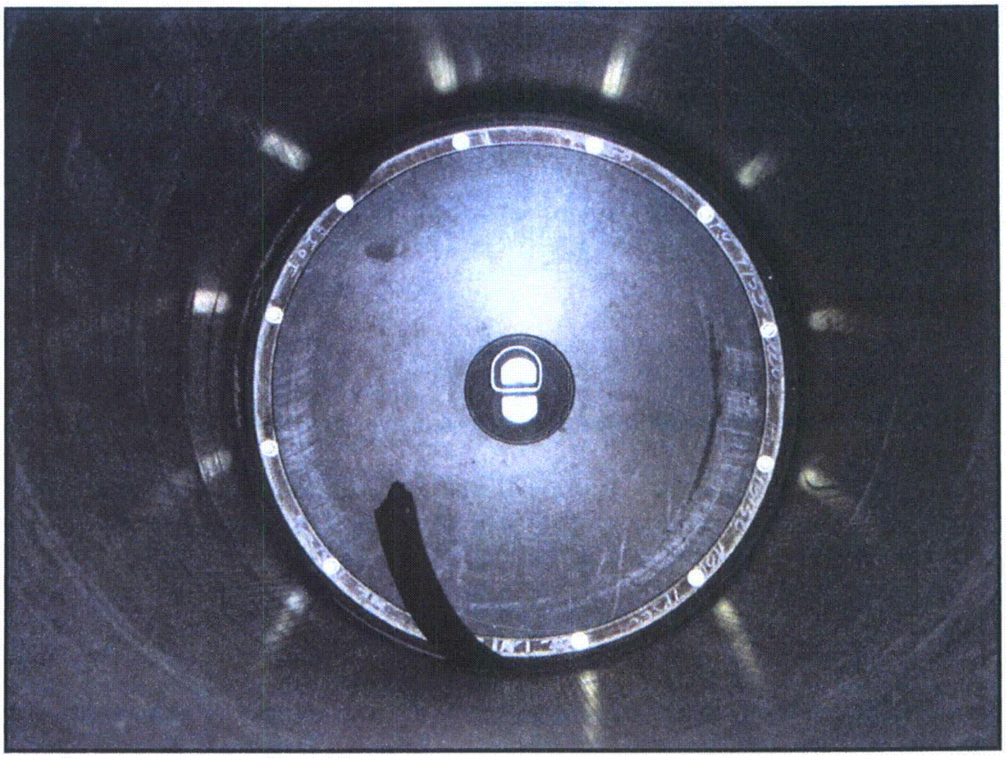

Figure 80 – View of NS30 #2 Bottom End Cap from the Lid End of the Shield Body Pipe

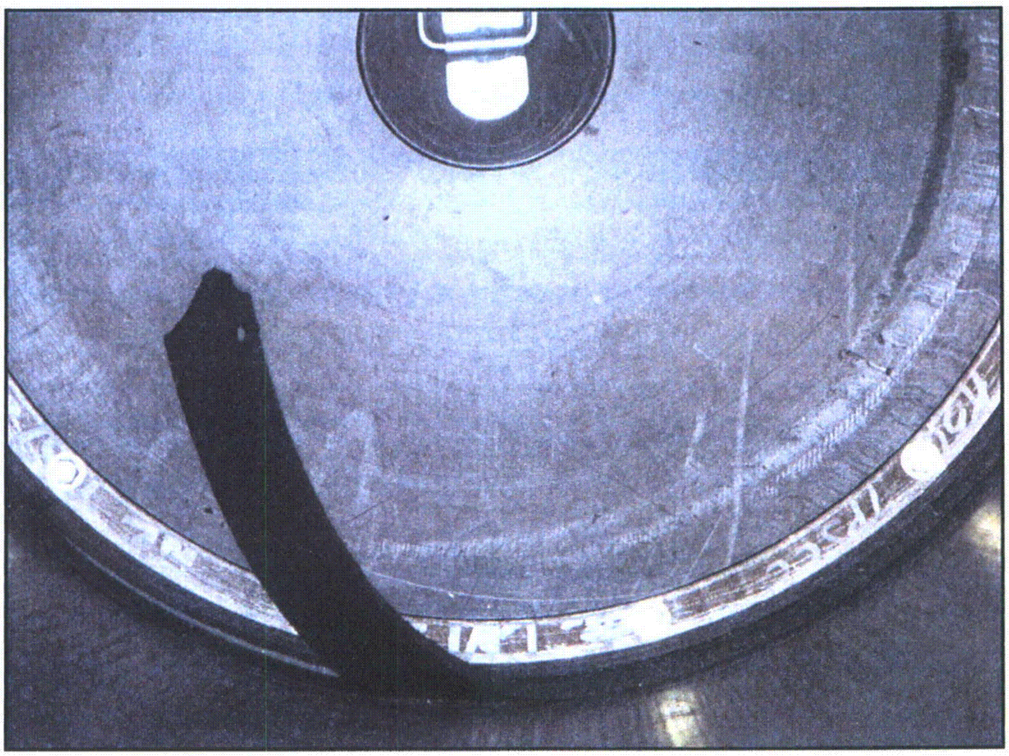

Figure 81 – View of NS30 #2 Bottom End Cap from the Lid End of the Shield Body Pipe (close-up of torn gasket)

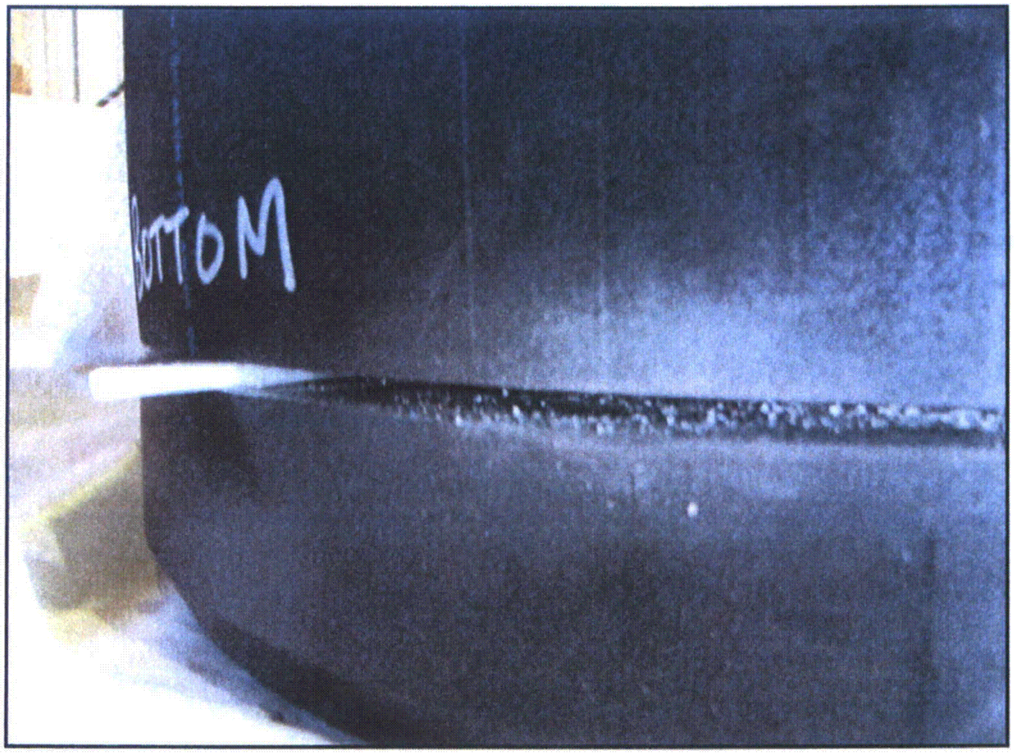

Figure 82 – NS30 #2 Bottom End Cap and Body Pipe Interface (separated by shims to facilitate removal of payload debris that bypassed gasket)

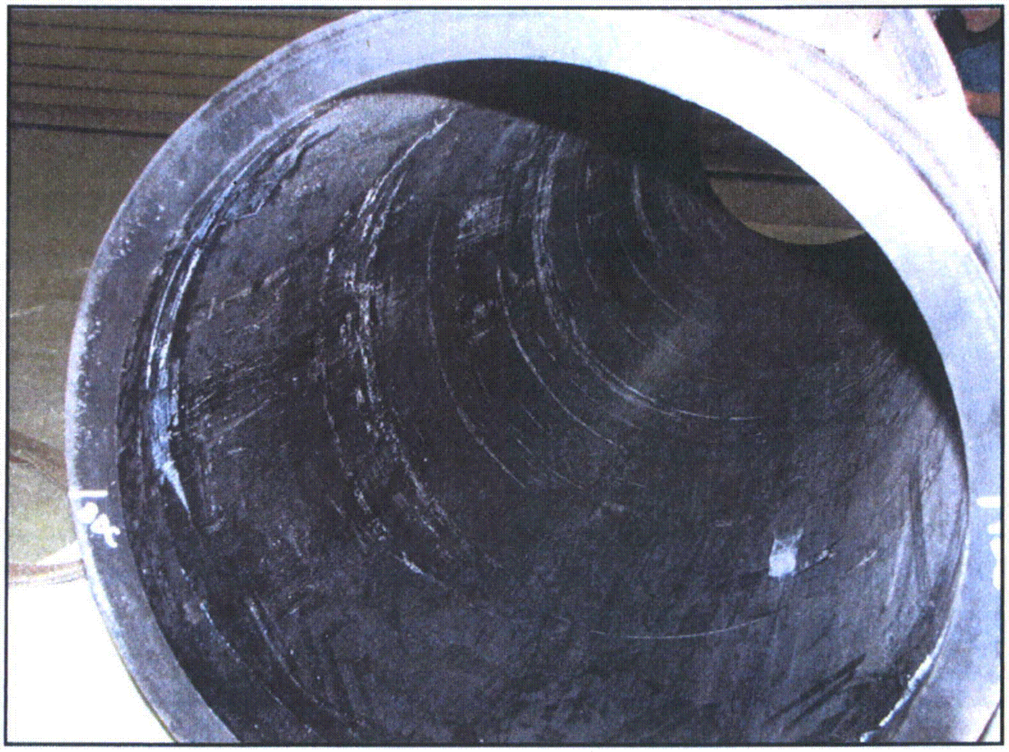

Figure 83 – NS30 #2 Body Pipe After Removal of Bottom End Cap

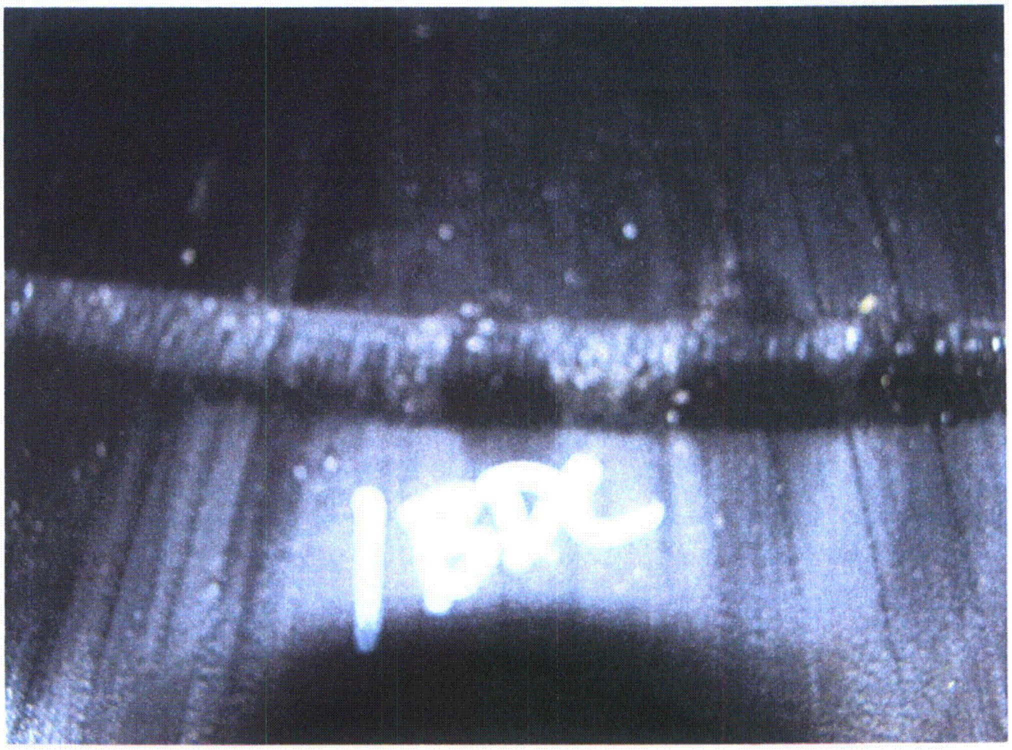

Figure 84 – NS30 #2 Body Pipe Interior Deformation Resulting from Interaction with Drum Ring

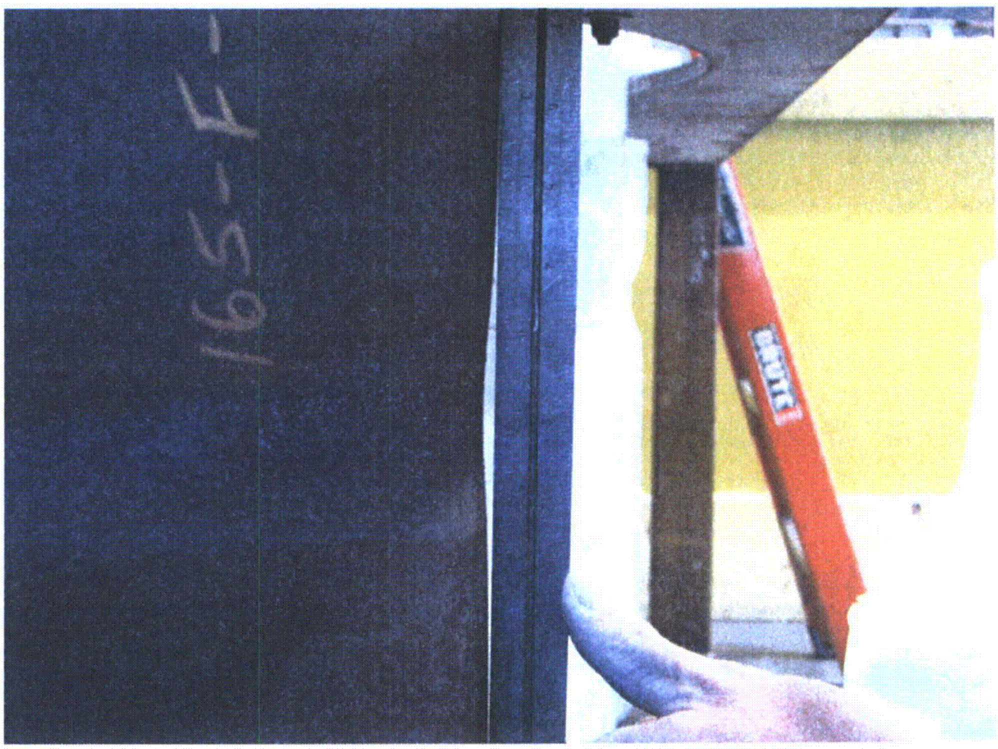

Figure 85 – NS30 #2 Body Pipe Exterior Deformation Resulting from Interaction with Canister Shell Deformed by Test Fixture Lower Centering Ring

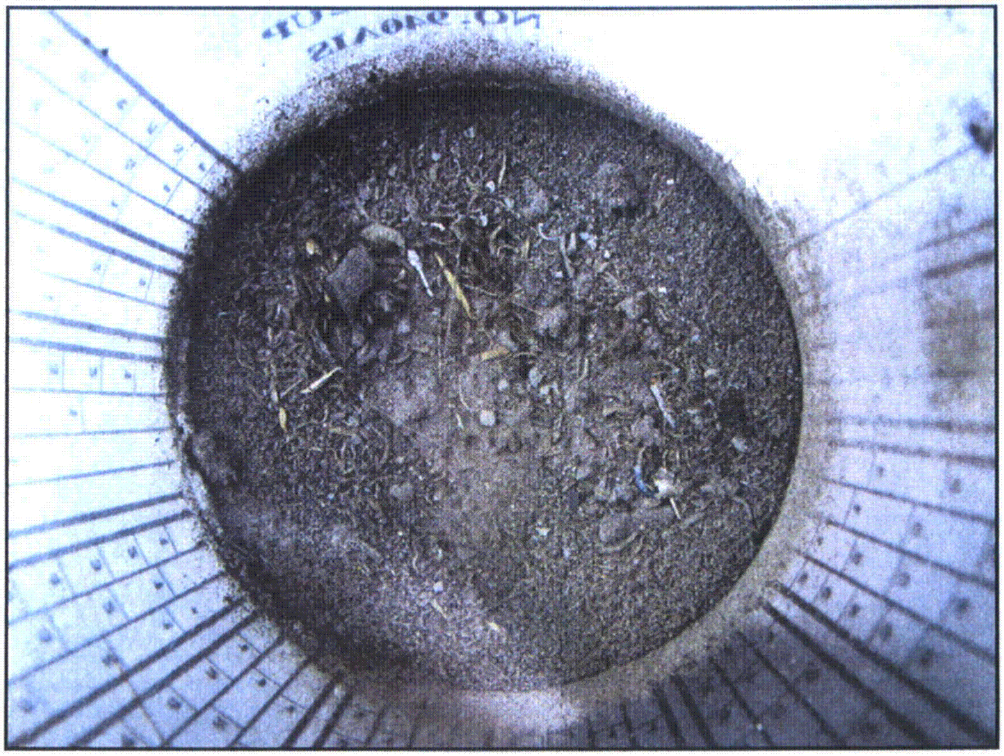

Figure 86 – Close-up of Debris Collected from All Surfaces External to the End Cap Gaskets and Internal to the Canister Confinement Boundary

IX. Appendix

A. DATA SHEET 1.1 – Component Weights

B. DATA SHEET 1.2 – Calibration Records

C. DATA SHEET 2.1 – Test #1, 30-Foot End Drop (Cold)

   a. Page 1
   b. Page 2
   c. Page 3
   d. Graph of Temperature Conditioning Test #1 – Cold Cycle
   e. Graph of Cold End Drop Test Temperature Conditioning
   f. End Limiter #1 – Post Cold End Drop Inspection

D. DATA SHEET 2.2 – Test #2, 30-Foot Side Drop (Cold)

   a. Page 1
   b. Page 2
   c. Graph of Cold Side Drop Test Temperature Conditioning
   d. NS30 #1 – Cold Drop Side Limiter Inspection

E. DATA SHEET 2.3 – Tests #1 & #2, 30-Foot Drops (Cold)

   a. Page 1
   b. CDX Grade Plywood Post Cold Drop Inspection
   c. Damage Assessment of NS30 #1 Cold Drop Test Article parts

F. DATA SHEET 2.4 – Test #3, 30-Foot End Drop (Hot)

   a. Page 1
   b. Page 2
   c. Page 3
   d. Graph of Temperature Conditioning Test #2 – Hot Cycle (iteration #1)
   e. Graph of Temperature Conditioning Test #2 – Hot Cycle (iteration #2)
   f. Graph of Hot End Drop Test Temperature Conditioning
   g. End Limiter #2 – Post Hot End Drop Inspection

G. DATA SHEET 2.5 – Test #4, 30-Foot Side Drop (Hot)

   a. Page 1
   b. Page 2
   c. Graph of Hot Side Drop Test Temperature Conditioning
   d. NS30 #2 – Hot Drop Side Limiter Inspection

H. DATA SHEET 2.6 – Tests #3 & #4, 30-Foot Drops (Hot)

a. Page 1

b. CDX Grade Plywood Post Hot Drop Inspection

c. Damage Assessment of NS30 #2 Hot Drop Test Article parts

I. ACCELERATION MEASUREMENTS

a. End Drop – Raw Data

b. End Drop – Filtered Data

c. Side Drop – Raw Data

d. Side Drop – Filtered Data

Appendix A – DATA SHEET 1.1 – Component Weights

PETERSEN INCORPORATED "A Winning Combination."	Procedure Number:	JSP-7953-01
	Revision Number:	1
	Revision Date:	08/31/09
	Page:	23 of 36

DATA SHEET 1.1 – Component Weights

Neutron Shielded Canister Test Fixture Tare Weights (lb)

2770 lbs.	306 LBS.	308 LBS.	105 LBS.
Body Assembly ①	End Limiter #1 ②	End Limiter #2 ③	End Cap Plate & Hardware ④
3076 LBS.	2875 LBS.	3078 LBS.	2875 LBS.
End Drop #1 Test Fixture ①+②=⑤	Side Drop #1 Test Fixture ①+④=⑥	End Drop #2 Test Fixture ①+③=⑦	Side Drop #2 Test Fixture ①+④=⑧

NS30 Neutron Shielded Canister Tare Weights (lb)

1668 LBS.	1666 LBS.
NS30 #1 ⑨	NS30 #2 ⑩

Payload Drum Weights (lb)

518 LBS.	510 LBS.	511 LBS.
Payload Drum # 1 ⓫	Payload Drum #2 ⓬	Payload Drum # 3 ⓭
511 LBS.	513 LBS	513 LBS.
Payload Drum # 4 ⓮	Payload Drum #5 ⓯	Payload Drum # 6 ⓰

Loaded NS30 Neutron Shielded Canister Weights (lb)

3207 LBS.	3203 LBS.
NS30 #1 ⑨+⓫+⓬+⓭=⓱ (3,100 - 3,200 lb)	NS30 #2 ⑩+⓮+⓯+⓰=⓲ (3,100 - 3,200 lb)

Loaded Neutron Shielded Canister and Test Fixture Weights (lb)

6283 LBS.	6082 LBS.	6281 LBS.	6078 LBS.
End Drop #1 ⑤+⓱	Side Drop #1 ⑥+⓱	End Drop #2 ⑦+⓲	Side Drop #2 ⑧+⓲

Test Engineer and Witness Records

[signature]	BART ANDERSON	9·25·09
Test Engineer Signature	Printed Name	Date
[signature]	JOE G. DANIEL	9·25·09
Witness Signature	Printed Name	Date

Appendix B – DATA SHEET 1.2 – Calibration Records

PETERSEN INCORPORATED
"A Winning Combination."

Procedure Number:	JSP-7953-01
Revision Number:	1
Revision Date:	08/31/09
Page:	24 of 36

DATA SHEET 1.2 – Calibration Records

Instrumentation Records

(If multiple load cells/scales are utilized, denote the corresponding component(s) that each load cell/scale was used to measure.)

Description	Number	Calibration Due Date
GSE 350 (10,000 lb CAP.) — Load Cell/Scale Description	PF 1034 — Petersen PF Number	9.30.2009
CARDINAL SCALE MODEL# 2240-50 — Load Cell/Scale Description	PF 1143 — Petersen PF Number	11.30.2010
M-D BUILDING PRODUCTS - DIGITAL LEVEL — ~~Load Cell/Scale Description~~	PF921 — Petersen PF Number	9.30.2010
ARMSTRONG : 0-100 Ft-lb CAP — Torque Wrench	PF948 — Petersen PF Number	3.31.2010
ARMSTRONG TORQUE WRENCH : 5-50 IN.lbs — ~~Strip Chart Recorder~~	PF771 — Petersen PF Number	9.30.2010
OMEGA DIGITAL THERMOMETER — Hand Held Temperature Probe	PF989 — Petersen PF Number	3.31.2010
OMEGA DATALOGGER THERMOMETER — Data Logger	XC0723-CCP — Serial Number	7.28.2010
BODY PIPE #1 (COLD) CUSTOMER SUPPLIED K-TYPE THERMOCOUPLE — Thermocouple Lead #1	XC0731-CCP — Serial Number	7.28.2010
BODY PIPE #2 (HOT) CUSTOMER SUPPLIED K-TYPE THERMOCOUPLE — Thermocouple Lead #2	XC0726-CCP — Serial Number	7.28.2010
PCB-PIEZOTRONICS - MODEL# 353B03 — Accelerometer #1	134496 — Serial Number	9.3.2010
PCB-PIEZOTRONICS - MODEL # 353B03 — Accelerometer #2	134497 — Serial Number	9.3.2010
RLC BODY #1 - (COLD) - CUSTOMER SUPPLIED K-TYPE THERMOCOUPLE — Other	XC0729-CCP — Serial Number	7.28.2010
RLC BODY #2 - (HOT) - CUSTOMER SUPPLIED KTYPE THERMOCOUPLE — Other	XC0725-CCP — Serial Number	7.28.2010
N19234 IEPE SIGNAL CONDITIONER — Other	XC0760-CCP 1449745 — Serial Number	9.1.2010

SONATEST 123 - U.T. MACHINE		10009000	7.10.2010
DIAL INDICATOR	JD 12.3.09	~~PF358~~ PF365	5.31.2010
O.D. MICROMETER	JD 12.3.09	~~PF365~~ PF358	7.31.2010
6" CALIPER		EM051	3.31.2010

Appendix C – DATA SHEET 2.1 – Test #1, 30-Foot End Drop (Cold)

Page 1

PETERSEN INCORPORATED "A Winning Combination."	Procedure Number: Revision Number: Revision Date: Page:	JSP-7953-01 1 08/31/09 25 of 36

DATA SHEET 2.1 – Test #1, 30-Foot End Drop (Cold)

.... Pre-Test Records				
Conditioning Iteration #_____ Set Point _____(°F)	Date & Time (mm/dd/yy & hh:mm)	Ambient Temp. (°F)	Internal Sensor (°F)	External Sensor (°F)
Start Conditioning				
Start +30 min.				
Start +60 min.				
Start +90 min.				
Start +120 min.				
Start +150 min.				
Start +180 min.				
Start +210 min.				
Start +240 min.				
Start +270 min.				
Start +300 min.				
Start +330 min.				
Start +360 min.				
Start +390 min.				
Start +420 min.				
Start +450 min.				
Start +480 min.				
Start +510 min.				
Start +540 min.				
Start +570 min.				
Start +600 min.				
Note: If time to reach conditioning set-point is greater than +600 min., use supplemental pages as necessary to record sensor temperatures.				
Stop Conditioning				
Stop +10 min.				
Stop +20 min.				
Stop +30 min.				
Stop +40 min.				
Stop +50 min.				
Stop +60 min.				
Stop +70 min.				
Stop +80 min.				
Stop +90 min.				
Stop +100 min.				
Stop +110 min.				
Stop +120 min.				
Note: If additional conditioning iterations with lower set-point are required to achieve internal temperature < -20 °F at the end of the 'X' dwell period, use supplemental pages as necessary to record sensor temperatures.				

SEE ATTACHED CHART.

SEE ATTACHED CHART.

Datasheet 2.1 – Page 1

Page 2

PETERSEN INCORPORATED "A Winning Combination."	Procedure Number:	JSP-7953-01
	Revision Number:	1
	Revision Date:	08/31/09
	Page:	26 of 36

Final Conditioning Iteration Set Point ____(°F)	Date & Time (mm/dd/yy & hh:mm)	Ambient Temp. (°F)	Internal Sensor (°F)	External Sensor (°F)
Start Conditioning				
Start +30 min.				
Start +60 min.				
Start +90 min.				
Start +120 min.				
Start +150 min.				
Start +180 min.				
Start +210 min.				
Start +240 min.				
Start +270 min.				
Start +300 min.		SEE ATTACHED CHART.		
Start +330 min.				
Start +360 min.				
Start +390 min.				
Start +420 min.				
Start +450 min.				
Start +480 min.				
Start +510 min.				
Start +540 min.				
Start +570 min.				
Start +600 min.				
Note: If time to reach final conditioning set-point is greater than +600 min., use supplemental pages as necessary to record sensor temperatures.				
Stop Conditioning				

Datasheet 2.1 – Page 2

Page 3

PETERSEN INCORPORATED "A Winning Combination."	Procedure Number: Revision Number: Revision Date: Page:	JSP-7953-01 1 08/31/09 27 of 36

Test Records

58.6°F	9·30·09 1:10 P.M.
Ambient Temperature (°F)	Test Date (mm/dd/yy) and Test Time (hh:mm)
30' 1"	89.8°
Measured Drop Test Height (in.)	Measured Longitudinal Angle (0° = horizontal)

Post-Test Records

Record Residual Height of End Impact Limitor and Damage to the Test Article Exterior Using the Space Below	Record Additional Comments Below or on a Separate Page
REFER TO APPENDIX "C" OF THE POST TEST SUMMARY REPORT.	REFER TO SECTION III OF THE POST TEST SUMMARY REPORT.

Test Engineer and Witness Records

Test Engineer Signature	Printed Name	Date
[signature]	BART ANDERSON	11·10·09

Witness Signature	Printed Name	Date
[signature]	JOE G. DANIEL	11·10·09

Datasheet 2.1 – Page 3

Graph of Temperature Conditioning Test #1 – Cold Cycle

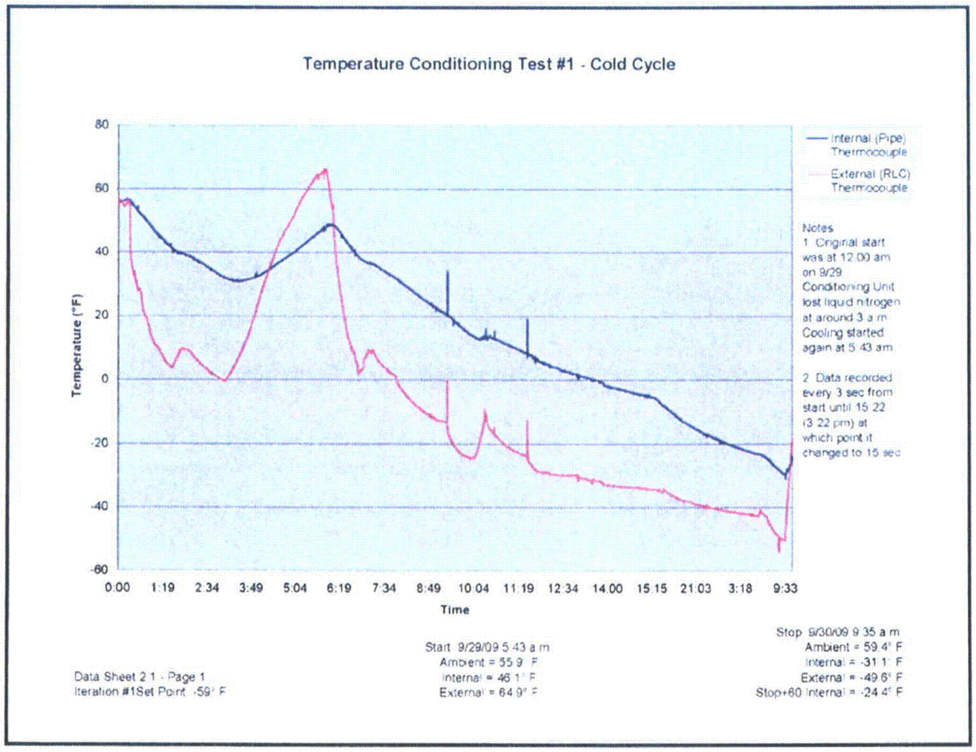

Graph of Cold End Drop Test Temperature Conditioning

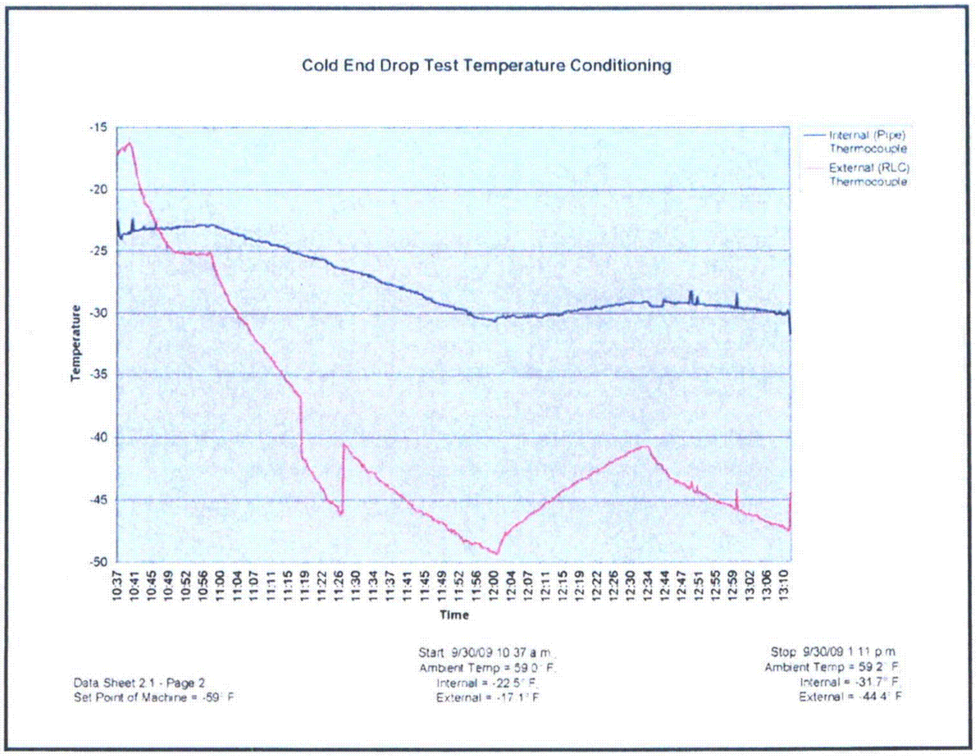

End Limiter #1 – Post Cold End Drop Inspection

END LIMITER #1 - POST COLD END DROP INSPECTION

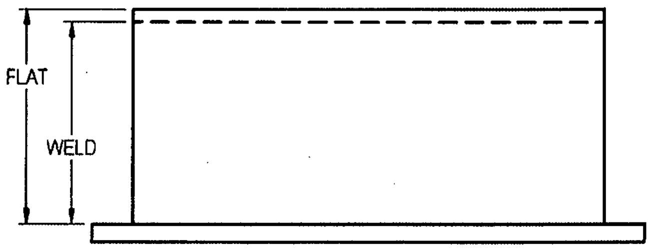

0° - FLAT = 11 3/4", WELD = 11 3/8"
90° - FLAT = 11 3/4", WELD = 11 3/8"
180° - FLAT = 11 3/4", WELD = 11 3/8"
270° - FLAT = 11 3/4", WELD = 11 3/8"

NOTES:
1. "FLAT" REFERS TO THE DIMENSION FROM "CRUSHED END" TO BASE PLATE.
2. "WELD" REFERS TO THE DIMENSION FROM "CRUSHED WELD AREA" TO BASE PLATE.
3. PRIOR TO DROP THE "FLAT" DIMENSION WAS 12"-12 1/16" AS PER DRAWING REQUIREMENT.

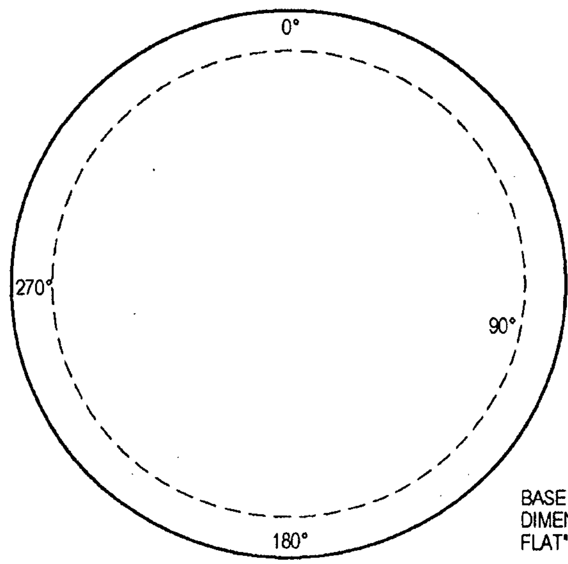

BASE PLATE WAS FLAT PRIOR TO DROP TEST. DIMENSIONS ARE FOR BASE PLATE "OUT OF FLAT" POST DROP.

0° = .280"
90° = .284"
180° = .315"
270° = .354"

Appendix D – DATA SHEET 2.2 – Test #2, 30-Foot Side Drop (Cold)

Page 1

PETERSEN INCORPORATED "A Winning Combination."	Procedure Number: Revision Number: Revision Date: Page:	JSP-7953-01 1 08/31/09 28 of 36

DATA SHEET 2.2 – Test #2, 30-Foot Side Drop (Cold)

Final Conditioning Iteration Set Point (°F)	Date & Time (mm/dd/yy & hh:mm)	Ambient Temp. (°F)	Internal Sensor (°F)	External Sensor (°F)
Start Conditioning				
Start +30 min.				
Start +60 min.				
Start +90 min.				
Start +120 min.				
Start +150 min.				
Start +180 min.				
Start +210 min.				
Start +240 min.				
Start +270 min.				
Start +300 min.				
Start +330 min.				
Start +360 min.				
Start +390 min.				
Start +420 min.				
Start +450 min.				
Start +480 min.				
Start +510 min.				
Start +540 min.				
Start +570 min.				
Start +600 min.				
Note: If time to reach final conditioning set-point is greater than +600 min., use supplemental pages as necessary to record sensor temperatures.				
Stop Conditioning				

SEE ATTACHED CHART.

Datasheet 2.2 – Page 1

Page 2

PETERSEN INCORPORATED "A Winning Combination."	Procedure Number: Revision Number: Revision Date: Page:	JSP-7953-01 1 08/31/09 29 of 36

Test Records

64.4°F	9.30.09 6:56 P.M.
Ambient Temperature (°F)	Test Date (mm/dd/yy) and Test Time (hh:mm)
30'1"	.5°
Measured Drop Test Height (in.)	Measured Longitudinal Angle (0° = horizontal)

Post-Test Records

Record Residual Height of Side Impact Limiters and Damage to the Test Article Exterior Using the Space Below	Record Additional Comments Below or on a Separate Page
REFER TO APPENDIX "D" OF THE POST TEST SUMMARY REPORT.	REFER TO SECTION IV OF THE POST TEST SUMMARY REPORT

Test Engineer and Witness Records

[signature]	BART ANDERSON	11.10.09
Test Engineer Signature	Printed Name	Date
[signature]	JOE G. DANIEL	11.10.09
Witness Signature	Printed Name	Date

Datasheet 2.2 – Page 2

Graph of Cold Side Drop Test Temperature Conditioning

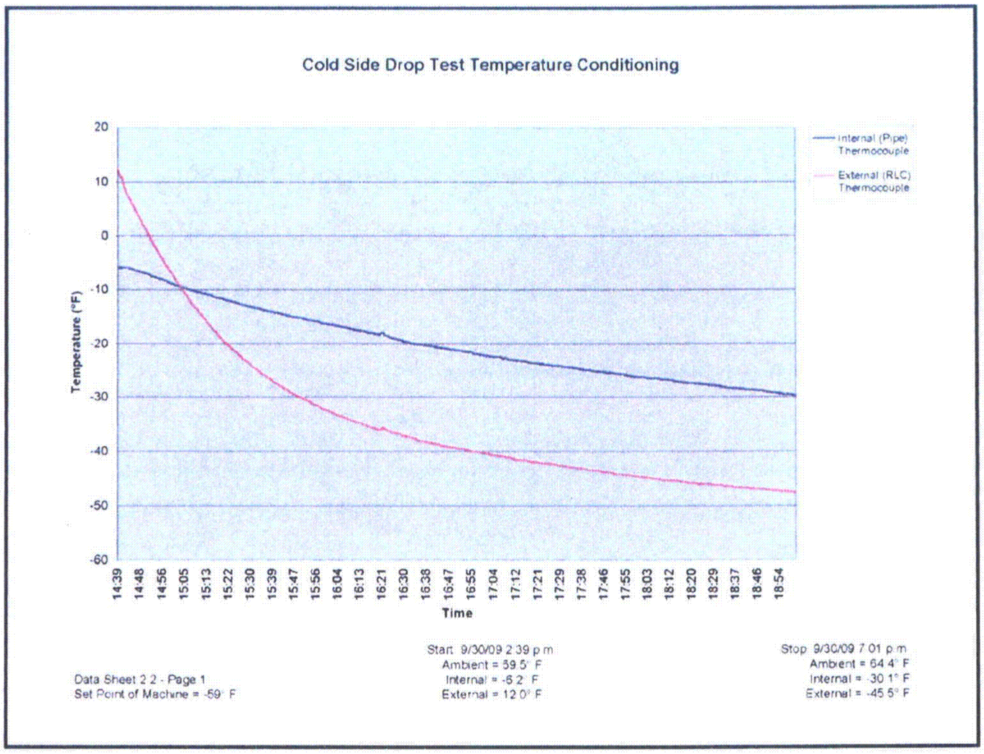

NS30 #1 – Cold Drop Side Limiter Inspection

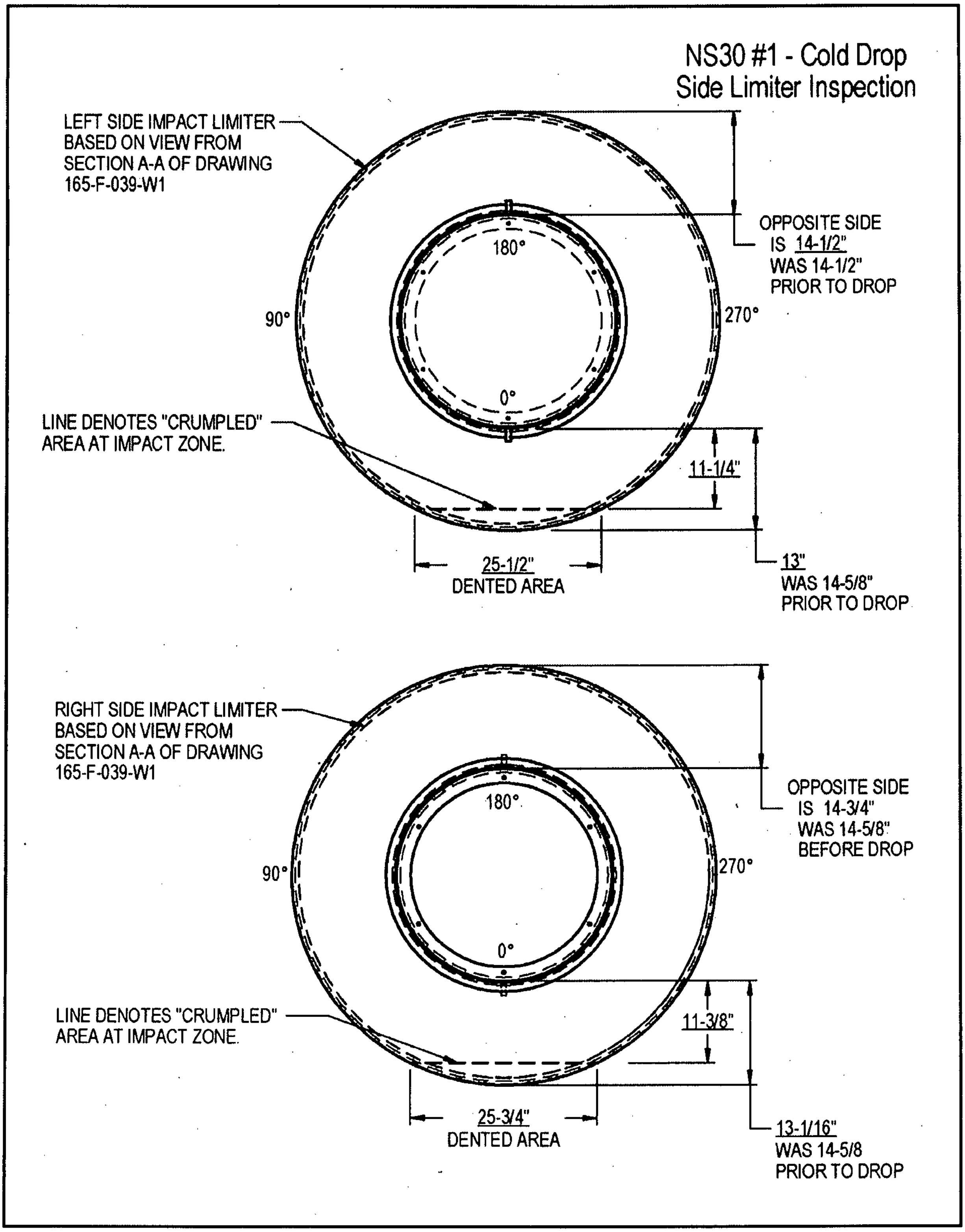

Appendix E – DATA SHEET 2.3 – Tests #1 & #2, 30-Foot Drops (Cold)

Page 1

PETERSEN INCORPORATED "A Winning Combination."	Procedure Number: Revision Number: Revision Date: Page:	JSP-7953-01 1 08/31/09 30 of 36

DATA SHEET 2.3 – Tests #1 & 2, 30-Foot Drops (Cold)

Post-Test Records

Record Visible Damage of Top and Bottom End Cap Assembly to Body Interfaces Using the Space Below	*Record Additional Comments Below or on a Separate Page*
REFER TO APPENDIX "E" AND SECTION V OF THE POST TEST SUMMARY REPORT.	
Record Visible Damage of Top End Cap, Bottom End Cap, and Body Using the Space Below	*Record Additional Comments Below or on a Separate Page*

Test Engineer and Witness Records

[signature]	BART ANDERSON	11·10·09
Test Engineer Signature	Printed Name	Date
[signature]	Joe G. Daniel	11·10·09
Witness Signature	Printed Name	Date

CDX Grade Plywood Post Cold Drop Inspection

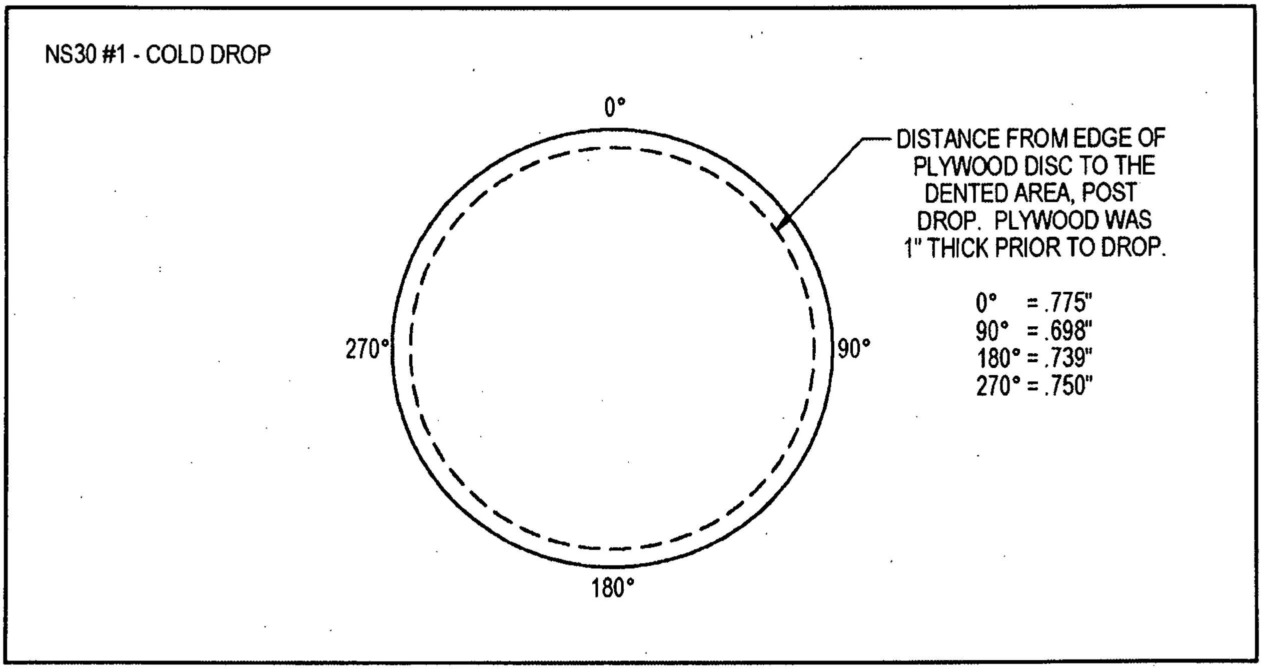

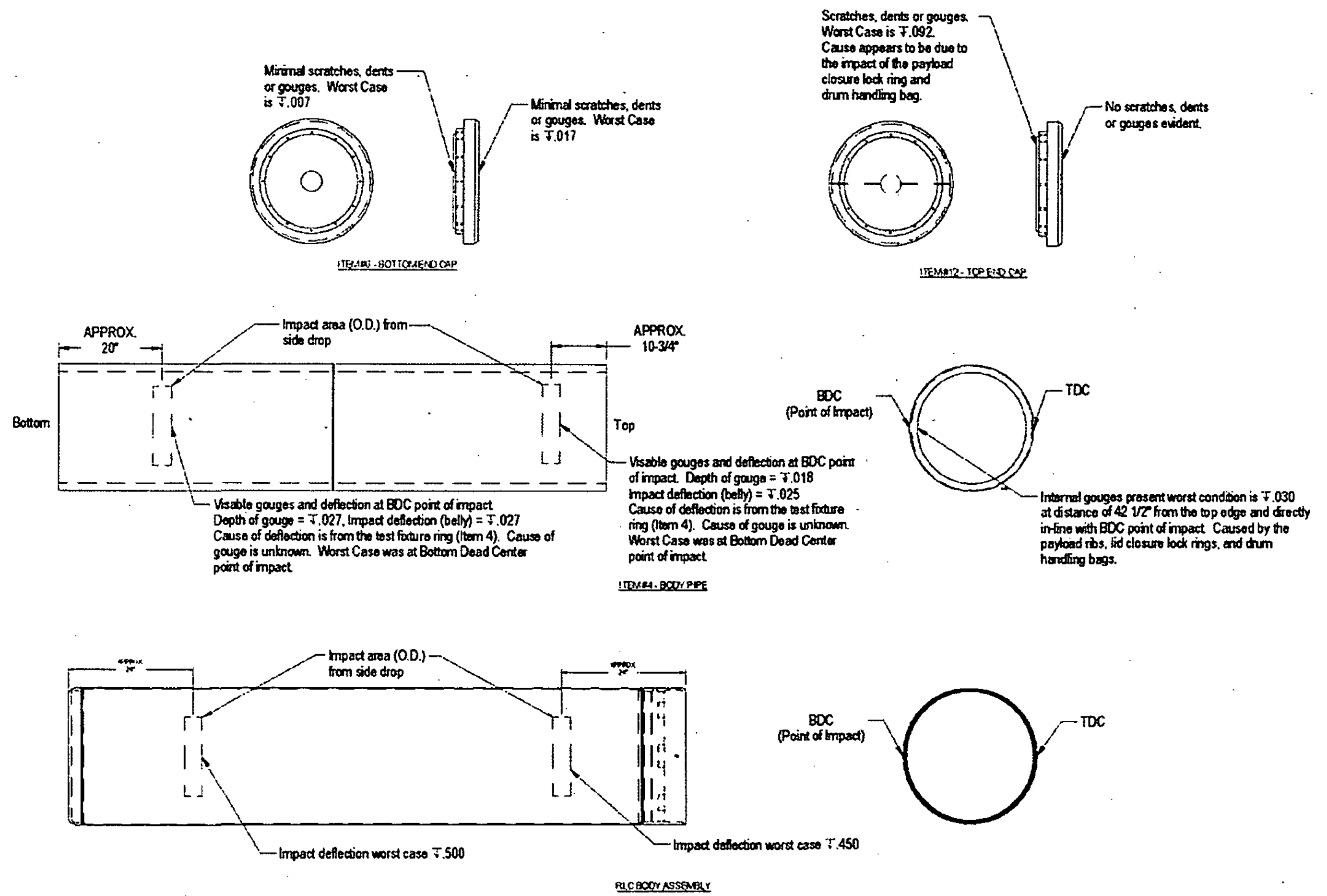

NS30 #1 - COLD DROP

Appendix F – DATA SHEET 2.4 – Test #3, 30-Foot End Drop (Hot)

Page 1

PETERSEN INCORPORATED "A Winning Combination."		
	Procedure Number:	JSP-7953-01
	Revision Number:	1
	Revision Date:	08/31/09
	Page:	31 of 36

DATA SHEET 2.4 – Test #3, 30-Foot End Drop (Hot)

Pre-Test Records				
Conditioning Iteration #_____ Set Point _____(°F)	Date & Time (mm/dd/yy & hh:mm)	Ambient Temp. (°F)	Internal Sensor (°F)	External Sensor (°F)
Start Conditioning				
Start +30 min.				
Start +60 min.				
Start +90 min.				
Start +120 min.				
Start +150 min.				
Start +180 min.				
Start +210 min.				
Start +240 min.				
Start +270 min.				
Start +300 min.				
Start +330 min.				
Start +360 min.				
Start +390 min.				
Start +420 min.				
Start +450 min.				
Start +480 min.				
Start +510 min.				
Start +540 min.				
Start +570 min.				
Start +600 min.				
Note: If time to reach conditioning set-point is greater than +600 min., use supplemental pages as necessary to record sensor temperatures.				
Stop Conditioning				
Stop +10 min.				
Stop +20 min.				
Stop +30 min.				
Stop +40 min.				
Stop +50 min.				
Stop +60 min.				
Stop +70 min.				
Stop +80 min.				
Stop +90 min.				
Stop +100 min.				
Stop +110 min.				
Stop +120 min.				
Note: If additional conditioning iterations with higher set-point are required to achieve internal temperature > 150 °F at the end of the 'X' dwell period, use supplemental pages as necessary to record sensor temperatures.				

SEE ATTACHED CHART.

SEE ATTACHED CHART.

Datasheet 2.4 – Page 1

Page 2

PETERSEN INCORPORATED "A Winning Combination."	Procedure Number:	JSP-7953-01
	Revision Number:	1
	Revision Date:	08/31/09
	Page:	32 of 36

Final Conditioning Iteration Set Point ______(°F)	Date & Time (mm/dd/yy & hh:mm)	Ambient Temp. (°F)	Internal Sensor (°F)	External Sensor (°F)
Start Conditioning				
Start +30 min.				
Start +60 min.				
Start +90 min.				
Start +120 min.				
Start +150 min.				
Start +180 min.				
Start +210 min.				
Start +240 min.				
Start +270 min.				
Start +300 min.				
Start +330 min.				
Start +360 min.				
Start +390 min.				
Start +420 min.				
Start +450 min.				
Start +480 min.				
Start +510 min.				
Start +540 min.				
Start +570 min.				
Start +600 min.				
Note: If time to reach final conditioning set-point is greater than +600 min., use supplemental pages as necessary to record sensor temperatures.				
Stop Conditioning				

SEE ATTACHED CHART.

Datasheet 2.4 – Page 2

Page 3

PETERSEN INCORPORATED "A Winning Combination."	Procedure Number: Revision Number: Revision Date: Page:	JSP-7953-01 1 08/31/09 33 of 36

Test Records

58.8°F	10·5·09 9:46 A.M.
Ambient Temperature (°F)	Test Date (mm/dd/yy) and Test Time (hh:mm)
30'1"	89.9°
Measured Drop Test Height (in.)	Measured Longitudinal Angle (0° = horizontal)

Post-Test Records

Record Residual Height of End Impact Limiter and Damage to the Test Article Exterior Using the Space Below	Record Additional Comments Below or on a Separate Page
REFER TO APPENDIX "F" OF THE POST TEST SUMMARY REPORT	REFER TO SECTION VI OF THE POST TEST SUMMARY REPORT.

Test Engineer and Witness Records

[signature]	BART ANDERSON	11·10·09
Test Engineer Signature	Printed Name	Date
[signature]	JOE G. DANIEL	11·10·09
Witness Signature	Printed Name	Date

Datasheet 2.4 – Page 3

Graph of Temperature Conditioning Test #2 – Hot Cycle (iteration #1)

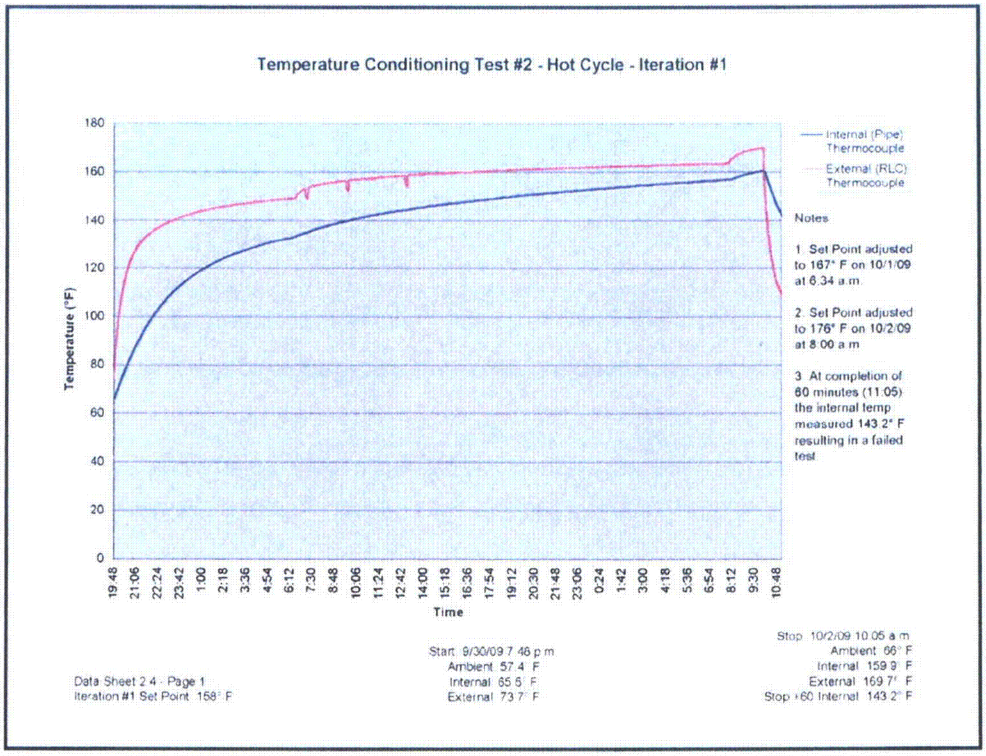

Graph of Temperature Conditioning Test #2 – Hot Cycle (iteration #2)

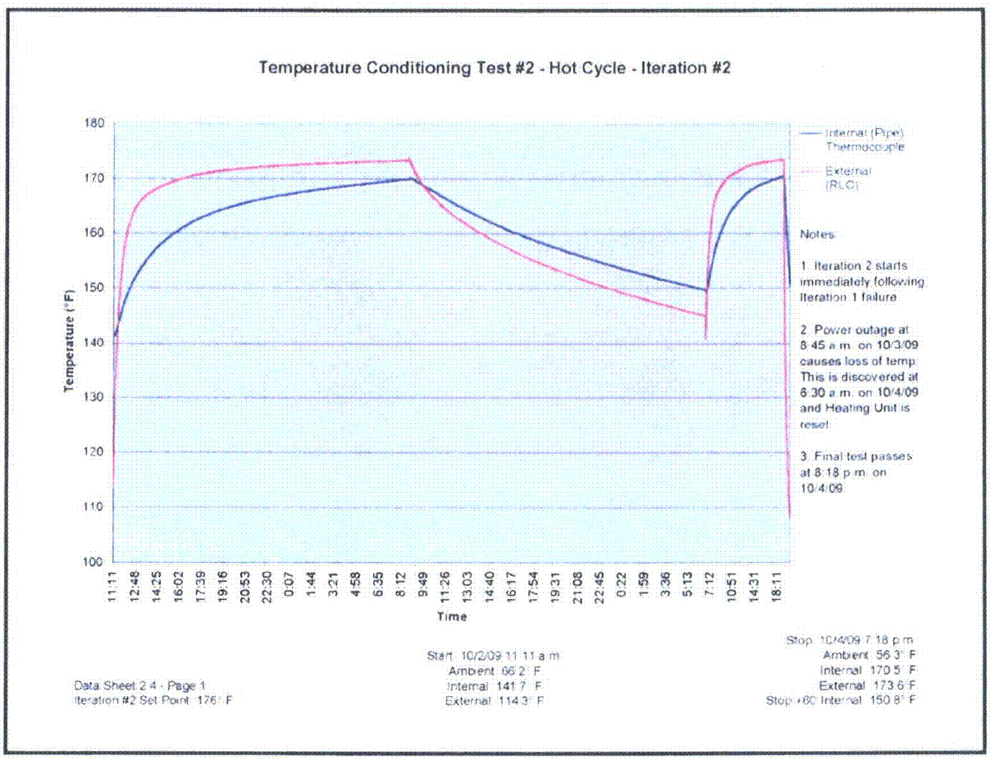

Graph of Hot End Drop Test Temperature Conditioning

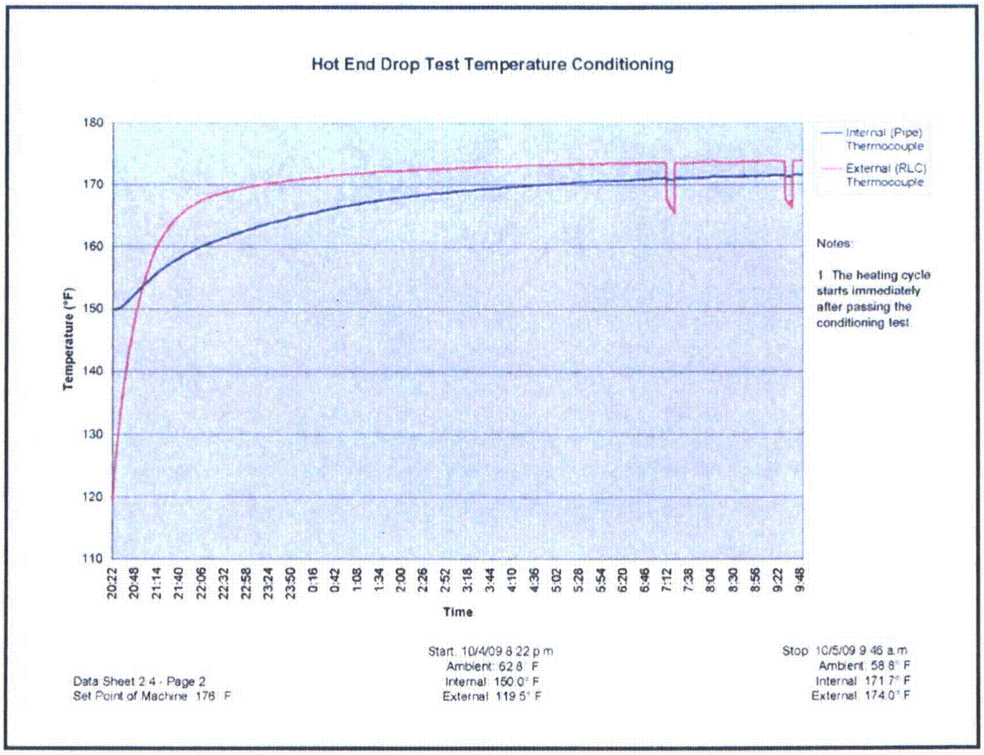

End Limiter #2 – Post Hot End Drop Inspection

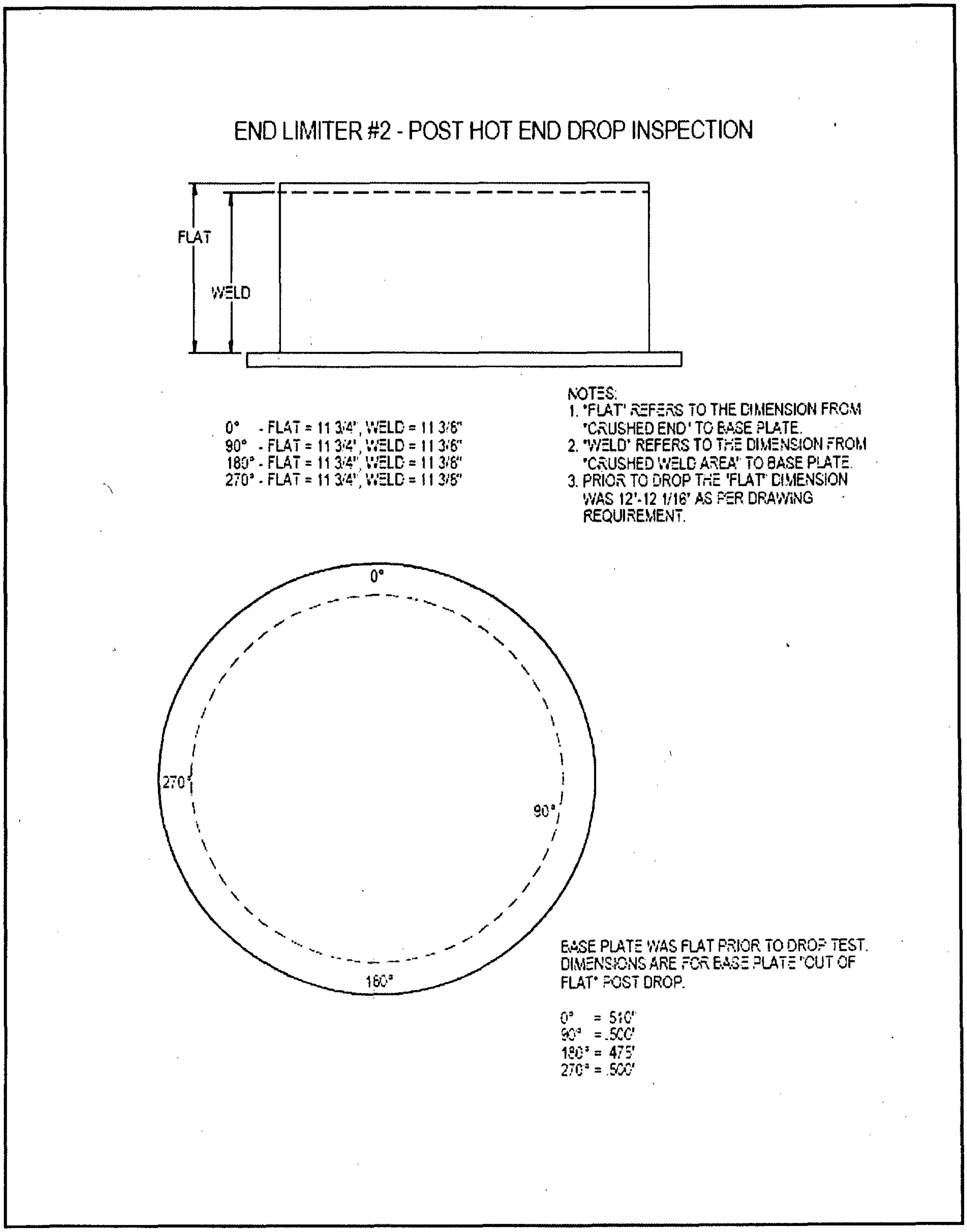

Appendix G –DATA SHEET 2.5 – Test #4, 30-Foot Side Drop (Hot)

Page 1

PETERSEN INCORPORATED "A Winning Combination."	Procedure Number:	JSP-7953-01
	Revision Number:	1
	Revision Date:	08/31/09
	Page:	34 of 36

DATA SHEET 2.5 – Test #4, 30-Foot Side Drop (Hot)

Final Conditioning Iteration Set Point _____(°F)	Date & Time (mm/dd/yy & hh:mm)	Ambient Temp. (°F)	Internal Sensor (°F)	External Sensor (°F)
Start Conditioning				
Start +30 min.				
Start +60 min.				
Start +90 min.				
Start +120 min.				
Start +150 min.				
Start +180 min.				
Start +210 min.				
Start +240 min.				
Start +270 min.				
Start +300 min.				
Start +330 min.				
Start +360 min.				
Start +390 min.				
Start +420 min.				
Start +450 min.				
Start +480 min.				
Start +510 min.				
Start +540 min.				
Start +570 min.				
Start +600 min.				
Note: If time to reach final conditioning set-point is greater than +600 min., use supplemental pages as necessary to record sensor temperatures.				
Stop Conditioning				

SEE ATTACHED CHART.

Datasheet 2.5 – Page 1

Printed copies of this procedure are uncontrolled and are to be used as reference only

Page 2

PETERSEN INCORPORATED "A Winning Combination."	Procedure Number: Revision Number: Revision Date: Page:	JSP-7953-01 1 08/31/09 35 of 36

Test Records

58.1°F	10·6·09 8:22 A.M.
Ambient Temperature (°F)	Test Date (mm/dd/yy) and Test Time (hh:mm)
30'1"	.1°
Measured Drop Test Height (in.)	Measured Longitudinal Angle (0° = horizontal)

Post-Test Records

Record Residual Height of Side Impact Limiters and Damage to the Test Article Exterior Using the Space Below	Record Additional Comments Below or on a Separate Page
REFER TO APPENDIX "G" OF THE POST TEST SUMMARY REPORT.	REFER TO SECTION VII OF THE POST TEST SUMMARY REPORT.

Test Engineer and Witness Records

[signature]	BART ANDERSON	11·10·09
Test Engineer Signature	Printed Name	Date
[signature]	JOE G. DANIEL	11·10·09
Witness Signature	Printed Name	Date

Datasheet 2.5 – Page 2

Graph of Hot Side Drop Test Temperature Conditioning

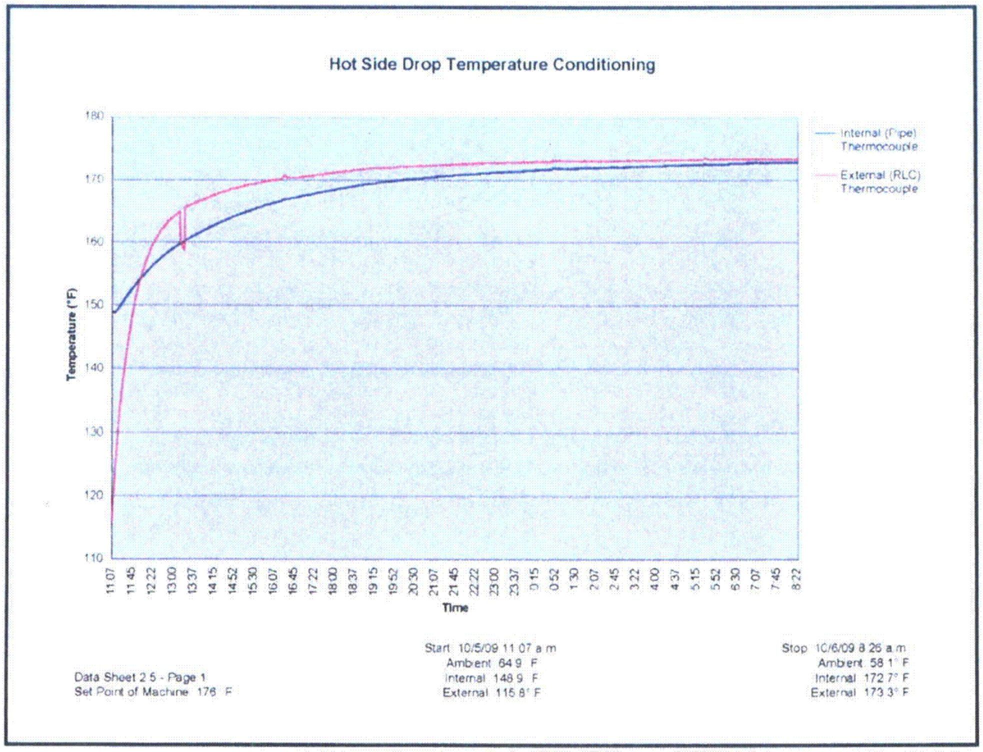

NS30 #2 – Hot Drop Side Limiter Inspection

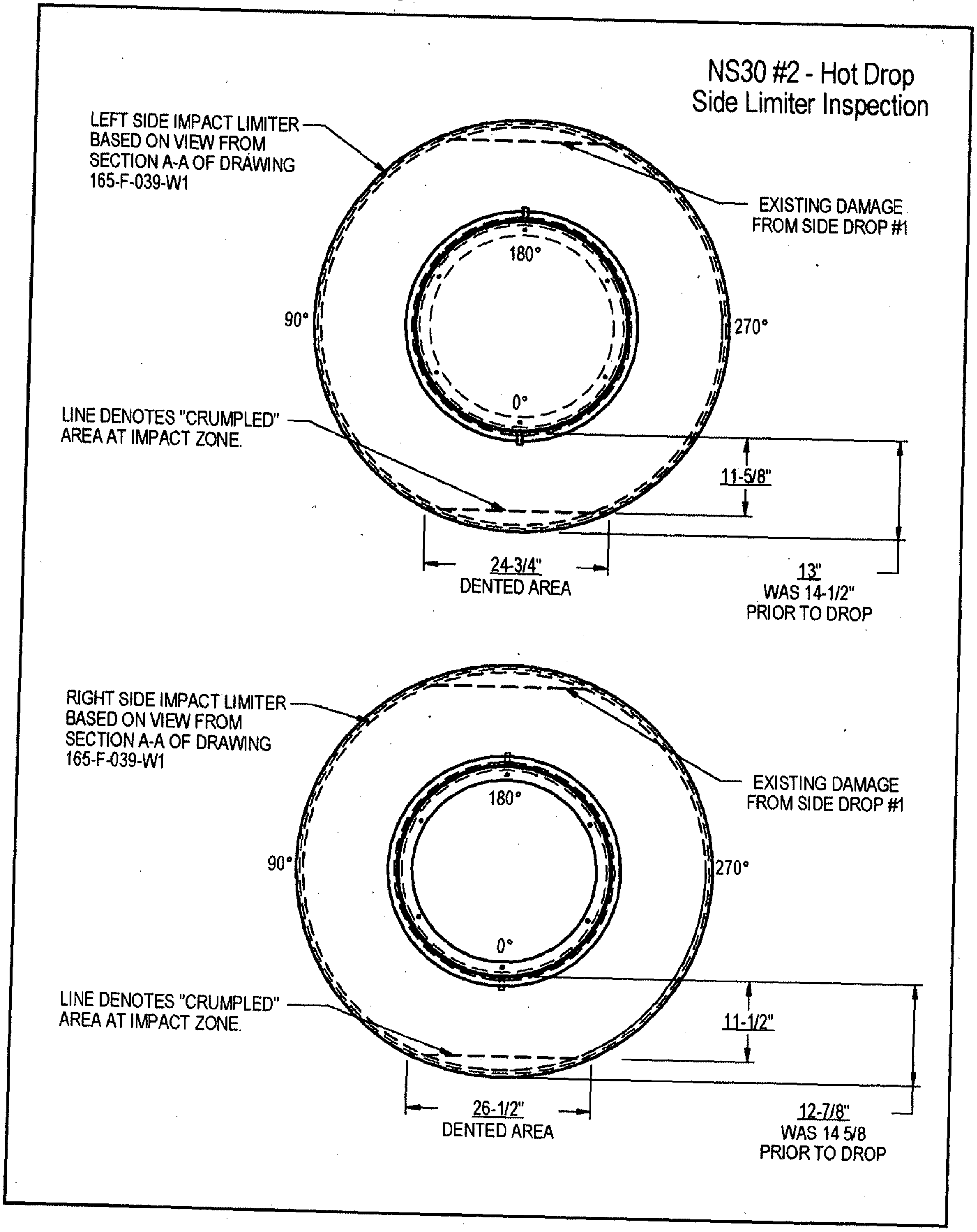

Appendix H – DATA SHEET 2.6 – Tests #3 & #4, 30-Foot Drops (Hot)

Page 1

PETERSEN INCORPORATED "A Winning Combination."	Procedure Number: Revision Number: Revision Date: Page:	JSP-7953-01 1 08/31/09 36 of 36

DATA SHEET 2.6 – Tests #3 & 4, 30-Foot Drops (Hot)

Post-Test Records	
Record Visible Damage of Top and Bottom End Cap Assembly to Body Interfaces Using the Space Below REFER TO APPENDIX "H" AND SECTION VIII OF THE POST TEST SUMMARY REPORT.	Record Additional Comments Below or on a Separate Page
Record Visible Damage of Top End Cap, Bottom End Cap, and Body Using the Space Below	Record Additional Comments Below or on a Separate Page

Test Engineer and Witness Records

[signature]	BART ANDERSON	11-10-09
Test Engineer Signature	Printed Name	Date
[signature]	JOE G. DANIEL	11-10-09
Witness Signature	Printed Name	Date

CDX Grade Plywood Post Hot Drop Inspection

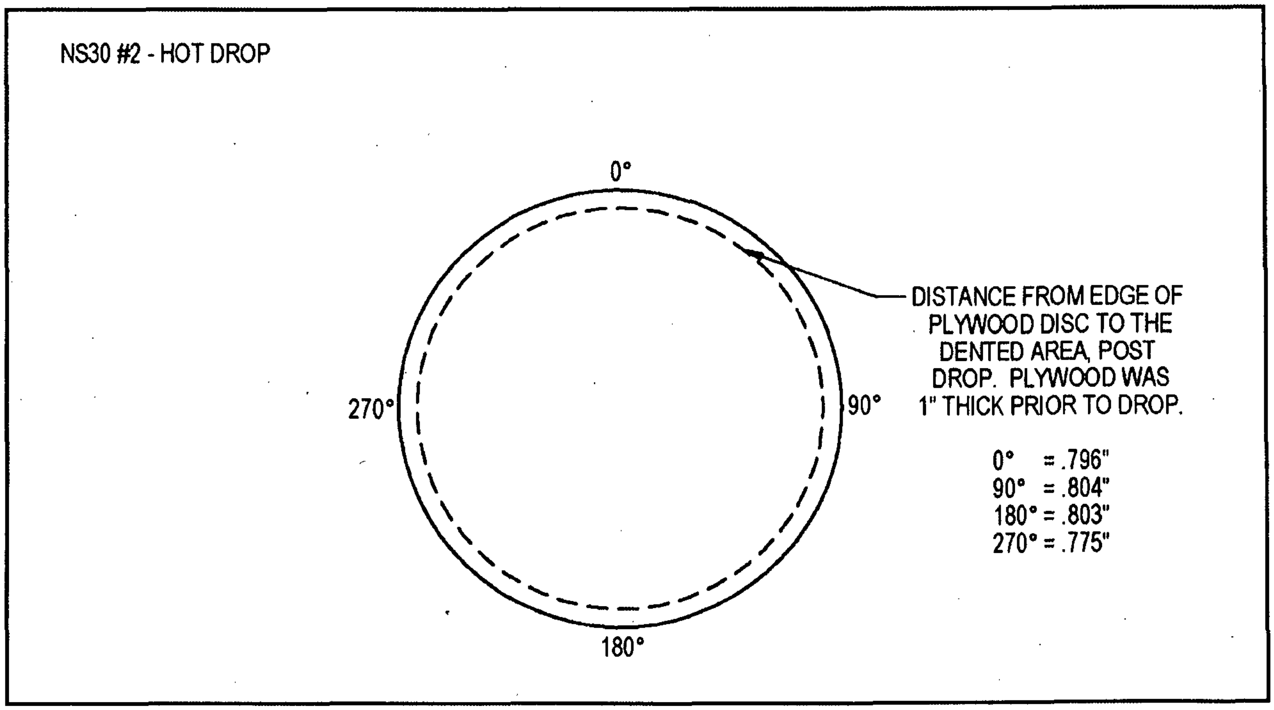

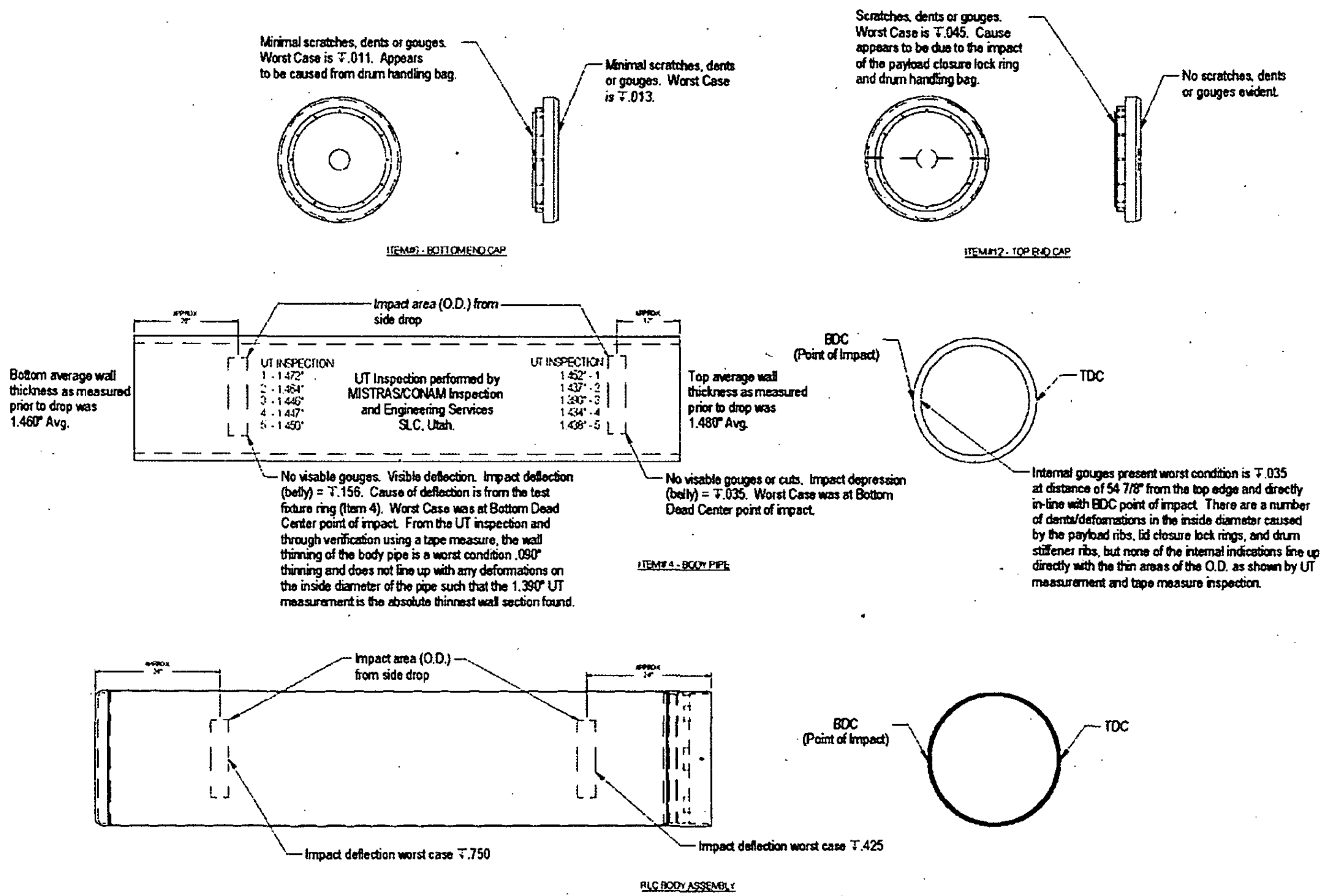

NS30 #2 - HOT DROP

Appendix I – ACCELERATION MEASUREMENTS

End Drop – Raw Data

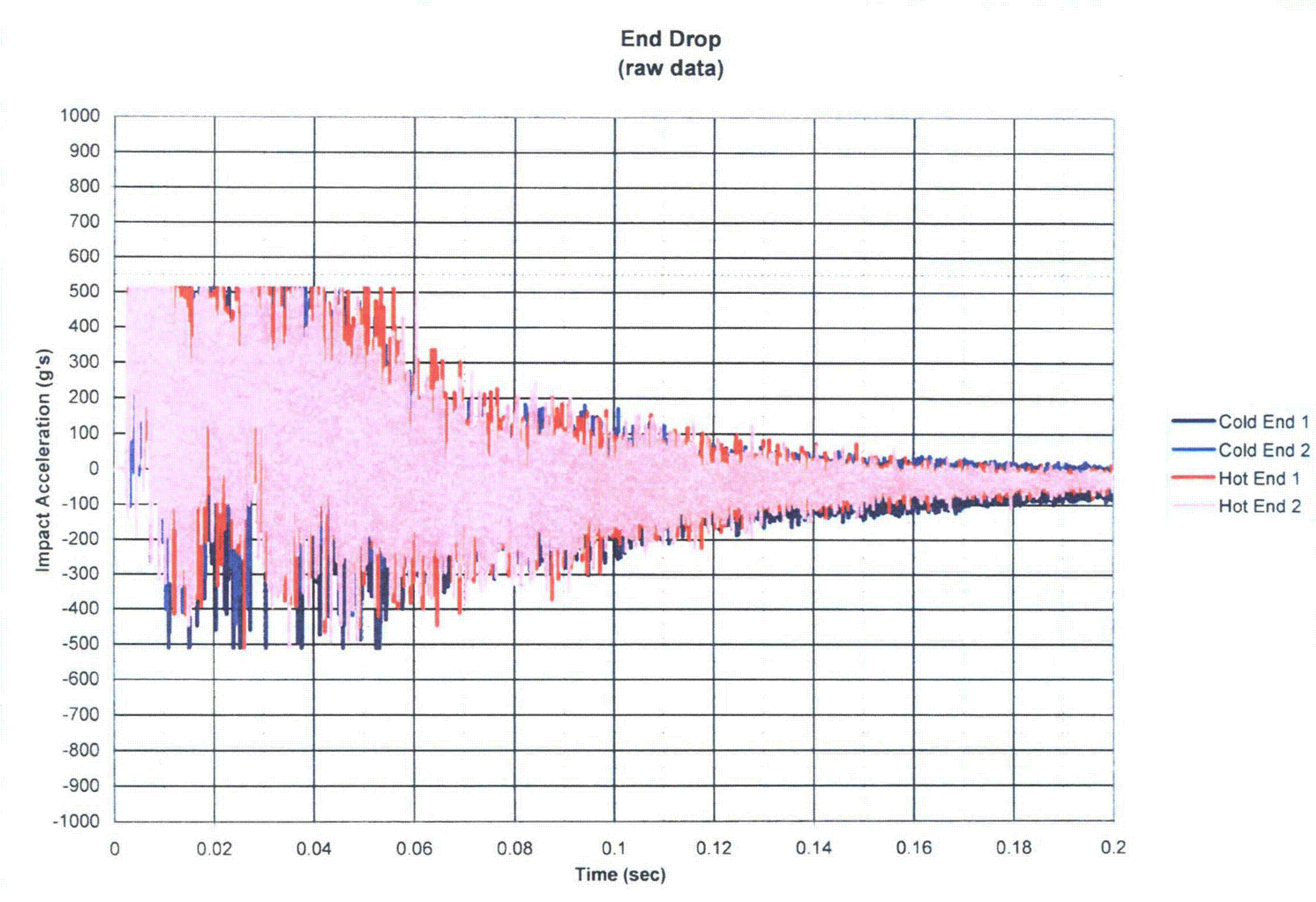

End Drop – Filtered Data

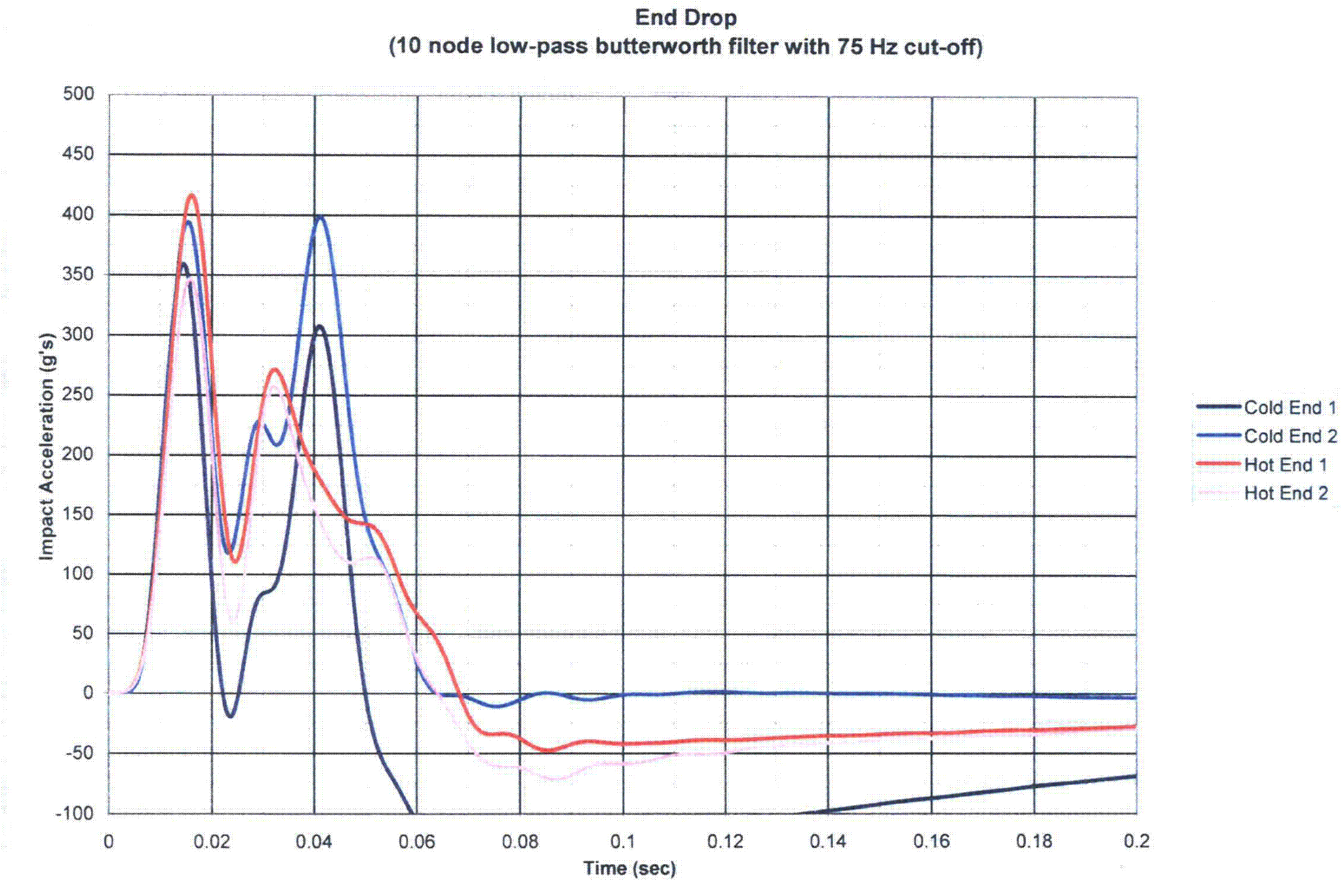

Side Drop – Raw Data

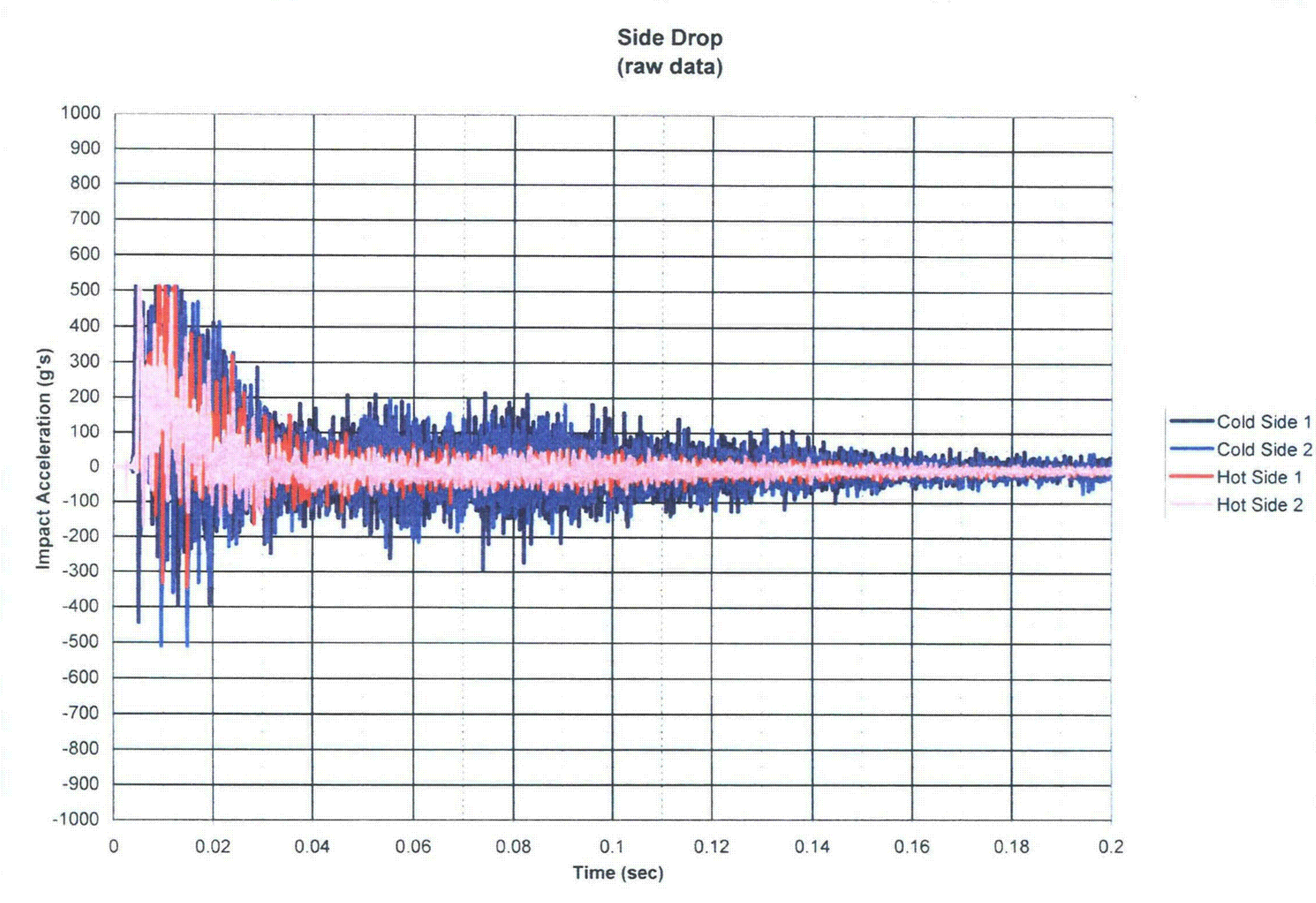

Side Drop – Filtered Data

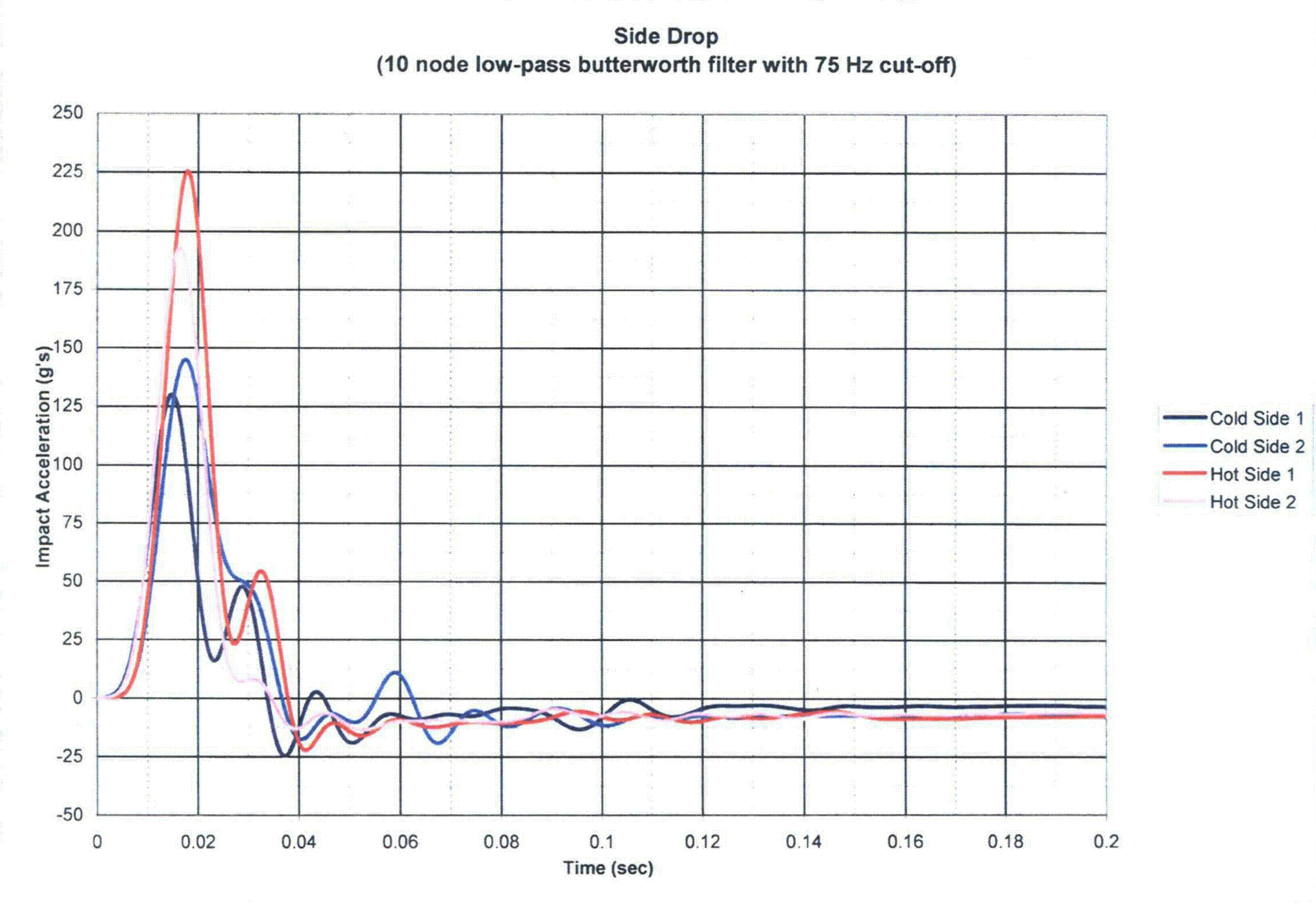

AREVA	AREVA Federal Services LLC
	CALCULATION

Document No: 01937.01.M0005.01-04	**Rev. No:** 0	
Project No: 01937.01.M005.01.00001.100	**Project Name:** RH Technical Support	

Title: Thermal Analysis of RH Shielded Canisters in RH-TRU 72-B Cask

Summary:

The purpose of this calculation is to document the thermal performance of the NS15 and NS30 shielded RH waste canisters in the RH-TRU 72-B packaging. The calculation demonstrates compliance with the applicable regulatory requirements as specified in 10 CFR 71 for Normal Conditions of Transport (NCT) and Hypothetical Accident Conditions (HAC).

Documentum No.: CALC-3002278-000

Software Utilized:	Version:	Storage Media Attached:
Thermal Desktop® & SINDA/FLUINT	5.1	1 CD

REV.	ORIGINATOR Typed / Signature / Date	CHECKED Typed / Signature / Date	APPROVED Typed / Signature / Date
0	GJ Banken GJ Banken 1/29/10	MC Lobo Mark Lobo 1/29/10	GL Clark GL Clark 2/1/10

REVISION HISTORY

REV.	CHANGES
0	Original Issue

TABLE OF CONTENTS

LIST OF FIGURES

LIST OF TABLES

1.0 Introduction

The Remote-Handled Transuranic Waste Shipping Cask (Model No. RH-TRU 72-B) is designed for the safe transport of remote-handled transuranic (RH-TRU) wastes from various sites around the United States. The purpose of this calculation is to document the thermal performance of the alternative NS15 and NS30 shielded RH waste canisters under NCT and HAC conditions when transported within the RH-TRU 72-B packaging. The NS15 and NS30 neutron shield inserts are supplemental internal additions to the RH-TRU waste canister assembly (removable lid design) and provide dose rate attenuation for neutron-emitting RH waste.

This calculation documents the thermal safety basis for adding the NS15 and NS30 neutron shield inserts to the RH-TRU Waste Canister Assembly as an alternative payload configuration for the RH-TRU 72-B packaging. The analysis confirms that the package design complies with all thermal acceptance criteria specified in 10 CFR 71[1].

1.1 Objective

The objectives of this calculation are:

- develop a thermal model of the waste canister assembly with the NS15 and NS30 neutron shield inserts within the existing and approved thermal model of the RH-TRU 72-B packaging,
- determine the combined thermal performance of the shielded canisters and the RH-TRU 72-B packaging under NCT and HAC conditions of transportation and for a variation in the decay heat distribution within the containers, and
- ensure that the RH-TRU 72-B packaging temperatures remain bounded by the previous safety evaluations for NCT and HAC conditions.

1.2 Purpose

The purpose of this calculation is to demonstrate compliance with the applicable regulatory requirements for the NS15 and NS30 shielded canisters as an alternative payload configuration for the RH-TRU 72-B packaging. The applicable regulatory requirements are specified in 10 CFR 71 [1] for Normal Conditions of Transport (NCT) and for Hypothetical Accident Conditions (HAC). Further guidance for the calculation is taken from NUREG-1617 [3] and Regulatory Guide 7.8 [4].

1.3 Scope

The scope of this calculation is limited to the transportation of the NS15 and NS30 shielded canisters, as defined by drawing X-106-503-SNP [5], within the RH-TRU 72-B packaging with a payload decay heat of fifty (50) watts or less.

2.0 Description of Thermal Design

The Remote-Handled Transuranic Waste Shipping Cask (Model No. RH-TRU 72-B) is an existing Type B packaging designed for the safe transport of remote-handled transuranic (RH-TRU) wastes from various sites around the United States. This section presents a description of the RH-TRU 72-B packaging and the payload canisters, their design features, the payload configurations, and the thermal load conditions evaluated.

2.1 Geometry

Design drawings of the RH-TRU 72-B packaging and the standard waste canisters are presented in the RH-TRU 72-B SAR [2]. Design information for the NS15 and NS30 neutron shield inserts is provided by design drawing X-106-503-SNP [5].

2.2 Principal Design Features

2.2.1 RH-TRU 72-B Packaging

The RH-TRU 72-B packaging is composed of an inner vessel which optionally provides an inner containment boundary, an outer cask which provides an outer containment boundary and acts as an environmental barrier, and energy absorbing impact limiters at each end of the outer cask. Polyurethane foam filled energy absorbers (impact limiters) are attached to each end of the outer cask to provide impact and thermal protection under normal and accident conditions of transport. The empty cask weighs approximately 37,000 lbs. Figure 2-1 illustrates an overview of the RH-TRU 72-B package.

The RH-TRU 72-B Cask is designed with a totally passive thermal system. The principal design features of this system consists of an external thermal fire shield surrounding a 4.375-in. cask wall and polyurethane foam impact limiters protecting the ends of the cask body. The fire shield consists of a 10 gauge stainless steel sheet (0.135-in. thick) offset from the outer cask body by a 12 gauge stainless steel wire wrap (0.105-in. diameter) on a 3-in. pitch. The cylindrical outer cask consists of a 1.50-in. thick, 41.13-in. O.D. stainless steel outer shell, a 1.875-in. thick lead shield, and a 1-in. thick, 32.375-in. I.D. stainless steel inner shell. The outer cask bottom end plate is 5-in. thick stainless steel, while the outer cask lid is 6-in. thick stainless steel. The 32-in. O.D. inner vessel of the cask is constructed of 0.375-in. thick stainless steel with a 1.50-in. thick stainless steel bottom end plate and a 6.50-in. thick stainless steel lid. Butyl rubber containment O-ring seals are used on the inner and outer containment boundaries. Impact protection is provided by polyurethane foam impact limiters covering each end of the outer cask. The polyurethane impact limiters also provide thermal protection during the hypothetical accident condition (HAC) fire.

2.2.2 Waste Canisters

The payload of the RH-TRU 72-B cask will consist of one RH waste canister, either a standard or shielded configuration. This calculation addresses only the NS15 and NS30 shielded waste canister configurations. All RH-TRU waste will be loaded directly into the payload canister or into inner containers which are then overpacked within the payload canister. The standard payload canister uses a 26-in. outside diameter 1/4-in. thin-wall cylinder fabricated of carbon or stainless steel as the outer shell. Including a lift pintle at the top of the payload canister, the overall length is 120½ inches. The payload canister is basically a one- or two-piece construction unit (fixed or removable lid versions, respectively, either of which may be configured with a through-pintle fill port and plug) capable of transporting RH-TRU waste.

This calculation addresses the addition of the NS15 and NS30 neutron shield inserts for the RH waste canister as an authorized payload configuration for shipment in the RH-TRU 72-B packaging. The NS15 and NS30 neutron shielded canisters contain supplemental internal neutron shielding components added to the RH-TRU waste canister assembly (removable lid design) and provide dose rate attenuation for neutron-emitting RH waste. The nominal dimensions for the NS30 and NS15 neutron shielded canisters are provided in drawing X-106-503-SNP [5].

The neutron shielding for the NS15 and NS30 neutron shield inserts is fabricated from pipe-grade extra-high molecular weight (EHMW), high density polyethylene (HDPE) plastic with a cell classification of 345444C or greater per ASTM D3350 [17]. The NS15 shield insert body pipe has a nominal wall thickness of 3.387-in. (3.288-in. minimum) and the NS30 shield insert body pipe has a nominal wall thickness of 1.454-in. (1.412-in. minimum). Both the NS15 and NS30 shield insert body pipes have a 24-in. outside diameter and the shield insert end caps have a nominal wall thickness of 5-in. Figure 2-2 illustrates an overview of the NS15 shielded waste canister. The overview of the NS30 shielded canister is similar except for the wall thickness of the shield insert.

2.3 Methodology

The methodology used to conduct the analysis was as follows:

1. The existing thermal models of the RH-TRU 72-B packaging for the transport of paper and metallic wastes under normal conditions of transport (NCT) and hypothetical accident conditions (HAC) were extracted from Reference [2] safety analysis report. Since these thermal models were developed under an earlier version of SINDA/FLUINT, the models were re-run and the results compared to the original results to ensure that the current version of the code produces similar results.
2. A 'solids' based thermal model of the 72-B canisters with the NS15 and NS30 neutron shield inserts was developed using the Thermal Desktop® computer program. The thermal model simulates the entire canister and included representation of the paper and metallic waste configurations, as appropriate, plus the waste containers that hold the waste.
3. A 'cask and impact limiter only' thermal model for NCT and HAC were created from the existing non-graphical, text based thermal models obtained from the Reference [2] safety analysis report by deleting the thermal definitions for the canister and payload contained within each thermal model.
4. A representation of the interior surfaces for the inner vessel (IV) of the 72-B cask was added to the 'solids' modeling of the NS15 and NS30 shielded canisters. This thermal representation of the IV surfaces is used to generate the radiation and conductance tie-ins between the shielded canisters and the cask and impact limiter portions of the RH-TRU 72-B packaging.
5. The combined thermal models of the shielded canisters and the 72-B packaging are then exercised using the SINDA/FLUINT computer program to predict the thermal performance of the shielded canisters within the 72-B packaging.

2.4 Design Basis Thermal Load Conditions

The shielded waste canister and RH-TRU 72-B package combinations are evaluated in accordance with 10 CFR 71 [1] and Regulatory Guide 7.8 [4] for the applicable NCT thermal loads. The load conditions are defined as follows:

- *NCT Hot*: An ambient temperature of 100 °F is used to evaluate the maximum temperatures within the cask with maximum decay heat and 10 CFR §71.71(c)(1) prescribed insolation.
- *NCT Hot, No Solar*: Same as NCT Hot, but without insolation. This case serves as the basis for evaluation of the maximum temperature at the accessible surfaces of the package in accordance with 10 CFR §71.43(g). 10 CFR §71.43(g) stipulates that for exclusive use packages, the maximum accessible surface temperature must be less than 185 °F for this condition.
- *HAC Hot:* Thermal conditions prior to the event are conservatively taken from the *NCT Hot* condition, followed by a thirty-minute transient with an ambient temperature of 1,475 °F with maximum decay heat, and then back to a steady-state ambient temperature of 100 °F with maximum decay heat and insolation per 10CFR71.71(c)(1). This load case evaluates the peak temperature achieved for the various cask components under the HAC fire event and the associated thermal stresses.

Cold environment conditions are not addressed by this evaluation since the minimum temperatures expected within the packaging and payload are bounded by -20 °F and -40 °F uniform temperature conditions established in the RH-TRU 72-B SAR [2].

2.5 Design Basis Thermal Loads

2.5.1 Insolation Loads

Maximum steady-state package temperatures with insolation are determined by using the insolation values delineated in 10 CFR §71.71(c)(1), averaged over 12 hours. This action conservatively bounds the transient thermal response that the payload and internal package components have to a diurnal (i.e., cyclic) solar load. The relatively large thermal mass and the polyurethane foam impact limiters will effectively isolate (i.e., decouples) the thermal response of the internal components from the cyclic variation in insolation heating applied to the outside of the package. To account for self-shading provided by the package surfaces in the horizontal orientation, the projected area of the package curved surfaces is used instead of their full area when calculating the total insolation incident on the package. A solar absorptivity of 0.52 is assumed for the stainless steel surfaces under NCT conditions. The solar absorptivity is increased to 0.8 after the HAC fire event to account for potential soot accumulation on the package surfaces.

2.5.2 Payload Decay Heat

The package payload is assumed to consist of a paper based waste stream with an assumed maximum decay heat loading of 50 watts. The decay heat is assumed to be equally distributed within the waste volume on a volumetric basis. Approximately the same total volume of waste can be accommodated by either canister design/payload definition. The thermal properties of the paper based waste stream are the same as presented in the RH-TRU 72-B SAR [2].

Table 2-1 - Insolation Data per 10CFR71.71(c)(1)

Form and Location of Surface	Total Insolation for a 12-hour Period (g-cal/cm^2)[(1)]
Flat surfaces transported horizontally; base surface	None
Flat surfaces transported horizontally; all other surfaces	800
Flat surfaces not transported horizontally	200
Curved surfaces	400

Notes:

(1) The 12-hour period covers the daylight hours. Insolation for the remaining 12 hours (nights) is zero. The 12-hour insolation values are converted to equivalent 12-hour averaged values for evaluation of package temperatures.

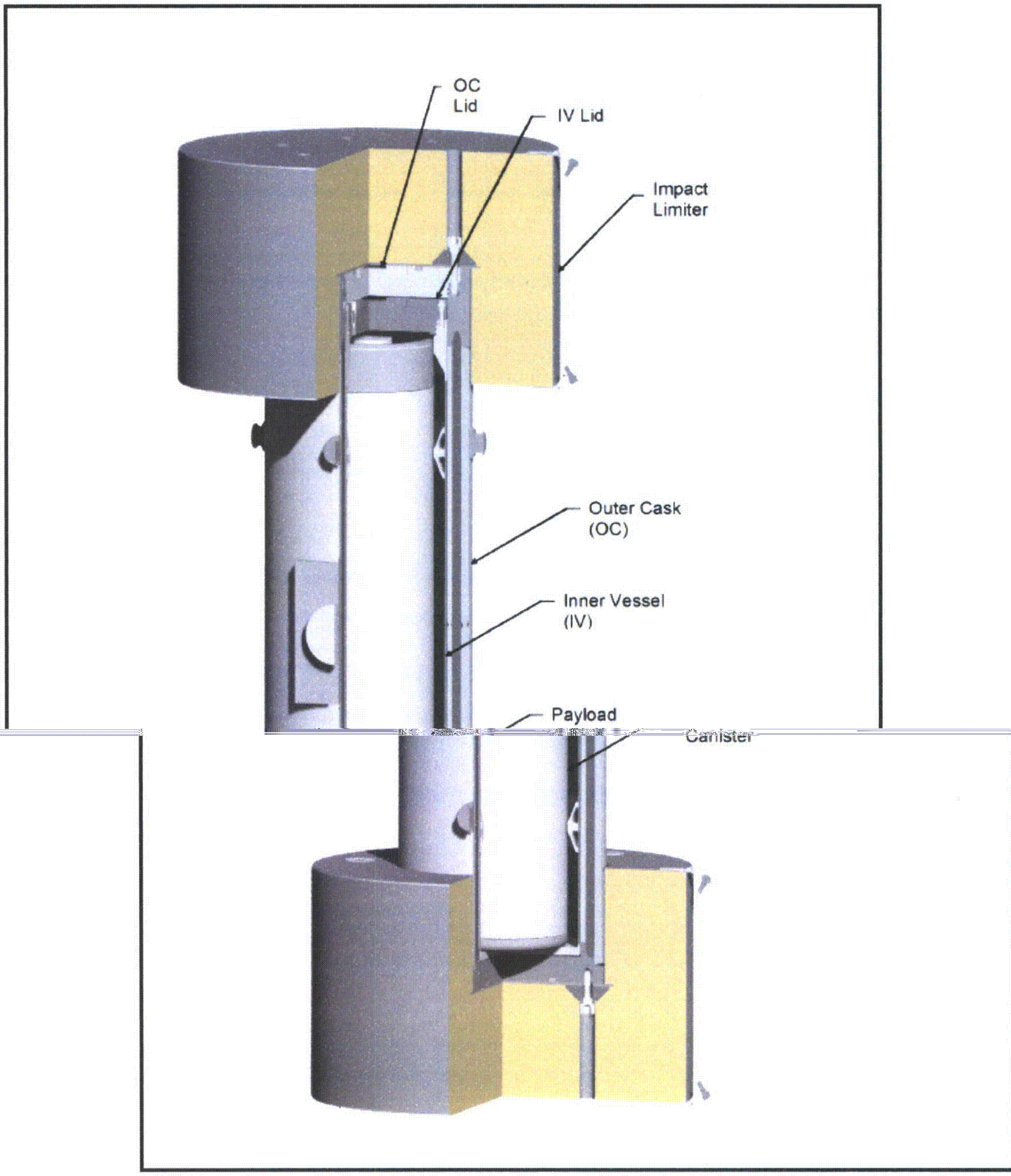

Figure 2-1 - Overview of RH-TRU 72-B Package

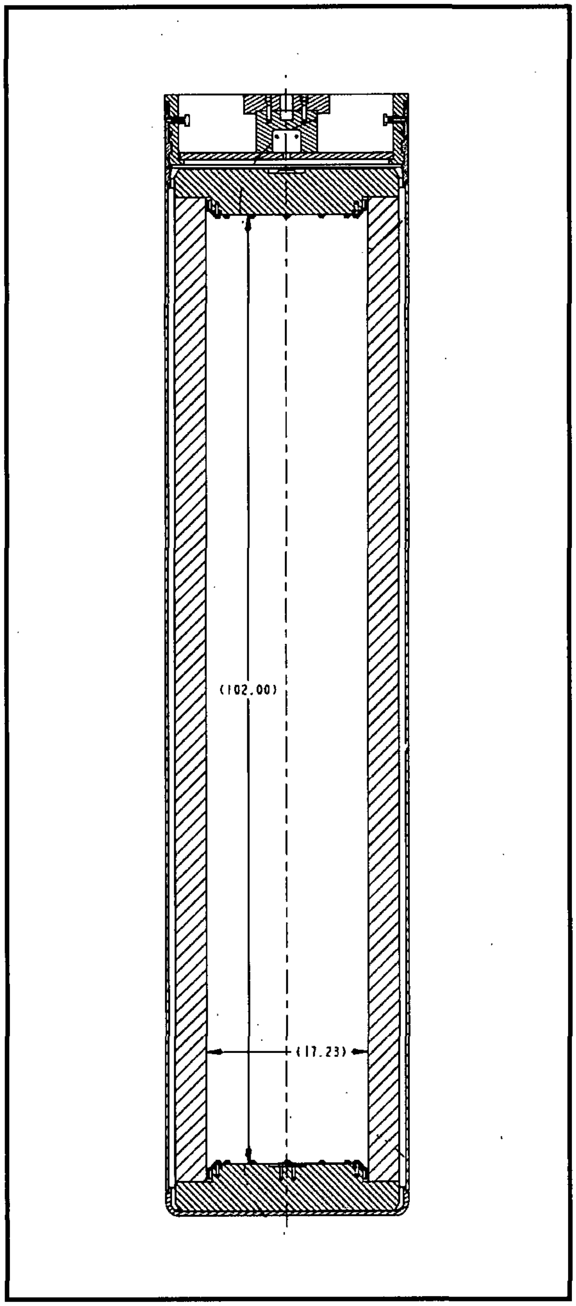

Figure 2-2 - Overview of NS15 Shielded Waste Canister

3.0 Material Specifications

This section presents the thermal properties used in the thermal model of the NS15 and NS30 shielded waste canisters within the RH-TRU 72-B packaging. The RH-TRU 72-B package is fabricated primarily of Type 304 stainless steel, lead, and polyurethane foam. The void spaces within the package are assumed to be filled with air at one atmosphere. Air also fills the gap between the outer cask (OC) outer shell and the thermal shield. The various waste containers to be transported will be constructed of carbon or stainless steel.

The shielded canister shell may be fabricated from carbon or stainless steel. For the purposes of this analysis the shell material is assumed to be ASTM A516 carbon steel since both the higher thermal conductivity and emissivity of carbon steel will bound the canister temperatures achieved under HAC conditions with stainless steel. The shield inserts are fabricated of high density polyethylene (HDPE) material. The void spaces within the waste canisters are assumed to be filled with air at one atmosphere.

3.1 Summary of Thermal Properties

The thermal properties for the RH-TRU 72-B packaging components are documented in the RH-TRU 72-B SAR [2].

The thermal properties of A516 carbon steel assumed for the fabrication of the waste canisters presented in Table 3-1 are taken from Table TCD, material group B, of the ASME Boiler and Pressure Vessel Code [7]. The density of A516 carbon steel is taken from an on-line database [8].

The thermal properties of the HDPE shielding material used for the NS15 and NS30 shield inserts is based on DriscoPlex® pipe material [6] (see product data sheet in Appendix 7.6). The thermal properties of the material presented in Table 3-2 are taken from [9], while its density is obtained from the product datasheet.

The thermal properties for air presented in Table 3-3 are derived from curve fits provided in [10]. Because the thermal conductivity of air varies significantly with temperature, the computer model calculates the thermal conductivity across the various air spaces as a function of the mean film temperature.

The payload within the shielded canisters is conservatively assumed to be paper and to exhibit the thermal conductivity of air in order to bound the potential temperature rise and temperature limit within the payload. This modeling assumption is consistent with the treatment established in the RH-TRU 72-B SAR [2] for paper based payloads.

3.2 Emissivity, Absorption, & Transmittance Data

Table 3-4 presents the surface emissivity assumed for the various surfaces in the shielded canister thermal model. The optical properties are based on the information contained in [11]. The emissivity and solar absorptivity for the RH-TRU 72-B packaging materials are documented in the safety analysis report [2].

3.3 Technical Specification of Components

The materials used in the RH-TRU 72-B package that are considered to be temperature sensitive are the butyl used for the O-ring seals and the polyurethane foam used in the impact limiters.

The RH-TRU 72-B SAR [2] presents the basis for the temperature limitations of the butyl rubber O-ring seals and the polyurethane foam. Per the RH-TRU 72-B SAR, the butyl rubber O-ring seals have an allowable temperature range of -40 °F to 225 °F and a short duration (8 hours) upper temperature limit of 360 °F. The allowable temperature range for the polyurethane foam during impact loadings is -20 °F to 300 °F. Temperature excursions to -40 °F will not permanently degrade the properties of the foam. Foam performance under hypothetical accident condition (HAC) transient conditions is discussed in Section 3.5 of the RH-TRU 72-B SAR [2].

Other package materials are stainless steel and lead. The melting points for these materials are 2,600 °F and 620 °F, respectively. The carbon steel, which may be used in the waste containers and the payload canister, has a melting temperature of approximately 2,750 °F.

The design temperature limit for the HDPE used for the shielded inserts is assumed to be the vicat softening temperature. Per data sheet in Appendix 7.6, the vicat softening temperature for the pipe-grade HDPE considered for this evaluation is 256 °F.

No specific temperature limit exists for the waste payload. Instead, the temperature limit for the waste material is discussed in Appendix 4.6 of the RH-TRU Payload Appendices.

Table 3-1 - Thermal Properties of ASTM A516 Carbon Steel

Temperature (°F)	Density (lb_m/in^3)	Thermal Conductivity (Btu/hr-ft-°F)	Specific Heat (Btu/lb_m-°F)
70	0.284	23.6	0.106
100		23.9	0.110
150		24.2	0.114
200		24.4	0.118
250		24.4	0.121
300		24.4	0.123
400		24.2	0.128

Table 3-2 - Thermal Properties of HDPE

Temperature (°F)	Density (lb_m/in^3)	Thermal Conductivity (Btu/hr-ft-°F)	Specific Heat (Btu/lb_m-°F)
-	0.035	0.25	0.46

Table 3-3 - Thermal Properties of Air

Temperature (°F)	Density lb_m/in^3)	Specific Heat (Btu/lb_m-°F)	Dynamic Viscosity (lb_m /ft-hr)	Thermal Conductivity (Btu/hr-ft-°F)	Prandtl No.	Coef. Of Thermal Exp. (°R^{-1})
-40	Use Ideal Gas Law w/ Molecular wt = 28.966 g/mole	0.240	0.03673	0.0121	Compute as $Pr = c_p\mu / k$	Compute as $\beta = 1/(°F+459.67)$
0		0.240	0.03953	0.0131		
50		0.240	0.04288	0.0143		
100		0.241	0.04607	0.0155		
200		0.242	0.05207	0.0178		
300		0.243	0.05764	0.0199		
400		0.245	0.06286	0.0220		

Table 3-4 - Surface Emissivity

Material	Assumed Conditions	Assumed Emissivity (ε)
Canister Shell (Carbon Steel)	Painted	0.8
HDPE Surfaces	Black	0.85
Inner Waste Containers Shell (Carbon Steel)	Oxidized or painted	0.8

4.0 Thermal Evaluation under Normal Conditions of Transport

This section presents the thermal analysis methodology and the evaluation of the thermal performance for the NS15 and NS30 shielded canisters and the RH-TRU 72-B packaging combination under NCT conditions to demonstrate compliance with the requirements of 10 CFR §71.43(g) and §71.71. The thermal evaluations are performed using conservative analytical techniques to assure that all materials are maintained within their applicable minimum and maximum allowable temperature during all modes of operation.

4.1 Thermal Model for NCT

The analytical thermal model of the shielded canisters within the RH-TRU 72-B packaging are developed for use with the Thermal Desktop® [12] and SINDA/FLUINT [13] computer programs. These programs work together to provide the functions needed to build, exercise, and post-process a thermal model. The SINDA/FLUINT and Thermal Desktop® computer programs have been validated for safety basis calculations for nuclear related projects [14].

The analytical thermal model of the RH-TRU 72-B packaging developed for the RH-TRU 72-B SAR [2] is re-used for the purposes of this calculation. The thermal model is set up as an axisymmetric, lumped-parameter, finite-difference 360° model. Complete details of the cask and impact limiter modeling are provided in the RH-TRU 72-B SAR. A summary description is also provided in Appendix 7.4.1. The NCT thermal evaluations assumed that the package is in its normal horizontal orientation for transportation.

The thermal modeling of the NS15 and NS30 shielded canister payloads are developed using the Thermal Desktop® computer program based on drawing X-106-503-SNP [5]. With the exception of the payload definition and the thickness of the high density polyethylene (HDPE) used for shielding, identical modeling approaches are used for the thermal models for the two canister designs. Approximately 1,270 thermal nodes are used to define and simulate the NS15 canister design and its enclosed payload, while approximately 1,385 thermal nodes are used for the NS30 canister design.

Waste will not be directly loaded into the NS15 shielded canister. Instead, the wasted is assumed to be contained within three (3) approximately 15-gallon waste containers which are then overpacked by the NS15 canister. Three alternative arrangements of the containers within the NS15 canister were examined to determine the sensitivity of the results to the use and placement of dunnage. While the results indicate a general insensitivity to container placement within the canister, the stacking of the three waste containers against the base of the canister was shown to yield a slightly higher payload temperature than the other placement assumptions.

The heat transfer between the various components within the shielded canisters is via radiation and conduction. All void spaces within the canister and cask cavity are assumed to be filled with air at atmospheric pressure.

A similar modeling approach is used for the payload definition for the NS30 canister, except that the waste is assumed to be contained within six (6) approximately 8-gallon containers that, in turn, are housed within three (3) approximately 30-gallon waste containers.

A paper based waste stream is assumed for the payload with a maximum decay heat loading of 50 watts for either canister configuration. The decay heat is assumed to be equally distributed within the waste volume on a volumetric basis. This is the same modeling approach used in the RH-TRU 72-B SAR [2].

Details of the thermal modeling used for the NS15 and NS30 shielded canister configurations are provided in Appendix 7.4.2.

4.2 Heat and Cold

4.2.1 Maximum Temperatures for NCT Conditions

Two ambient conditions are evaluated for NCT conditions: NCT Hot (i.e., 100 °F with regulatory solar averaged over 12 hours) and NCT Hot, No Solar (i.e., 100 °F with no insolation loading). See Section 2.4 for a description of each ambient condition. Table 4-1 presents the resulting package temperatures for the transportation of the NS15 shielded canister, while Table 4-2 presents the same type of results for the NS30 shielded canister. The maximum temperatures seen for the NS15 and NS30 neutron shield inserts are 141 °F and 137 °F, respectively. The temperature levels achieved under NCT conditions demonstrate that all component temperatures for the NS15 and NS30 canister configurations are within their respective limits.

Figure 4-1 illustrates the temperature distribution within the NS15 shielded canister and payload under the NCT Hot condition. The temperature distribution on the left side of the figure includes the waste drums and waste payload, while the illustration on the right side of the figure presents the temperature distribution within the canister shell and the NS15 shield insert only. Figure 4-2 illustrates similar temperature distributions for the NS30 shielded canister.

4.2.2 Minimum Temperatures for NCT Conditions

Cold environment conditions are not addressed by this evaluation since, given sufficient time, the minimum temperatures expected within the packaging and payload are bounded by -20 °F and -40 °F uniform temperature conditions established in the RH-TRU 72-B SAR [2]. These minimum temperature levels are within the allowable temperature limits for all components of the NS15 and NS30 shielded canisters.

4.3 Maximum Normal Operating Pressure

The RH-TRU 72-B package has a design pressure of 150 psig. The major factors affecting the pressure within the sealed IV are:

- Radiolytic gas generation (or consumption),
- Temperature-related pressure change,
- Barometric pressure change,
- Chemical reactions,
- Biological gas generation, and/or
- Thermal decomposition.

The determination of the maximum normal operating pressure (MNOP) is not within the scope of this calculation.

4.4 Evaluation of Package Performance for Normal Conditions of Transport

The combined thermal performance of the NS15 and NS30 shielded RH waste canisters in the RH-TRU 72-B packaging has been evaluated for the applicable NCT conditions of transportation and for a maximum decay heat loading of 50 W within the canisters. The evaluations found that the resulting component temperatures remained within their specified allowable limits for all cases. Further, the computed temperatures for the RH-TRU 72-B packaging components were essentially the same as those predicted in the RH-TRU 72-B SAR [2] for similar ambient conditions. Thus the NS15 and NS30 shielded RH waste canisters will not impact the safety basis of the RH-TRU 72-B packaging.

Table 4-1 - Maximum NCT Temperatures for NS15 Shielded Canister

Location / Component	Temperature (°F) [1]		
	NCT With Insolation	NCT Without Insolation	Allowable Temperature
Waste Centerline	247	225	N/A
NS15 Shield Insert	141	119	256
Canister Shell	133	111	800
IV Shell	128	105	800
IV Void Space Bulk Avg	127	104	N/A
OC Inner Shell	126	103	800
OC Lead Shield	126	103	620
OC Outer Shell	126	103	800
OC Thermal Shield	125	103	2,600
OC Upper Ring Forging	125	102	800
IV O-Ring Seal	125	103	225
OC O-Ring Seal	125	102	225
IV Lid	125	103	800
OC Lid	125	103	800
Impact Limiter Foam	132	104	300
Impact Limiter Shell	133	105	2,600

Table Note: 1) Temperatures assume a total payload decay heat loading of 50 W.

Table 4-2 - Maximum NCT Temperatures for NS30 Shielded Canister

Location / Component	Temperature (°F) [1]		
	NCT With Insolation	NCT Without Insolation	Allowable Temperature
Waste Centerline	234	214	N/A
NS30 Shield Insert	137	115	256
Canister Shell	132	110	800
IV Shell	128	105	800
IV Void Space Bulk Avg	127	104	N/A
OC Inner Shell	126	103	800
OC Lead Shield	126	103	620
OC Outer Shell	126	103	800
OC Thermal Shield	125	103	2,600
OC Upper Ring Forging	125	103	800
IV O-Ring Seal	126	103	225
OC O-Ring Seal	125	103	225
IV Lid	126	103	800
OC Lid	125	103	800
Impact Limiter Foam	132	104	300
Impact Limiter Shell	133	105	2,600

Table Note: Temperatures assume a total payload decay heat loading of 50 W.

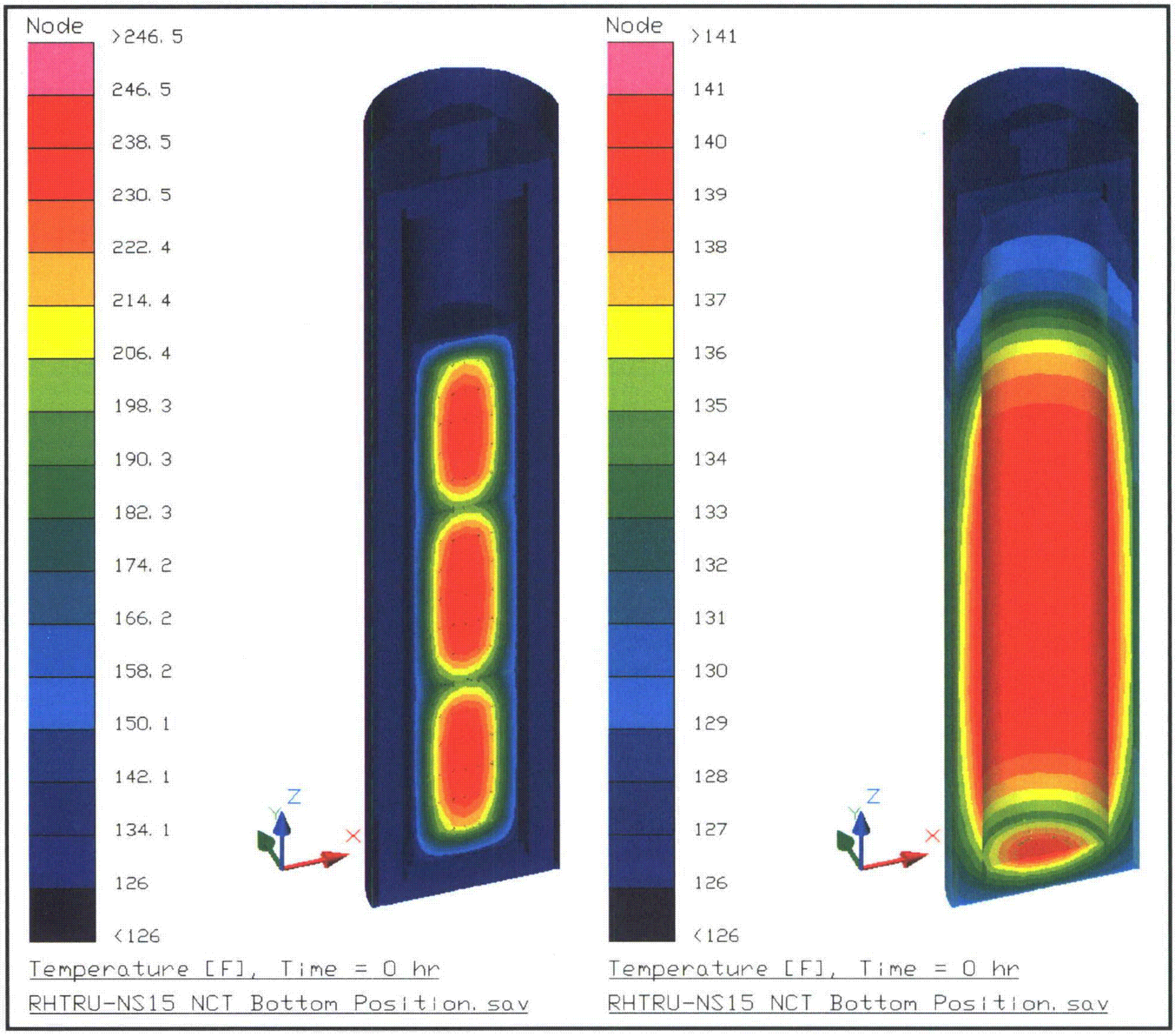

Figure 4-1 - NCT Temperature Distribution within NS15 Shielded Canister

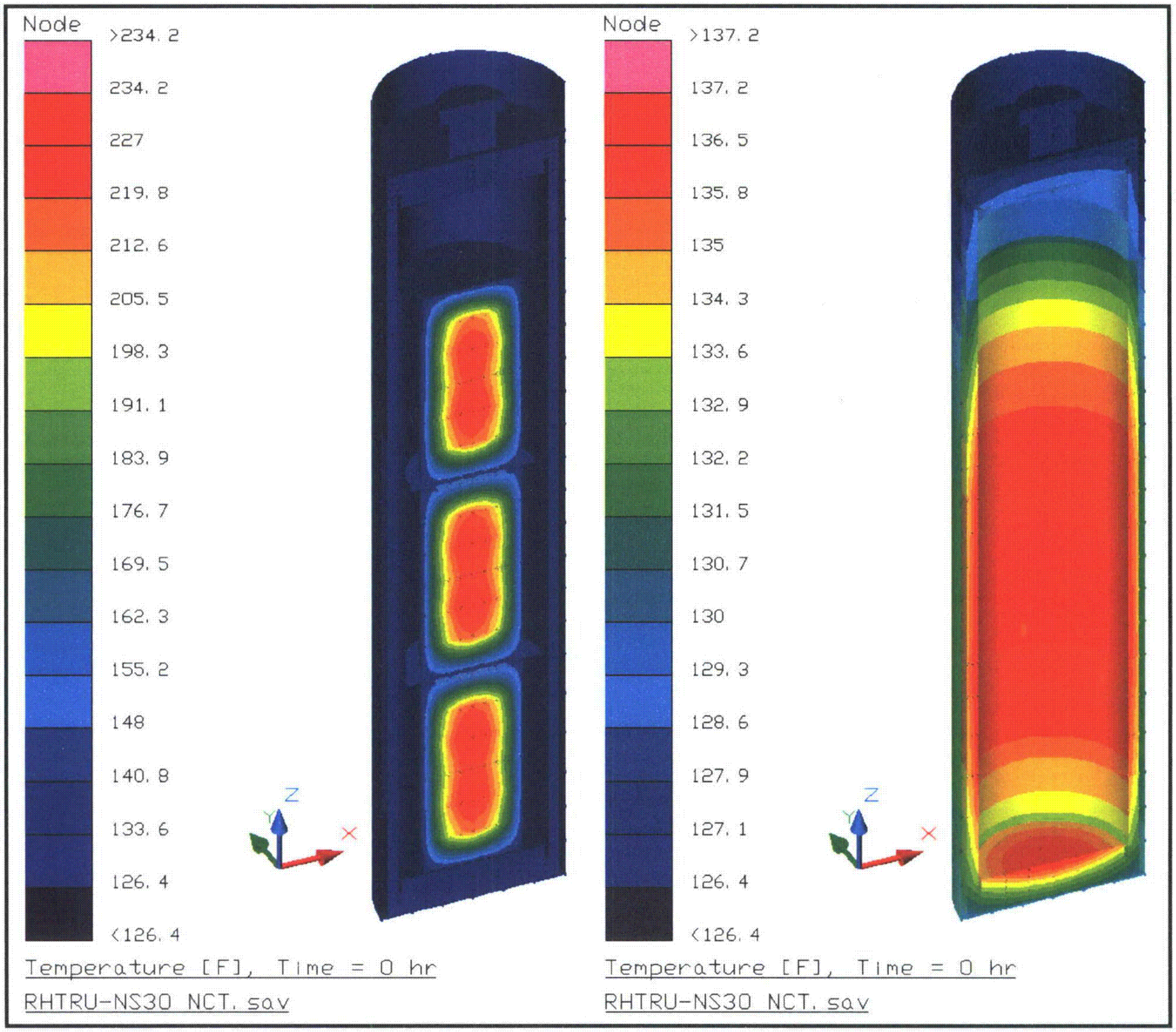

Figure 4-2 - NCT Temperature Distribution within NS30 Shielded Canister

5.0 Thermal Evaluation under Hypothetical Accident Conditions

This section presents the thermal analysis methodology and the evaluation of the thermal performance for the NS15 and NS30 shielded canisters and the RH-TRU 72-B packaging combination under the hypothetical accident condition (HAC) specified in 10 CFR §71.73(c)(4).

5.1 Initial Conditions

The initial conditions assumed for the package prior to the HAC event are described in the RH-TRU 72-B SAR [2]. A summary of the modifications made to the NCT thermal model of the packaging to simulate the assumed package conditions prior to and during the HAC event are as follows:

- The simulated worst-case damage arising from the postulated HAC free and puncture drops were made to the impact limiters. This included reducing the foam thickness to bound the amount of foam lost due to thermal decomposition during the fire event,
- No significant thermal damage is predicted for the RH-TRU 72-B cask body as a result of the free drop events,
- Included credit for the thermal conductance through the wire wrap supporting the thermal shield to maximize the heat flow into the package. This conductance was conservatively ignored for NCT,
- Increased the emissivity of all external surfaces to 0.8 and the solar absorptivity to account for possible oxidation and/or soot accumulation on the surfaces,
- Assumed an initial temperature distribution within the package equivalent to the steady-state conditions with a 100 °F ambient and no insolation.

The RH-TRU 72-B SAR [2] describes the initial conditions and the expected level of damage sustained by the RH-TRU 72-B package from the 10 CFR 71.73 prescribed free and puncture drops. The total gross weight of the loaded NS15 or NS30 shielded canisters is 3,100 lb, or a factor of approximately 2.6 less than the 8,000 lb gross weight for the removable or fixed lid standard payload canisters. As such, the expected level of package damage would be less with an NS15 or NS30 shielded canister payload. Free drop testing of an NS30 shielded canister, which structurally bounds the NS15 shielded canister, in a RH-TRU 72-B surrogate test fixture demonstrated that no significant damage is sustained by the shield insert as a result of the free drop [16]. Therefore, the analytical models of the shielded canisters for NCT condition described in Appendix 7.4.2 are also valid for the HAC evaluation.

5.2 Fire Test Conditions

The fire test conditions analyzed to address the 10 CFR §71.73(c) requirements are as follows:

- The initial ambient conditions are assumed to be 100 °F ambient with no insolation,
- At time = 0, a fully engulfing fire environment consisting of a 1,475 °F ambient with an effective emissivity of 0.9 is used to simulate the average flame temperature of the hydrocarbon fuel/air fire event.

- The convection heat transfer coefficients between the package and the ambient during the 30-minute fire event are based on an average gas velocity of 9 m/sec. Following the 30-minute fire event the convection coefficients are based on still air,
- The ambient condition of 100 °F with insolation is assumed following the 30-minute fire event. A solar absorptivity of 0.8 is assumed for the exterior surfaces to account for potential soot accumulation on the package surfaces.

The transient analysis is continued for 11.5 hours after the end of the 30-minute fire to capture the peak package temperatures. The peak O-ring seal temperatures were determined by extending the transient time period to 24 hours.

5.3 Maximum Temperatures and Pressure

Table 5-1 and Table 5-2 present the predicted maximum temperatures for NS15 and NS30 shielded canister configurations, respectively, under HAC conditions. The results show that all component temperatures remain with allowable limits. The peak temperature of the HDPE shield inserts is seen to remain below the design limit of 256 °F for both configurations. Further, the fact that the canister shell also remains below this temperature level demonstrates that the HDPE temperature limit would not have been exceeded even if direct contact existed between the components.

Figure 5-1 illustrates the temperature response of the RH-TRU 72-B packaging with the NS15 canister payload. A similar response is seen with the NS30 canister. The illustrated temperature response is essentially the same as presented in the RH-TRU 72-B SAR [2]. Figure 5-2 and Figure 5-3 illustrate the temperature response of the NS15 and NS30 canister payloads, respectively.

5.4 Maximum Thermal Stresses

The temperature levels and transient response seen for the NS15 and NS30 canisters under HAC conditions are similar to that seen for the base payload for the RH-TRU 72-B packaging. As such, the thermal stresses presented in the RH-TRU 72-B SAR [2] are also applicable to the NS15 and NS30 canisters.

5.5 Evaluation of Package Performance for Hypothetical Accident Conditions of Transport

The combined thermal performance of the NS15 and NS30 shielded RH waste canisters in the RH-TRU 72-B packaging has been evaluated for the applicable HAC conditions of transportation and for a maximum decay heat loading of 50 W within the canisters. The evaluations found that the resulting component temperatures remained within their specified allowable limits for all cases. Further, the computed temperatures for the RH-TRU 72-B packaging components were essentially the same as those predicted in the RH-TRU 72-B SAR [2] for accident conditions. Thus the NS15 and NS30 shielded RH waste canisters will not impact the safety basis of the RH-TRU 72-B packaging.

Table 5-1 - HAC Temperatures for NS15 Shielded Canister

Location / Component	Temperature (°F) [1]			
	End of Fire	Peak	Post-fire Steady-State	Allowable Temperature
Waste Centerline	225	244	244	N/A
NS15 Shield Insert	119	189	138	256
Canister Shell	113	229	130	800
IV Shell	151	323	125	800
IV Void Space Bulk Avg	284	406	124	N/A
OC Inner Shell	416	488	123	800
OC Lead Shield	527	544	123	620
OC Outer Shell	605	606	123	800
OC Thermal Shield	1,231	1,231	123	2,600
OC Upper Ring Forging	105	159	123	800
IV O-Ring Seal	103	142	123	360/225
OC O-Ring Seal	107	145	123	360/225
IV Lid	105	159	123	800
OC Lid	106	150	123	800
Impact Limiter Foam	N/A	N/A	N/A	N/A
Impact Limiter Shell	1,427	1,427	131	2,600

Table Note 1: Temperatures assume a total payload decay heat loading of 50 W.

Table 5-2 - HAC Temperatures for NS30 Shielded Canister

Location / Component	Temperature (°F) [1]			
	End of Fire	Peak	Post-fire Steady-State	Allowable Temperature
Waste Centerline	214	232	232	N/A
NS30 Shield Insert	115	206	135	256
Canister Shell	113	232	129	800
IV Shell	151	323	125	800
IV Void Space Bulk Avg	284	406	124	N/A
OC Inner Shell	416	488	123	800
OC Lead Shield	527	544	123	620
OC Outer Shell	605	606	123	800
OC Thermal Shield	1,231	1,231	123	2,600
OC Upper Ring Forging	105	160	123	800
IV O-Ring Seal	107	149	123	360/225
OC O-Ring Seal	104	149	123	360/225
IV Lid	109	160	123	800
OC Lid	107	151	123	800
Impact Limiter Foam	N/A	N/A	N/A	N/A
Impact Limiter Shell	1,427	1,427	131	2,600

Table Note 1: Temperatures assume a total payload decay heat loading of 50 W.

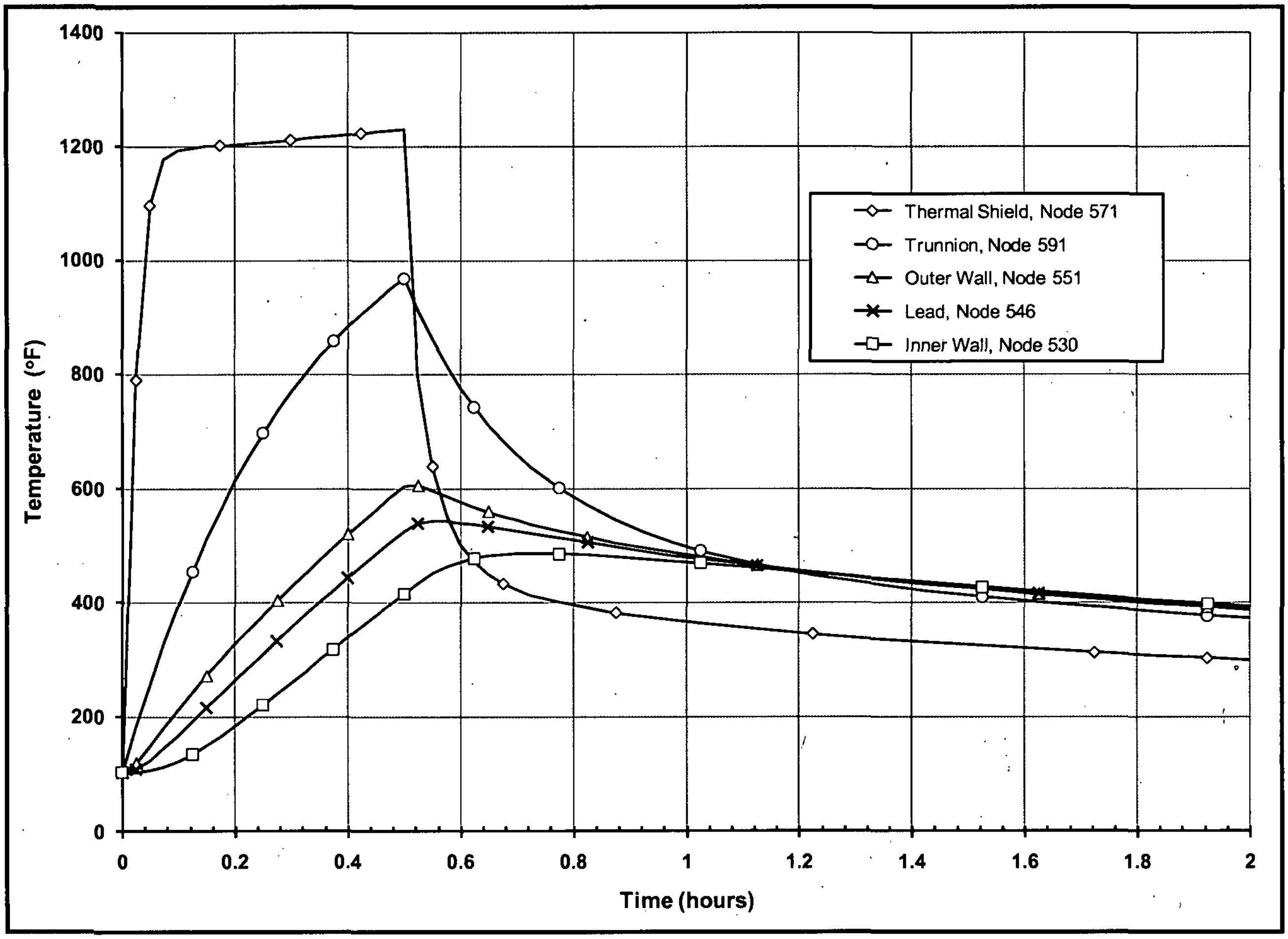

Figure 5-1 - HAC Temperature Response for RH-TRU 72-B Package with NS15 Shielded Canister Payload

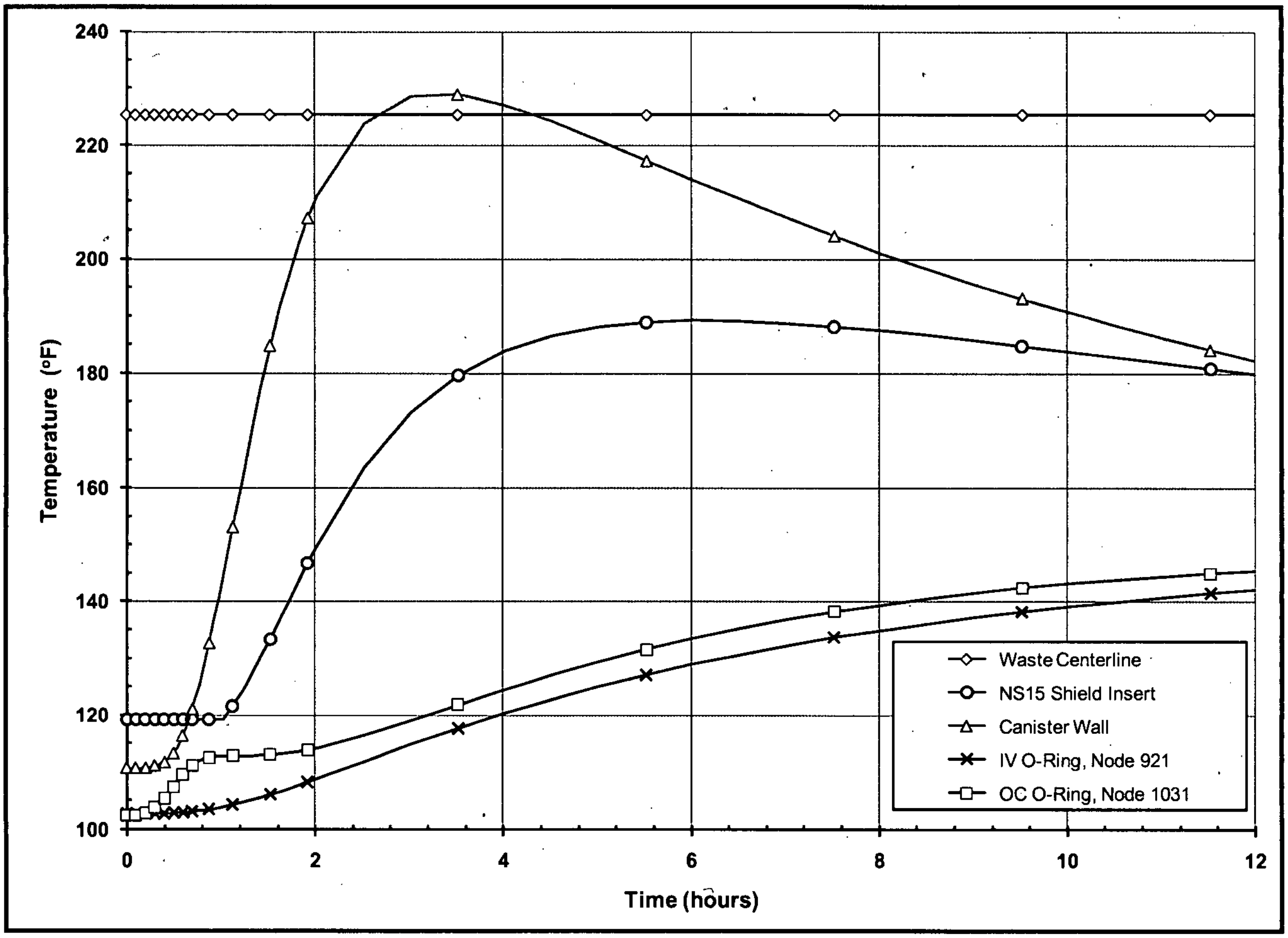

Figure 5-2 - HAC Temperature Response for NS15 Shielded Canister Payload

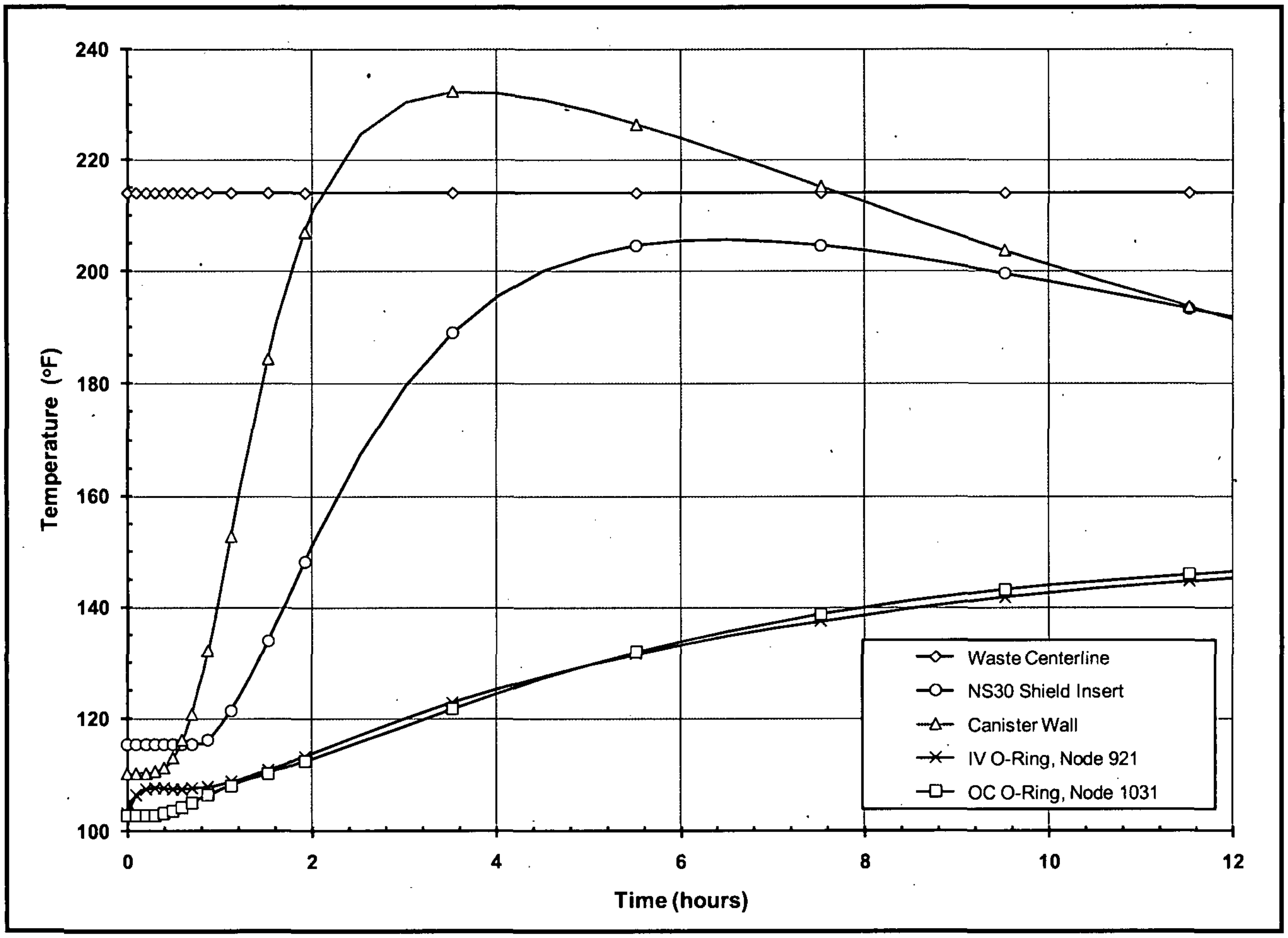

Figure 5-3 - HAC Temperature Response for NS30 Shielded Canister Payload

6.0 Conclusion

The thermal evaluations presented in this calculation demonstrate that both the NS15 and NS30 shielded RH waste canisters with a maximum payload decay heat loading of 50 watts comply with all the thermal acceptance criteria specified in 10 CFR 71[1]. The evaluations were conducted using conservative assumptions and methods. The evaluations included sensitivity analyses for assumed placement of the waste payload within the canister and for centered or eccentric location of the cylindrical shells within one another. The thermal response seen for the RH-TRU 72-B packaging components are seen as being essentially the same as those predicted in the RH-TRU 72-B SAR [2] under both NCT and HAC conditions. As such, the addition of the NS15 and NS30 shielded RH waste canisters as alternative payloads will not impact the safety basis of the RH-TRU 72-B packaging.

7.0 Appendices

7.1 References

1. Title 10, Code of Federal Regulations, Part 71 (10 CFR 71), *Packaging and Transportation of Radioactive Materials*, United States Nuclear Regulatory Commission (USNRC), 01-01-02 Edition.
2. RH-TRU 72-B Safety Analysis Report, Rev. 4, June 2006.
3. NUREG-1609, "*Standard Review Plan for Transportation Packages for Radioactive Material*", Spent Fuel Project Office, Office of Nuclear Material Safety and Safeguards, U.S. Nuclear Regulatory Commission, Washington, DC 20555-0001, March 1999.
4. Regulatory Guide 7.8, *Load Combinations for the Structural Analysis of Shipping Casks for Radioactive Material*, Revision 1, U. S. Nuclear Regulatory Commission, March 1989.
5. Drawing X-106-503-SNP, Rev. 0, *RH-TRU Waste Canister Assembly, NS15 & NS30, Neutron Shielded Design*, prepared for U.S. Department of Energy by AREVA Federal Services LLC, 1/28/2010.
6. DriscoPlex® PE3608/(PE3408) Pipe, Pipe and Fittings Data Sheet, Bulletin PP 109, September 2006 (see also Appendix 7.6).
7. American Society of Mechanical Engineers (ASME) Boiler and Pressure Vessel Code, 1998 Edition, ASME International, New York, NY.
8. Matweb, Online Material Data Sheets, www.matweb.com.
9. Handbook of Polyethylene Pipe, Second Edition, Plastic Pipe Institute, Irving TX, 75062, www.plasticpipe.org.
10. Rohsenow, Hartnett, and Choi, *Handbook of Heat Transfer*, 3rd edition, McGraw-Hill Publishers, 1998.
11. G. G. Gubareff, J. E. Janssen, and R. H. Torborg, *Thermal Radiation Properties Survey*, 2nd Edition, Honeywell Research Center, 1960.
12. Thermal Desktop®, Version 5.1, Cullimore & Ring Technologies, Inc., Littleton, CO, 2007.
13. SINDA/FLUINT, Systems Improved Numerical Differencing Analyzer and Fluid Integrator, Version 5.1, Cullimore & Ring Technologies, Inc., Littleton, CO, 2007.
14. AFS-TR-VV-006, Rev. 0, *Thermal Desktop and SINDA/FLUINT Testing and Acceptance Report, V5.1, Windows XP*, AREVA Federal Services LLC, September 2008.
15. Calculation Number 01937.01.M0005.01-02, *72-B Thermal Scoping Analysis*, Rev. 0, AREVA Federal Services LLC.
16. Engineering Report: 7953-R-027, 30-foot Free Drop Post-Test Summary Report for the NS30 Neutron Shielded Canister, Petersen Incorporated, November 2009.
17. ASTM D 3350, *Standard Specification for Polyethylene Plastics Pipe and Fittings Materials*, ASTM International, West Conshohocken, PA, 2003, DOI: 10.1520/C0033-03, www.astm.org.

7.2 Sample Input File

The input files are too large for inclusion directly into this calculation. Instead, the input and output files are provided on a CDROM.

7.3 Computer Run Record

AREVA	COMPUTER RUN RECORD		
Computer Run Identification	**Verification of Existing RH-TRU 72-B Thermal Models**		
Software Verification	Verified under AFS-EN-PRC-013, Rev. 01		
Analysis Software	Thermal Desktop™ & SINDA/FLUINT™, Version 5.1		
Hardware Description	Pentium M, Windows XP operating system for computer DLT6000		
Disk Storage Description	All files stored on CD-ROM in folder named: **RH-TRU 72-B Verification**		
Disk File Storage	File Description	File Name	Creator
	ASCII Input	RH-TRU_50Watt_NCT.inp RH-TRU_50Watt_HAC.inp RH-TRU_300Watt_NCT.inp RH-TRU_300Watt_HAC.inp frcvv-sqft.f	G Banken
	Binary Database	-none-	G Banken
	ASCII Output	RH-TRU_NCT_50W.out RH-TRU_50W_HAC.out RH-TRU_NCT_300W.out RH-TRU_300Watt_HAC.out	G Banken
	Binary Output	-none-	G Banken
	Spreadsheets	none	
Printed Attachments	Description		

COMPUTER RUN RECORD

Computer Run Identification	**NS15 Shielded Canister**		
Software Verification	Verified under AFS-EN-PRC-013, Rev. 01		
Analysis Software	Thermal Desktop™ & SINDA/FLUINT™, Version 5.1		
Hardware Description	Pentium M, Windows XP operating system for computer DLT6000		
Disk Storage Description	All files stored on CD-ROM in folder named: **NS15 Safety Evaluation**		
Disk File Storage	File Description	File Name	Creator
	ASCII **Input**	RHTRU-NS15_NCT_Bottom_Position.inp/cc RHTRU-NS15_NCT_Middle_Position.inp/cc RHTRU-NS15_NCT_Top_Position.inp/cc RHTRU-NS15_NCT_Eccentric.inp/cc RHTRU-NS15_NCT_NoSolar.inp RHTRU-NS15_HAC.inp RHTRU-NS15_HAC_PostSS.inp RHTRU-NS15_NCT_Bottom_Position.rad RHTRU-NS15_NCT_Middle_Position.rad RHTRU-NS15_NCT_Top_Position.rad RH-TRU Optical Properties.rco RH-TRU Material Properties.tdp RH-TRU_Cask_NCT.dat / RH-TRU_Cask_HAC.dat frcvv-sqft.f	G Banken
	Binary Database	RHTRU-NS15_NCT_Bottom_Position.dwg RHTRU-NS15_NCT_Middle_Position.dwg RHTRU-NS15_NCT_Top_Position.dwg RHTRU-NS15_NCT_Eccentric.dwg	G Banken
	ASCII Output	RHTRU-NS15_NCT_Bottom_Position.out/usr1 RHTRU-NS15_NCT_Middle_Position.out/usr1 RHTRU-NS15_NCT_Top_Position.out/usr1 RHTRU-NS15_NCT_Eccentric.out/usr1 RHTRU-NS15_NCT_NoSolar.out/usr1 RHTRU-NS15_HAC.out/usr1 RHTRU-NS15_HAC_PostSS.out/usr1	G Banken
	Binary Output	RHTRU-NS15_NCT_Bottom_Position.sav RHTRU-NS15_NCT_Middle_Position.sav RHTRU-NS15_NCT_Top_Position.sav RHTRU-NS15_NCT_Eccentric.sav RHTRU-NS15_NCT_NoSolar.sav RHTRU-NS15_HAC.sav RHTRU-NS15_HAC_PostSS.sav	G Banken
	Spreadsheets	RHTRU-72B Shielded Canister Results.xls	

AREVA	**COMPUTER RUN RECORD**		
Computer Run Identification	**NS30 Shielded Canister**		
Software Verification	Verified under AFS-EN-PRC-013, Rev. 01		
Analysis Software	Thermal Desktop™ & SINDA/FLUINT™, Version 5.1		
Hardware Description	Pentium M, Windows XP operating system for computer DLT6000		
Disk Storage Description	All files stored on CD-ROM in folder named: **NS30 Safety Evaluation**		
Disk File Storage	File Description	File Name	Creator
	ASCII **Input**	RHTRU-NS30_NCT.inp RHTRU-NS30_NCT_NoSolar.inp RHTRU-NS30_HAC.inp RHTRU-NS30_HAC_PostSS.inp RHTRU-NS30.cc RHTRU-NS30.rad RH-TRU Optical Properties.rco RH-TRU Material Properties.tdp RH-TRU_Cask_NCT.dat RH-TRU_Cask_HAC.dat frcvv-sqft.f	G Banken
	Binary Database	RH-TRU NS30 Canister.dwg	G Banken
	ASCII Output	RHTRU-NS30_NCT.out/usr1 RHTRU-NS30_NCT_NoSolar.out/usr1 RHTRU-NS30_HAC.out/usr1 RHTRU-NS30_HAC_PostSS.out/usr1	G Banken
	Binary Output	RHTRU-NS30_NCT.sav RHTRU-NS30_NCT_NoSolar.sav RHTRU-NS30_HAC.sav RHTRU-NS30_HAC_PostSS.sav	G Banken
	Spreadsheets	RHTRU-72B Shielded Canister Results.xls	

7.4 Thermal Model Details

This section presents details of the thermal modeling used to simulate the NS15 and NS30 shielded canisters within the RH-TRU 72-B packaging. The analytical thermal model of the shielded canisters within the RH-TRU 72-B packaging is developed for use with the Thermal Desktop® [12] and SINDA/FLUINT [13] computer programs. These programs work together to provide the functions needed to build, exercise, and post-process a thermal model. The Thermal Desktop® computer program provides graphical input and output display functions, as well as computing the thermal mass, conduction, and radiation exchange conductors for the defined geometry and thermal/optical properties. Thermal Desktop® is designed to run as an application module within the AutoCAD™ design software. As such, all of the CAD tools available for generating geometry within AutoCAD™ can be used for generating a thermal model. In addition, the use of the AutoCAD™ layers tool presents a convenient means of segregating the thermal model into its various elements.

The SINDA/FLUINT computer program is a general purpose code that handles problems defined in finite difference (i.e., lumped parameter) and/or finite element terms and can be used to compute the steady-state and transient behavior of the modeled system. Although the code can be used to solve any physical problem governed by diffusion-type equations, specialized functions used to address the physics of heat transfer and fluid flow make the code primarily a thermal code. The SINDA '85 computer program used to produce the thermal results presented in the RH-TRU 72-B [2] safety analysis report is an early predecessor to Version 5.1 of the SINDA/FLUINT software used for this evaluation.

Together, the Thermal Desktop® and SINDA/FLUINT codes provide the capability to simulate steady-state and transient temperatures using temperature dependent material properties and heat transfer via conduction, convection, and radiation. While complex algorithms may also be programmed into the solution process to, for example, compute heat transfer coefficients as a function of the local conditions, this capability of the code has not been utilized for this evaluation.

The SINDA/FLUINT and Thermal Desktop® computer programs have been validated for safety basis calculations for nuclear related projects [14].

7.4.1 Thermal Model for RH-TRU 72-B Packaging

The analytical thermal model of the RH-TRU 72-B packaging developed for the RH-TRU 72-B SAR [2] is re-used for the purposes of this calculation. The thermal model for NCT provides an axisymmetric, 360° representation of the RH-TRU 72-B cask body and impact limiters, as illustrated in Figure 7-1 to Figure 7-4. The modeling is defined via non-graphical, textual modeling language that defines a lumped-parameter, finite-difference representation of the package. Similar modeling is used for HAC conditions, except for the simulation of the non- axisymmetric effect of the trunnions and the side drop and puncture pin damage. To address these HAC related aspects of the thermal modeling, the thermal modeling for the lead shield, outer vessel, thermal shield, and the impact limiters are extended to three dimensions. Figure 7-5 illustrates the revised thermal modeling for the impact limiters to capture the pre-fire drop damage. Full details of the modeling and the assumptions used in its development are provided in the RH-TRU 72-B SAR. The following bullet items identify the basis of this thermal modeling:

- The thermal analyses are based on coding for the SINDA '85/FLUINT finite difference code
- All internal voids are assumed to be filled with air at one (1) atmosphere
- Solar heat input is based on projected surface area of the package and a solar absorptivity of $\alpha = 0.52$ for NCT and $\alpha = 0.8$ for HAC
- Convective heat transfer from the exterior of the package is based on natural convection for NCT and post-fire HAC conditions and on forced convection during the 30-minute HAC fire. These convection coefficients are determined from the local Nusselt number based on local air temperature (average of the local external surface temperature and the ambient temperature) and the surface area. The Nusselt number is calculated as a function of the Grashof and Prandtl numbers
- External radiation from packaging and impact limiter surfaces is calculated assuming a surface emissivity of $\varepsilon = 0.3$ for NCT and $\varepsilon = 0.8$ for HAC

7.4.2 Thermal Model for NS15 and NS30 Shielded Canisters

The thermal modeling of the NS15 and NS30 shielded canisters and waste payload are developed using the Thermal Desktop® computer program [12] based on the geometry provided by drawing X-106-503-SNP [5]. With the exception of the payload definition and the thickness of the high density polyethylene (HDPE) used for shielding, identical modeling approaches are used for the thermal models for the NS15 and NS30 canister designs. Approximately 1,270 thermal nodes are used to define the NS15 canister design and its enclosed payload, while approximately 1,385 thermal nodes are used for the NS30 canister design. The interface of the graphics based modeling of the NS15 and NS30 shielded canisters with the textual based thermal modeling of the RH-TRU 72-B cask body is provided via a series of shell surfaces illustrated in Figure 7-6 whose location and surface area match precisely the nodal distribution in the text based modeling of the RH-TRU 72-B cask body.

The shell for both shielded payload canister configurations is identical to the unshielded configuration with a 26-in. outside diameter and a ¼-in. thick wall fabricated of painted ASTM A516 carbon steel. Including the lifting pintle at the top of the payload canister, the overall length of the modeled canister is 120½ inches. Given the combination of the relative thinness of the shell, the conductivity of carbon steel, and the relatively low heat flux associated with a 50 W decay heat payload, the shell of the canister is modeled with a single thermal node in the radial direction. Axial thermal resolution is provided with thermal nodes spaced approximately every 5 inches along the shell's length. The lid and base of the canister shell as modeled with one node for the ¼-in. thickness and 5 nodes in the radial direction. The lifting pintle is modeled with solid elements using 30 thermal nodes. The heat transfer between the waste canister shell and the RH-TRU 72-B cask body is modeled as conduction and radiation across the nominal 2.625-in. gap in the same fashion as the thermal modeling defined in the RH-TRU 72-B SAR [2]. The radial gap between the canister and the RH-TRU 72-B inner vessel is mechanically maintained within ½-in. of nominal spacing by the use of spacer rings and support rails. Figure 7-7 illustrates the thermal interface between the waste canister and the inner surfaces of the cask cavity. Heat transfer between the base and lid ends of the canister and the cask inner surfaces is modeled as conduction and radiation across 0.125-in. and 0.5-in. gaps, respectively. The relatively void space associated with the region around the lifting pintle on the canister effectively isolates the top of the canister from the underside of the cask lid.

The HDPE neutron shielding material for the NS15 canister is modeled with a nominal thickness of 3.387-in. and an outer diameter of 24 inches. The top and bottom end caps have a 5-in. thickness. The neutron shielding material for the NS30 canister is modeled with a nominal thickness of 1.454-in. The outer diameter and the thickness of the top and bottom end caps are the same as that for the NS15 shield insert. Figure 7-8 illustrates the thermal model of the NS15 shield insert in the waste canister. Except for sidewall thickness, the thermal modeling for the NS30 shield insert is similar.

Five thermal nodes are used to model the HDPE wall thickness of the NS15 shield insert and three nodes are used for the NS30 shield insert. The 5-in. node spacing in the axial direction matches that used for the canister shell. The top and bottom end caps are simulated with 9 thermal nodes in the radial direction and 6 nodes across the thickness. Radial heat transfer between the HDPE insert and the canister shell wall is simulated as conduction and radiation across the nominal 0.75-in. gap between the components. The use of a uniform radial gap is appropriate for NCT and HAC evaluations even though the RH-TRU 72-B package is transported horizontally since the increase in the radial gap on one side of the HDPE insert will be offset by a corresponding smaller gap on the opposing side. In addition, ignoring the narrow line contact that will exist for the horizontal package orientation will yield conservative temperature estimates for NCT conditions, while the bounding temperature achieved under HAC conditions can be conservatively estimated by assuming the inner surface reaches a temperature equivalent to that achieved by the outer surface.

Axial heat transfer between the HDPE insert and the base and lid ends of the canister is modeled as conduction and radiation across 0.125-in. and 0.375-in. gaps, respectively. The HDPE insert is conservatively assumed to have shifted forwarded slightly under horizontal transportation from its vertical loading position. Maintaining a tight contact between the bases of the insert and canister shell will yield lower NCT temperatures for the insert and payload and lower HAC temperatures for the base of the canister shell since the thermal mass of the HDPE insert will not be as closely coupled to help absorb the heat flux during the fire event.

The payload for the NS15 canister is assumed to be contained within three (3) approximately 16-gallon containers. Each waste container and its contents are represented by 119 thermal nodes. The containers are assumed to be full of waste whose volumetric heat generation is evenly distributed and whose effective thermal conductivity is equal to that of air. The shell of the containers is simulated as 0.04-in. thick carbon steel.

Three alternative placements of the waste containers within the canister are considered: first, the containers are assumed to be stacked on the bottom of the canister cavity, the second configuration assumes the use of approximately 19.9-in. of dunnage at the bottom of the canister to elevate the top of the uppermost container to near the top of the canister cavity, and the third placement configuration assumes approximately 7.5-in. of dunnage at both the top and bottom of the canister to center the waste containers within the canister. The second placement configuration further assumes the use of slip sheets or some other separator between the containers, while the first and third container arrangement assumes the containers are in close, near physical contact with one another. The dunnage required for these various placement configurations are not specifically modeled, but are assumed to have the thermal conductance of an equivalent airspace. Even containers in near physical contact with one another are assumed to have an approximate airspace of 0.375-in. between their end face surfaces because the rolled rims and dished ends prevent tighter contact. Figure 7-9 illustrates the bottom and top positioning configurations of the waste containers, while Figure 7-10 illustrates the center positioning scheme.

To assess the effect of eccentric placement within the horizontal cask, a sensitivity evaluation was conducted for the bottom positioning configuration for the waste containers described above. The changes to the thermal modeling for the eccentric placement consisted of reducing the mean gap between the lower half of the horizontally oriented drums, poly insert, and canister and their adjacent component to one half of the gap assumed for the concentric placement of the components. The corresponding mean gap between the upper half of these same components was increased by 50% over that assumed for the concentric placement of the components. The thermal conductance due to the line contact between the components is conservatively ignored. All other aspects of the thermal model remained the same as discussed above.

The modeling approach used for the payload definition for the NS30 canister is similar to that for the N15 canister, except that the waste is assumed to be contained within six (6) approximately 8-gallon containers that, in turn, are housed within three (3) approximately 30-gallon drums. Figure 7-11 illustrates the assumed payload configuration for the NS30 shielded canister configuration. As with the payload definition for the NS15 canister, each waste container is assumed to be full of waste whose volumetric heat generation is evenly distributed and whose effective thermal conductivity is equal to that of air. The shell of the containers is simulated as 0.04-in. thick carbon steel. The shell and the contents are represented by 68 thermal nodes for each container.

The waste containers are assumed to be centered radially within the 30-gallon drums, to be in near contact with one another and the bottom of the drum, and within 0.75-in. of the drum lid. The near contact condition is simulated as a 0.125-in. gap to account for the axial offset provided by the rolled rims on the containers. The drums are assumed to be centered within the HDPE neutron shielding and in near physical contact with one another. Again, the near physical contact is simulated via 0.375-in. airspace because the rolled rims and dished ends prevent tighter contact. The 30-gallon drums are simulated as carbon steel shell elements with a thickness of 0.045-in.

7.5 Verification of Existing RH-TRU 72-B Thermal Models

The modeling approach of using a mixture of lumped-parameter and 'solids' modeling, together with the use of Version 5.1 of the SINDA/FLUINT computer program, was validated as producing similar results for both NCT and HAC codes when running the thermal models developed for the SINDA '85 code. This validation is documented in a scoping evaluation conducted on the NS15 and NS30 shielded insert concepts [15]. Table 7-1 summarizes the comparative results obtained between the original SINDA '85 modeling and that obtained using the modeling approach utilized in this evaluation. As seen, the results are very similar, thus verifying the modeling approach.

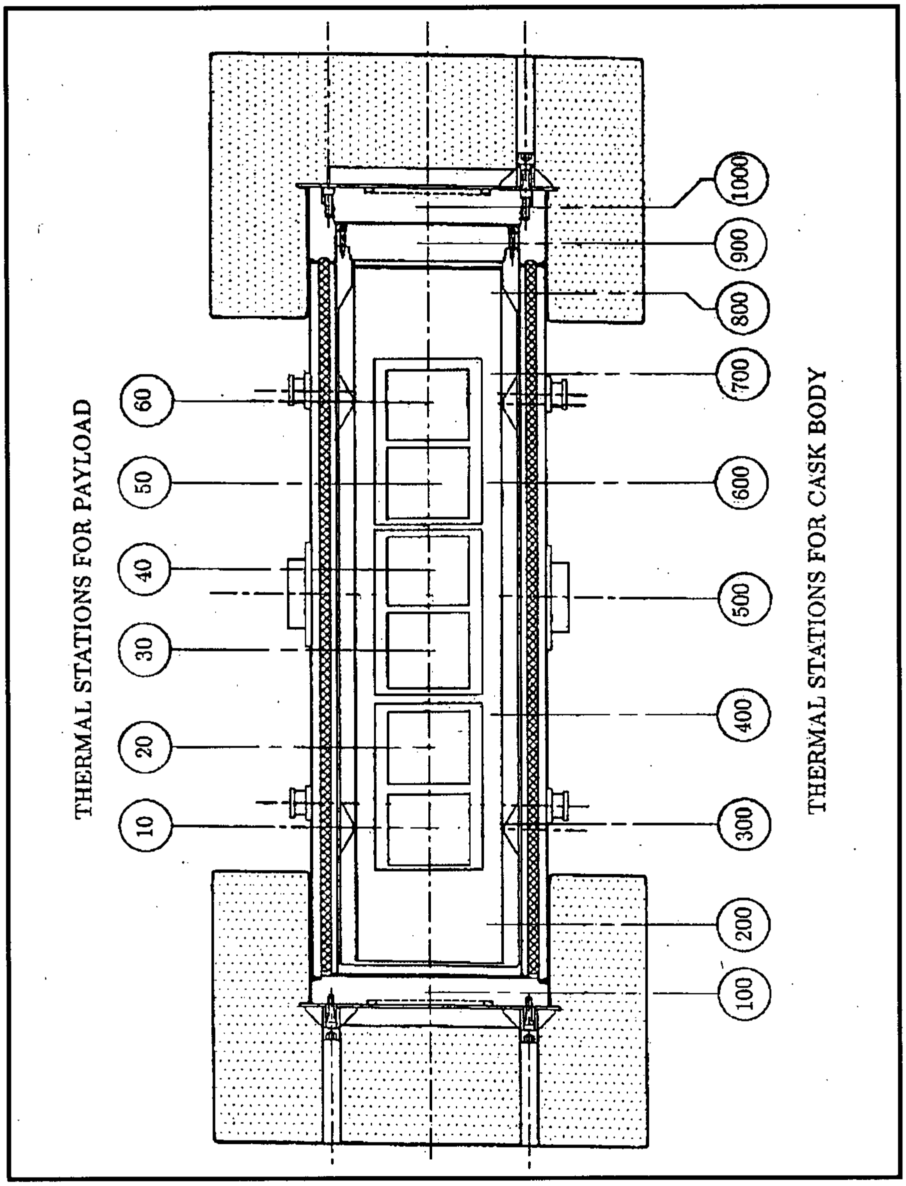

Figure 7-1 - Thermal Model Layout for RH-TRU 72-B Packaging

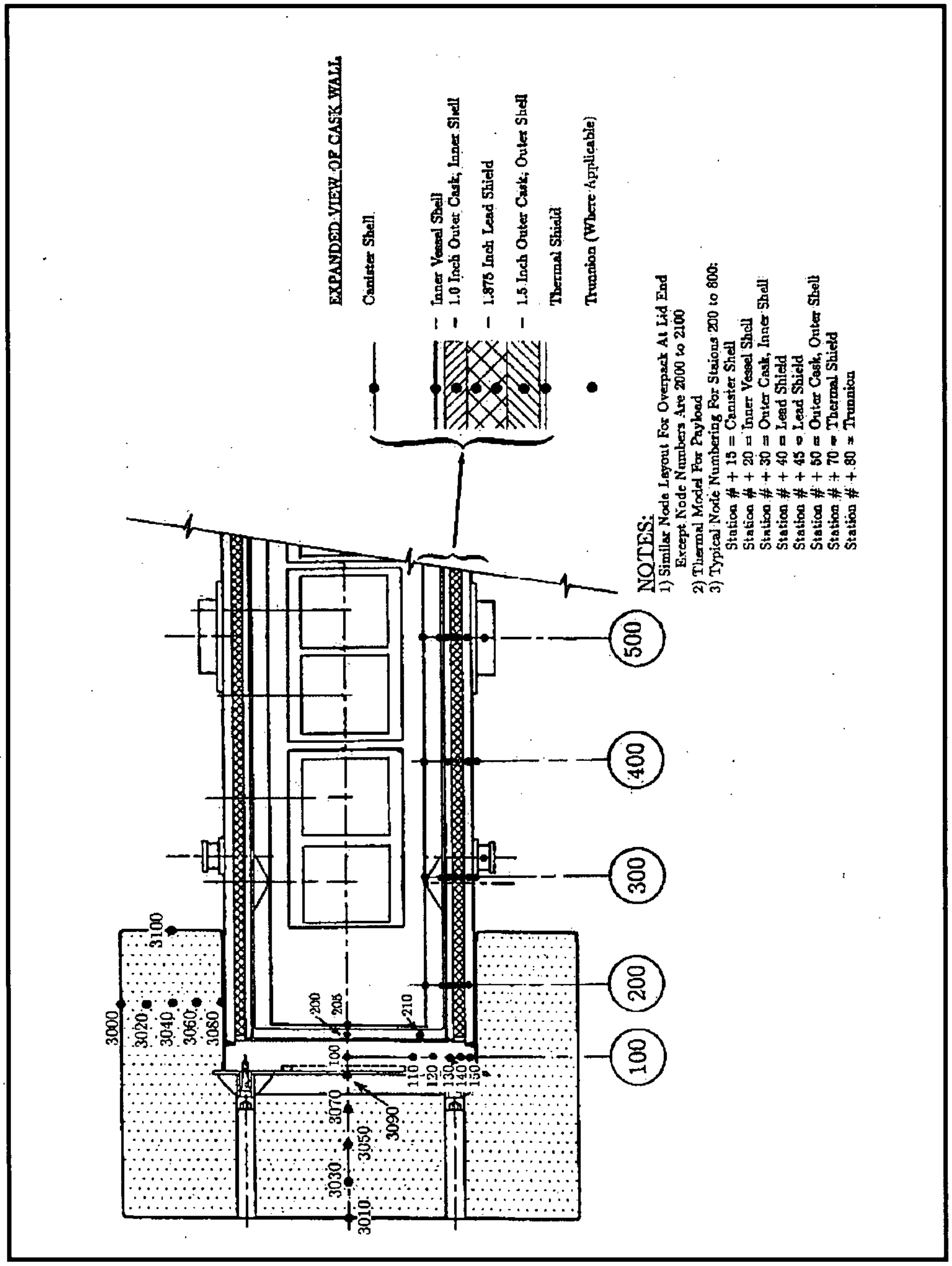

Figure 7-2 - Thermal Node Identification Scheme for Cask Body & Limiters

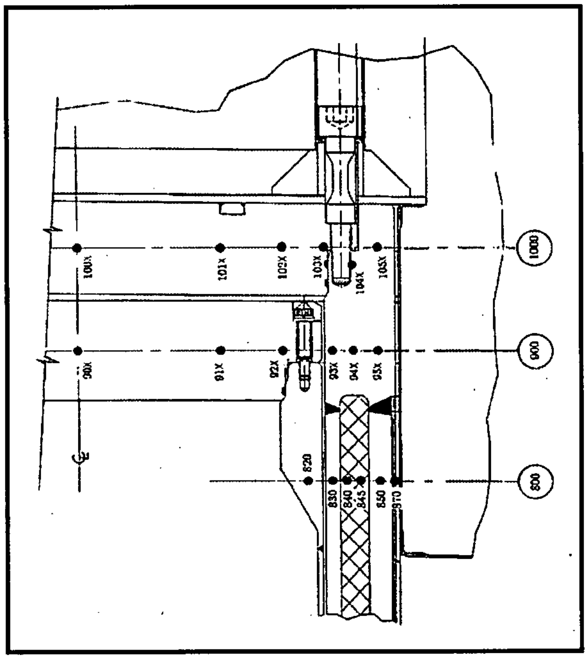

Figure 7-3 - Thermal Node Identification Scheme for Cask Lid End

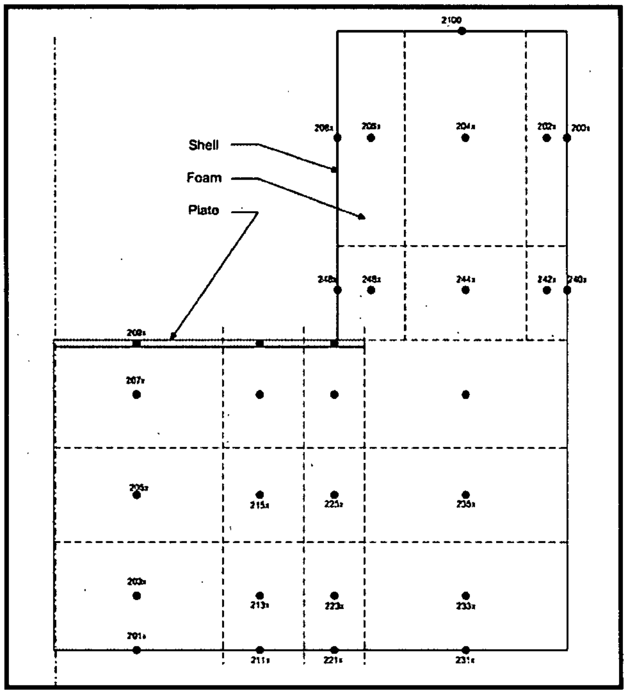

Figure 7-4 - Thermal Node Identification Scheme for Cask Lid End Impact Limiter

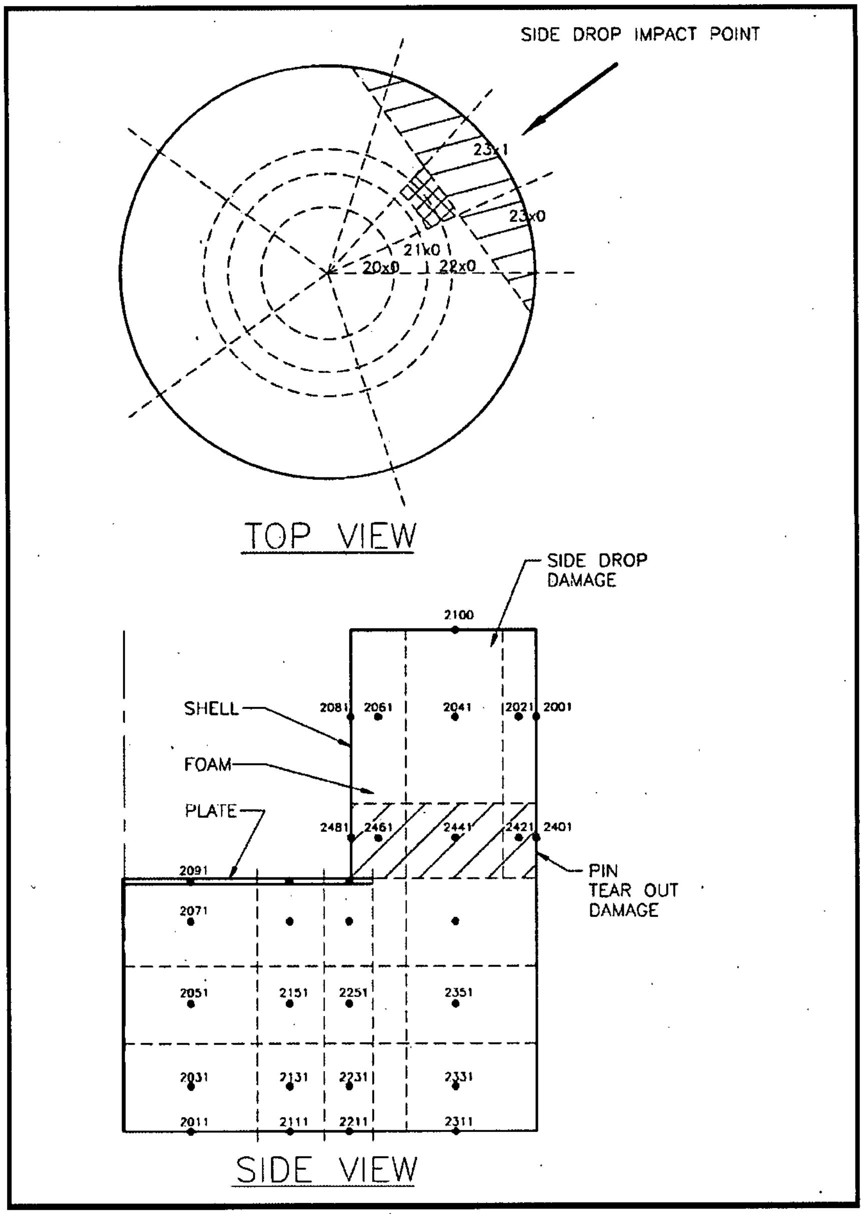

Figure 7-5 - Thermal Node Identification Scheme for Side Drop and Puncture Bar Damage to Impact Limiter

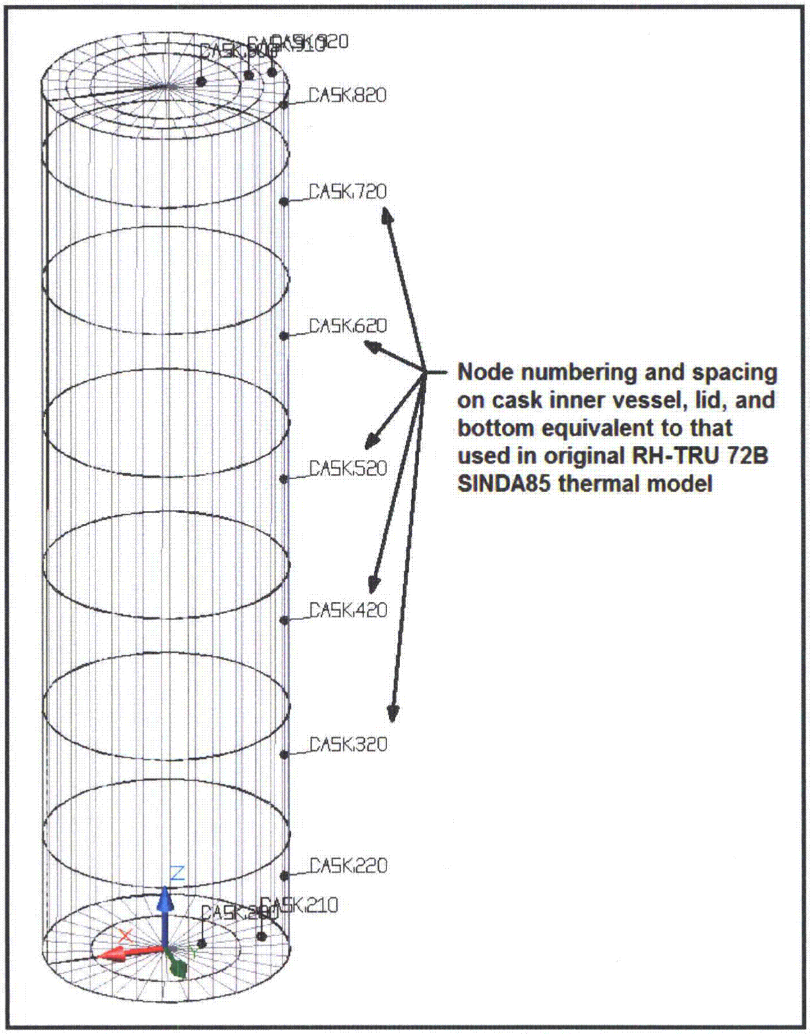

Figure 7-6 - Graphical Representation of RH-TRU 72-B Inner Vessel Sidewall, Base, and Lid Surfaces

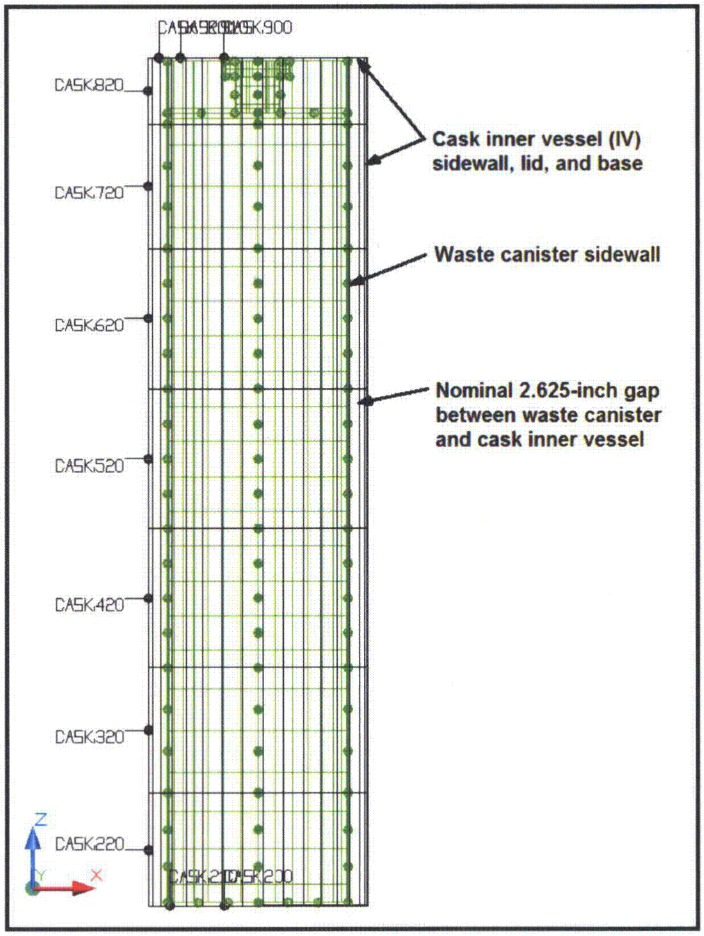

Figure 7-7 - Thermal Interface Scheme between RH-TRU 72-B Cask Model and Waste Canister Model

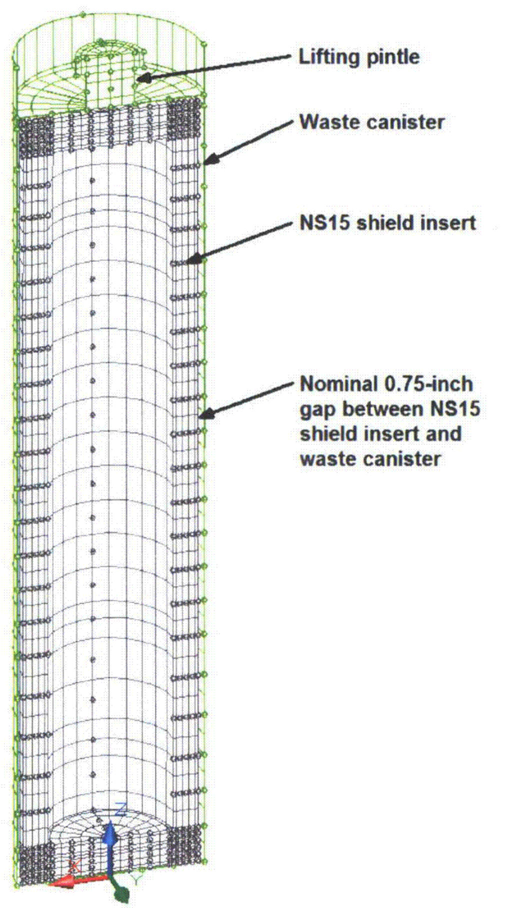

Figure 7-8 - Thermal Model Layout of NS15 Shielded Canister

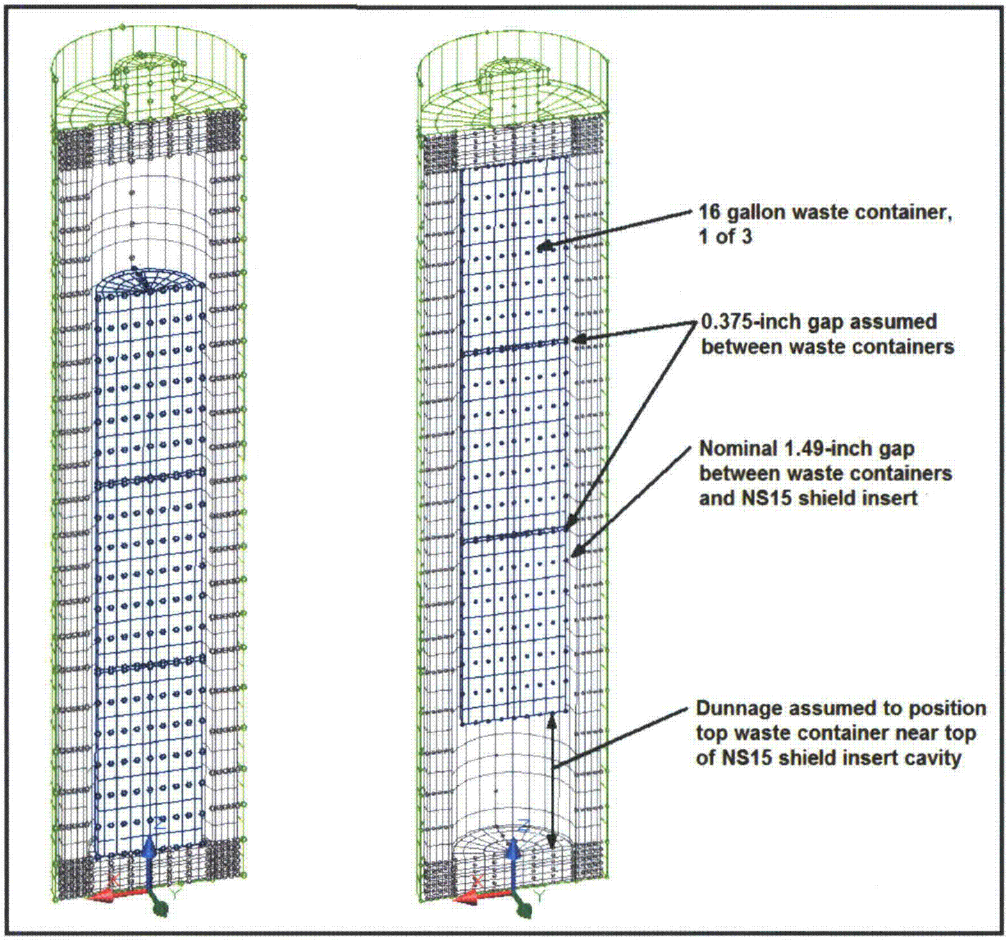

Figure 7-9 - Thermal Modeling of Waste Containers within NS15 Shielded Canister – Bottom and Top Positioning

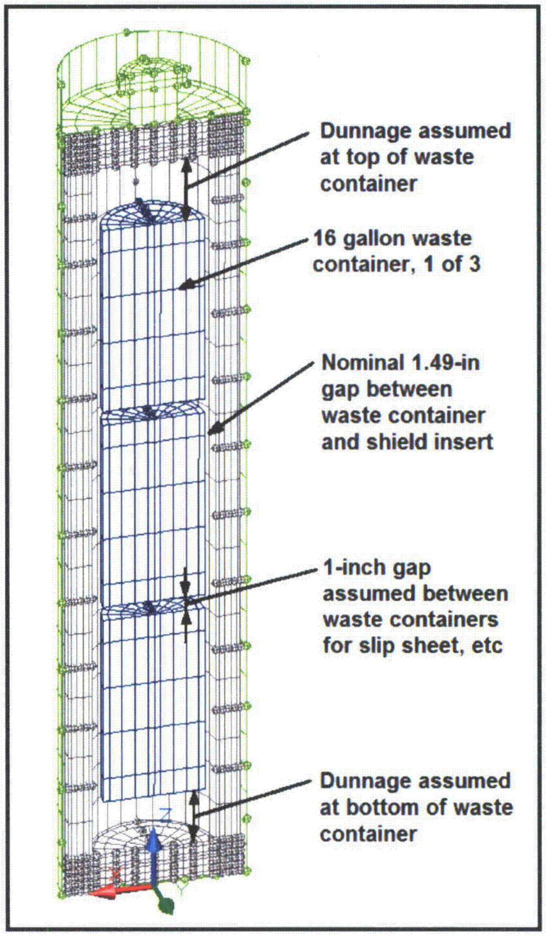

Figure 7-10 - Thermal Model Layout for Middle Positioning of Waste Containers within NS15 Shielded Canister

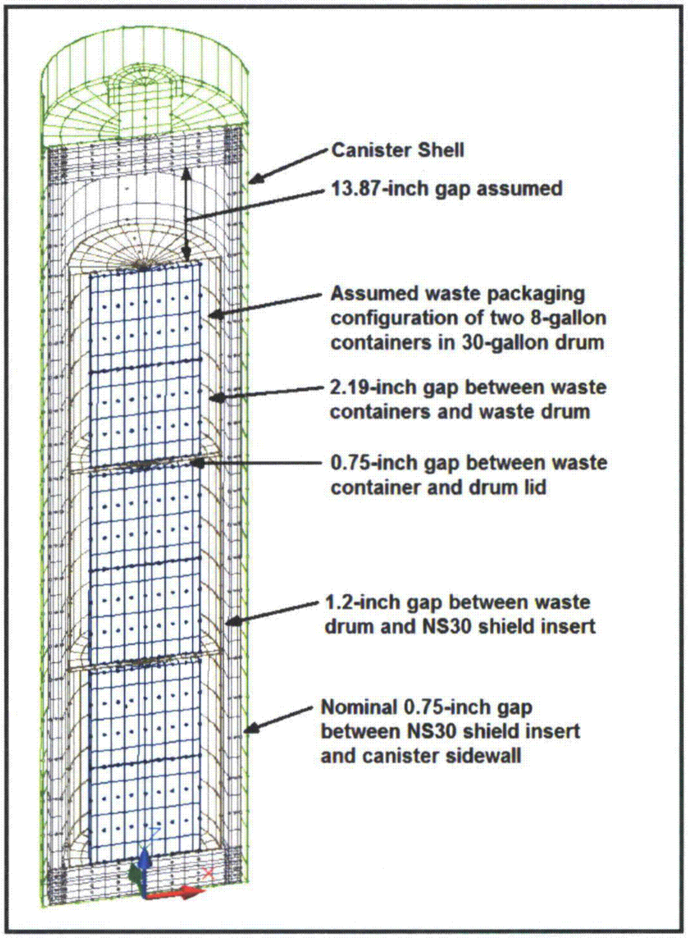

Figure 7-11 - Thermal Model Layout for Nested Waste Containers within NS30 Shielded Canister

Table 7-1 - Comparison of Results for Baseline HAC Thermal Models

Location	50 Watt Payload		300 Watt Payload	
	SAR Results	Re-Run	SAR Results	Re-Run
Waste Centerline	*219 °F*	214 °F	*196 °F*	197 °F
Canister Shell	*263 °F*	265 °F	*247 °F*	244 °F
IV Inner Shell	*327 °F*	328 °F	*343 °F*	343 °F
OC Inner Shell	*488 °F*	488 °F	*497 °F*	497 °F
OC Lead Shield	*544 °F*	544 °F	*554 °F*	554 °F
OC Outer Shell	*601 °F*	602 °F	*611 °F*	611 °F
OC Thermal Shield	*1,232 °F*	1,232 °F	*1,231 °F*	1,226 °F
OC Upper Ring Forging	*154 °F*	159 °F	*166 °F*	170 °F
IV O-Ring Seal	*150 °F*	151°F	*159 °F*	160 °F
OC O-Ring Seal	*149 °F*	150 °F	*158 °F*	158 °F
IV Lid	*148 °F*	151 °F	*157 °F*	160 °F
OC Lid	*150 °F*	150 °F	*159 °F*	158 °F
Impact Limiter Shell	*1,424 °F*	1,427 °F	*1,425 °F*	1,427 °F

7.6 Material Data Sheets

For more information and technical assistance contact:

Performance Pipe, a division of
Chevron Phillips Chemical Company LP
P.O. Box 269006
Plano, TX 75026-9006
800.527.0662

PERFORMANCE PIPE
A Division of Chevron Phillips Chemical Company LP

DriscoPlex®
PE3608 / (PE3408) Pipe
Pipe and Fittings Data Sheet

Typical Material Physical Properties of DriscoPlex® PE3608 / (PE3408)

High Density Polyethylene Materials

Property	Unit	Test Procedure	Typical Value
Material Designation	---	PPI TR-4	PE3608
Cell Classification	---	ASTM D3350	345464C
Pipe Properties			
Density	gms / cm³	ASTM D1505	0.955 (black)
Melt Index Condition 190 / 2.16	gms / 10 minutes	ASTM D1238	0.08
Hydrostatic Design Basis 73°F (23°C)	psi	ASTM D2837	1600
Hydrostatic Design Basis 140°F (60°C)	psi	ASTM D2837	800
Color; UV Stabilizer [C] [E]	---	ASTM D3350	Min 2% carbon Black Color UV Stabilizer
Material Properties			
Flexural Modulus 2% Secant - 16:1 span; depth, 0.5 in / min	psi	ASTM D790	>110,000
Tensile Strength at Yield	psi	ASTM D638 Type IV	3200
Elongation at Break 2 in / min., Type IV bar	%	ASTM D638	>700
Elastic Modulus	psi	ASTM D638	>150,000
Hardness	Shore D	ASTM D2240	62
PENT	hrs	ASTM F1473	>100
Thermal Properties			
Vicat Softening Temperature	°F	ASTM D1525	256
Brittleness Temperature	°F	ASTM D746	-103
Thermal Expansion	in / in / °F	ASTM D696	1.0×10^{-4}

Bulletin: PP 109 Revision Date September, 2006

Another quality product from Chevron Phillips Chemical Company LP, The Woodlands, Texas

AREVA	AREVA Federal Services LLC
	CALCULATION

Document No: 01937.01.M005-03	Rev. No: 0	Page: 1 of 41
Project No: 01937.01.M005	Project Name: RH Technical Support, RH-TRU 72-B SAR, Rev. 5	

Title: 72-B with NS15 and NS30 Shielded Canister Shielding Analysis

Summary:

The NS15 and NS30 shielded canisters are used to transport remote handled transuranic waste in the 72-B package. Activity limits are developed for gamma and neutron generating isotopes of interest that result in a dose rate of 1000 mrem/hr at a distance of 1-m from the package surface.

Documentum Number: CALC-3002163-000

Software Utilized:	Version:	Storage Media Attached:
MCNP5	1.40	1 CD

REV.	ORIGINATOR Typed / Signature / Date	CHECKED Typed / Signature / Date	APPROVED Typed / Signature / Date
0	RJ Migliore (neutron) [signature] 1/28/10 B Day (gamma) [signature] 1/28/10	W Zhang 01/28/10 [signature]	DS Hillstrom [signature] 1/29/10

AFS-EN-FRM-002 Rev. 02 (Issued July 27, 2009)
Reference: AFS-EN-PRC-002 Calculations

REVISION HISTORY

REV.	CHANGES
0	Original Issue

TABLE OF CONTENTS

LIST OF FIGURES

LIST OF TABLES

1.0 Introduction

The 72-B package is used to transport remote-handled transuranic waste. The license is being modified to allow shielded canisters filled with waste of potentially high neutron activity. The purpose of this calculation is to determine the activity limit for each isotope of interest that results in a dose rate of 1000 mrem/hr at a distance of 1-m from the package surface subsequent to an accident. MCNP v1.40 [3] is used for the neutron analysis, and a simple point-kernel approach is used for the gamma analysis.

2.0 Methodology

The methodology follows the established methodology used to determine the nuclide activity limits in the RH-TRU 72B SAR [1]. A list of common nuclides that may be present in the waste is summarized in Table 1. Each nuclide may be gamma emitting, neutron emitting, or both.

The objective is to compute a gamma activity limit, A_G, and a neutron activity limit, A_N, for each isotope of interest so that the 10 CFR 71.51(a)(2) hypothetical accident condition (HAC) dose rate limit of 1000 mrem/hr at a distance of 1-m from the package surface cannot be exceeded. If a nuclide is both a gamma and neutron emitter, a combined activity limit A_{GN} is computed as $1/[(1/A_G)+(1/A_N)]$. All radionuclides that do not have gamma energies and do not undergo spontaneous fission or whose maximum allowable activity is calculated to be greater than 1×10^8 curies are classified as "unlimited."

A 72-B package may transport either an NS30 or NS15 shielded canister assembly. A test was performed using the shielded canister to determine the amount of release under HAC [12]. Based on this test, 0.23% of the contents migrated out of the shielded canister. Therefore, it is conservatively assumed under HAC that the radionuclides contained within each canister reconfigure into two point sources that represent 98% and 2% of the total activity. The 2% value bounds the 0.23% value determined by experiment. Point sources are used to represent the source to conservatively minimize the distance from the source to the dose rate location. The maximum dose rate will occur when the distance from the sources to the 1-m location is minimized. The larger magnitude point source is assumed to migrate to the inside of polyethylene shield to the closest possible location to the damaged surface of the 72-B package. The smaller magnitude point source is assumed to migrate to a location outside the polyethylene shield and in-line with the larger source.

Under HAC, the 72-B package dose rate at 1-m in the radial direction is more limiting than the dose rate at 1-m in the axial direction. Because of the impact limiters, the distance from the point source to the dose location is significantly farther at the ends compared to the sides, yet the axial and radial neutron shielding is comparable in both directions. Therefore, the maximum side dose rate at 1-m bounds the maximum end dose rate at the same distance from the package surface.

Once the most restrictive combined neutron and gamma activities A_{GN} are known, the sum of activity partial fractions for any combination of the radionuclides for each canister must be less than or equal to unity, or:

$$\sum_{i=1}^{n} \frac{a_i}{A_{GN_i}} \leq 1$$

where, for a particular payload mix, a_i is the actual curie content of radionuclide "i" and A_{GNi} is the limiting curie content of radionuclide "i".

2.1 Neutron Methodology

For the neutron emitting isotopes, MCNP5 v1.40 [3] is used to compute the dose rates for each isotope of interest. The dose rate is computed at 1-m from the surface of the damaged package. ANSI/ANS-6.1.1-1977 flux-to-dose rate conversion factors are used in the calculations [5]. These factors for neutrons are provided in Table 2.

The neutron source is computed in ED-042 [2] for the isotopes of interest. The total neutron spectrum is provided in Table 3 and Table 5 of ED-042. Each spectrum is entered in MCNP as a histogram distribution. Note that the lowest energy group of the source is conservatively set between 0.1 and 0.5 MeV in MCNP, although the actual group boundary is 0 to 0.5 MeV in ED-042. The number of source neutrons in that group is not changed. Therefore, the source neutrons in the lowest energy group will conservatively have a slightly larger average energy than the actual source. For convenience, the total source strength is set to 1 n/s in all MCNP models.

Note that data for Am-242m are provided for two metastable states (0.048 and 2.2 MeV) in ED-042, although only the 0.048 MeV source is utilized in the current calculation. The excluded 2.2 MeV Am-242m isotope has a half life of only 14 ms (see Table 1 of ED-042) and therefore will not be present in the waste.

No fissile material is included in the models to minimize self-shielding. Because no fissile material is included, no subcritical neutron multiplication is performed by MCNP. It has been determined in conjunction with the RH-TRU 72-B SAR that a conservative factor of 2.7 may be utilized to account for subcritical neutron multiplication (see Section 5.5.2 of [1]). This subcritical multiplication factor was determined by surrounding a point source with a sphere comprised of 325 g Pu-239 and a 30% polyethylene/70% water mixture. The U-238 spectrum, which has the lowest average energy of the isotopes under consideration and hence highest subcritical multiplication factor, was conservatively utilized for the point source in that analysis. Given the similarity between the baseline RH-TRU 72-B configuration and the RH-TRU 72-B configured with the NS30 or NS15 shielded canister, this subcritical neutron multiplication factor is applicable to the current analysis.

Once the neutron dose rate is known for a 1 n/s source, the source strength may be scaled up to the limit of 1000 mrem/hr at 1-m by utilizing the total neutron source strength (per gram) and the specific activity of the nuclide (Ci/g). The total neutron source strength (n/s/g) is provided in Table 2 and Table 4 of ED-042. The details of this calculation are shown in Section 4.1.

2.2 Gamma Methodology

Because of the large number of gamma emitting isotopes (169), and the thick gamma shielding of the 72-B package, explicit computation of the activity limits using MCNP for the gamma emitting isotopes is prohibitively expensive. Rather, a simplified point-kernel approach is utilized to produce results that are conservative in comparison to those obtained from a fully representative Monte Carlo analysis. The primary conservatism is using iron buildup factors in place of lead, which overestimates the dose rate. This methodology is also present in the 72-B SAR, Section 5.4.1 [1].

The dose rate from an isotropic point-source, as a function of gamma energy, is simply [9]:

$$D(E) = \frac{S(E)B(E,x)C(E)}{4\pi R^2} e^{-x}$$

where D(E) is the dose rate as a function of gamma energy, E (mrem/hr), S(E) is the source strength as a function of gamma energy, E (γ/s; 1 curie = $3.7(10)^{10}$ γ/s), B(E,x) is the buildup factor as a function of gamma energy, E, and mean free paths, x(E), C(E) is the gamma flux-to-dose rate conversion factor (γ/cm²-s to mrem/hr), and R is the radial distance from the source to the receptor (cm).

Gamma energy and intensity data is provided in Kinsey, et al [8]. All gamma energies less than 0.100 MeV are conservatively rounded to 0.100 MeV for the purpose of linear interpolation in Table 3, Table 4, and Table 5.

The number of mean free paths, x(E), is:

$$x(E) = \sum_{i=1}^{n} \mu_i(E) t_i$$

where $\mu_i(E)$ is the attenuation coefficient (as a function of gamma energy) of shield "i", and t_i is the thickness of shield "i" in centimeters. The number of mean free paths is a non-dimensional number.

The attenuation coefficient for shield "i" is:

$$\mu_i(E) = \left[\frac{\mu_1(E)}{\rho}\right]\rho_1 + \left[\frac{\mu_2(E)}{\rho}\right]\rho_2 + \left[\frac{\mu_3(E)}{\rho}\right]\rho_3 + \cdots + \left[\frac{\mu_n(E)}{\rho}\right]\rho_n$$

where, for a material containing "n" different elements, $\mu_x(E)$ and ρ_x are the mass attenuation coefficient (as a function of gamma energy) and partial density for element "x." The units for the attenuation coefficient are cm^{-1}. The units for mass attenuation coefficient are cm²/g. Table 6 presents a summary of the partial density for each major element of the three gamma attenuation materials (i.e., carbon steel, Type 304 stainless steel, and lead). Gamma attenuation in the polyethylene is not credited. Table 4 summarizes the mass attenuation coefficients for each element as a function of gamma energy, as taken from ANSI/ANS 6.4.3-1991 [10]. Mass attenuation coefficients used in the subsequent shielding calculations are linearly interpolated from the data in Table 4.

Gamma-ray isotropic point-source buildup factors are determined by conservatively assuming iron as the dominant shielding material. Although the actual buildup factors will lie somewhere between iron (atomic number, Z = 26) and lead (Z = 82), use of iron as the buildup factor will conservatively bound the maximum isotopic quantity (curies) allowed for transport because the buildup factor increases as the atomic number decreases.

Buildup factors are determined using the geometric progression (G-P) function as presented in ANSI/ANS 6.4.3-1991 [10]. The G-P function accurately reproduces buildup factor data for deep penetrations in shields (i.e., >20 mean free paths thick). The buildup factor, as a function of gamma energy, E, and mean free paths, x, using the G-P function is:

$$B(E,x) = 1+(b-1)\frac{(K^x-1)}{(K-1)} \quad \text{for } K \neq 1$$

$$B(E,x) = 1+(b-1)x \quad \text{for } K = 1$$

$$K(x) = cx^a + d\left[\frac{\tanh\left(\frac{x}{X_K}-2\right)-\tanh(-2)}{1-\tanh(-2)}\right]$$

The coefficients a, b, c, d, and X_K, as a function of gamma energy, are provided in Table 5. These coefficients are linearly interpolated for a given gamma energy.

Gamma flux-to-dose rate conversion factors are determined using the values delineated in ANSI/ANS 6.1.1-1977 [5], and presented in Table 3. The data in Table 3 are linearly interpolated to determine the conversion factor for a given gamma energy.

An example gamma dose rate calculation is presented in Section 5.3 for Co-60.

Table 1 – RH-TRU 72-B Radionuclide Inventory

^{3}H	^{90m}Zr	^{123m}Te	^{160}Tb	^{223}Fr	^{236}Pu
^{10}Be	^{93}Zr	^{125m}Te	^{166m}Ho	^{223}Ra	^{238}Pu
^{14}C	^{95}Zr	^{127}Te	^{168}Tm	^{224}Ra	^{239}Pu
^{22}Na	^{93m}Nb	^{127m}Te	^{182}Ta	^{225}Ra	^{240}Pu
^{32}P	^{94}Nb	^{129}Te	^{198}Au	^{226}Ra	^{241}Pu
^{33}P	^{95}Nb	^{129m}Te	^{207}Tl	^{228}Ra	^{242}Pu
^{35}S	^{95m}Nb	^{125}I	^{208}Tl	^{225}Ac	^{243}Pu
^{45}Ca	^{99}Tc	^{129}I	^{209}Tl	^{227}Ac	^{244}Pu
^{46}Sc	^{99m}Tc	^{131}I	^{209}Pb	^{228}Ac	^{241}Am
^{49}V	^{103}Ru	^{134}Cs	^{210}Pb	^{227}Th	^{242}Am
^{51}Cr	^{106}Ru	^{135}Cs	^{211}Pb	^{228}Th	^{242m}Am
^{54}Mn	^{103m}Rh	^{137}Cs	^{212}Pb	^{229}Th	^{243}Am
^{55}Fe	^{106}Rh	^{133}Ba	^{214}Pb	^{230}Th	^{245}Am
^{59}Fe	^{107}Pd	^{137}Ba	^{207}Bi	^{231}Th	^{240}Cm
^{57}Co	^{108}Ag	^{137m}Ba	^{210}Bi	^{232}Th	^{242}Cm
^{58}Co	^{108m}Ag	^{141}Ce	^{211}Bi	^{234}Th	^{243}Cm
^{60}Co	^{109m}Ag	^{142}Ce	^{212}Bi	^{231}Pa	^{244}Cm
^{59}Ni	^{110}Ag	^{144}Ce	^{213}Bi	^{233}Pa	^{245}Cm
^{63}Ni	^{110m}Ag	^{143}Pr	^{214}Bi	^{234}Pa	^{246}Cm
^{64}Cu	^{109}Cd	^{144}Pr	^{209}Po	^{234m}Pa	^{247}Cm
^{65}Zn	^{113m}Cd	^{144m}Pr	^{210}Po	^{232}U	^{248}Cm
^{73}As	^{115m}Cd	^{146}Pm	^{211}Po	^{233}U	^{250}Cm
^{79}Se	^{114}In	^{147}Pm	^{212}Po	^{234}U	^{247}Bk
^{85}Kr	^{114m}In	^{148}Pm	^{213}Po	^{235}U	^{249}Bk
^{86}Rb	^{115m}In	^{148m}Pm	^{214}Po	^{236}U	^{250}Bk
^{87}Rb	^{119m}Sn	^{146}Sm	^{215}Po	^{237}U	^{249}Cf
^{89}Sr	^{121m}Sn	^{147}Sm	^{216}Po	^{238}U	^{250}Cf
^{90}Sr	^{123}Sn	^{151}Sm	^{218}Po	^{239}U	^{251}Cf
^{88}Y	^{126}Sn	^{150}Eu	^{211}At	^{240}U	^{252}Cf
^{90}Y	^{124}Sb	^{152}Eu	^{217}At	^{237}Np	^{254}Cf
^{90m}Y	^{125}Sb	^{154}Eu	^{219}Rn	^{238}Np	^{252}Es
^{91}Y	^{126}Sb	^{155}Eu	^{220}Rn	^{239}Np	^{253}Es
^{88}Zr	^{126m}Sb	^{152}Gd	^{222}Rn	^{240}Np	^{254}Es
^{90}Zr	^{123}Te	^{153}Gd	^{221}Fr	^{240m}Np	^{254m}Es

Table 2 – Neutron Flux-to-Dose Rate Conversion Factors [5]

Energy (MeV)	C(E) (n/cm^2-s to mrem/hr)	Energy (MeV)	C(E) (n/cm^2-s to mrem/hr)
2.50E-08	3.67E-03	5.00E-01	9.26E-02
1.00E-07	3.67E-03	1.0	1.32E-01
1.00E-06	4.46E-03	2.5	1.25E-01
1.00E-05	4.54E-03	5.0	1.56E-01
1.00E-04	4.18E-03	7.0	1.47E-01
1.00E-03	3.76E-03	10.0	1.47E-01
1.00E-02	3.56E-03	14.0	2.08E-01
1.00E-01	2.17E-02	20.0	2.27E-01

Table 3 – Gamma Flux-to-Dose Rate Conversion Factors [5]

Energy (MeV)	C(E) (γ/cm^2-s to mrem/hr)	Energy (MeV)	C(E) (γ/cm^2-s to mrem/hr)
0.100	2.83E-04	0.800	1.68E-03
0.150	3.79E-04	1.000	1.98E-03
0.200	5.01E-04	1.400	2.51E-03
0.250	6.31E-04	1.800	2.99E-03
0.300	7.59E-04	2.200	3.42E-03
0.350	8.78E-04	2.600	3.82E-03
0.400	9.85E-04	2.800	4.01E-03
0.450	1.08E-03	3.250	4.41E-03
0.500	1.17E-03	3.750	4.83E-03
0.550	1.27E-03	4.250	5.23E-03
0.600	1.36E-03	4.750	5.60E-03
0.650	1.44E-03	5.000	5.80E-03
0.700	1.52E-03		

Table 4 – Mass Attenuation Coefficients [10]

γ-Energy (MeV)	Silicon	Chromium	Manganese	Iron	Nickel	Lead
0.100	1.73E-01	2.92E-01	3.10E-01	3.43E-01	4.10E-01	5.36E+00
0.150	1.40E-01	1.67E-01	1.72E-01	1.83E-01	2.05E-01	1.92E+00
0.200	1.25E-01	1.31E-01	1.32E-01	1.38E-01	1.49E-01	9.43E-01
0.300	1.07E-01	1.04E-01	1.03E-01	1.06E-01	1.11E-01	3.77E-01
0.400	9.54E-02	9.04E-02	8.95E-02	9.20E-02	9.53E-02	2.17E-01
0.500	8.70E-02	8.17E-02	8.07E-02	8.28E-02	8.55E-02	1.51E-01
0.600	8.04E-02	7.52E-02	7.42E-02	7.61E-02	7.84E-02	1.18E-01
0.800	7.06E-02	6.57E-02	6.49E-02	6.64E-02	6.83E-02	8.47E-02
1.000	6.34E-02	5.90E-02	5.82E-02	5.96E-02	6.12E-02	6.84E-02
1.500	5.17E-02	4.81E-02	4.75E-02	4.86E-02	4.99E-02	5.10E-02
2.000	4.47E-02	4.20E-02	4.15E-02	4.25E-02	4.37E-02	4.54E-02
3.000	3.67E-02	3.55E-02	3.51E-02	3.61E-02	3.73E-02	4.20E-02
4.000	3.23E-02	3.23E-02	3.20E-02	3.30E-02	3.44E-02	4.18E-02
5.000	2.96E-02	3.05E-02	3.04E-02	3.14E-02	3.28E-02	4.26E-02

Table 5 – Iron Exposure Buildup Factor Coefficients [10]

γ-Energy (MeV)	b	c	a	X_K	d
0.100	1.389	0.557	0.144	14.11	-0.0791
0.150	1.660	0.743	0.079	14.12	-0.0476
0.200	1.839	0.911	0.034	13.23	-0.0334
0.300	1.973	1.095	-0.009	11.86	-0.0183
0.400	1.992	1.187	-0.027	10.72	-0.0140
0.500	1.967	1.240	-0.039	8.34	-0.0074
0.600	1.947	1.247	-0.040	8.20	-0.0096
0.800	1.906	1.233	-0.038	7.93	-0.0110
1.000	1.841	1.250	-0.048	19.49	0.0140
1.500	1.750	1.197	-0.040	15.90	0.0110
2.000	1.712	1.123	-0.021	7.97	-0.0057
3.000	1.627	1.059	-0.005	11.99	-0.0132
4.000	1.553	1.026	0.005	12.93	-0.0191
5.000	1.483	1.009	0.012	13.12	-0.0258

3.0 Shielding Model

3.1 *Configuration of Source and Shielding*

The calculation is concerned only with dose rates under hypothetical accident conditions (HAC). Under normal conditions of transport (NCT), the dose rates will be determined by measurement.

It is assumed that the waste remains within the shielded canister in which it is loaded. However, the waste in each shielded canister is conservatively assumed to configure into two point sources. 98% of the source is assumed to configure inside the polyethylene shielding, while the remaining 2% of the source is assumed to configure outside the polyethylene shielding but inside the canister. Treating the source as point sources conservatively neglects self shielding effects.

The 72-B cask geometry in the MCNP models is the same as in the baseline 72-B SAR neutron shielding analysis. The input file listed in Section 5.5.7 of the 72-B SAR is used as the basis for the geometry [1]. A sketch of the baseline 72-B model showing puncture damage is provided in Figure 1. The NS30 and NS15 shielded canister models are based upon the dimensions of [6], conservatively account for minimum tolerance shield thicknesses and maximum damage due to HAC drops, and are shown in Figure 2 and Figure 3. The side thicknesses are computed by subtracting the maximum scratch depth (¼-in from Note 3 of [6]) from the minimum thickness. The end thickness of 2.66-in is only applicable near the interface of the lid with the wall, as the ends are much thicker through the center. It is computed as (5-1/16)-(2+1/16)-1/4 = 2.63-in, where ¼-in is the scratch depth. This value is slightly different than the 2.66-in used, although the difference is negligible. The outer 0.25-in carbon steel of the shielded canisters is the same as the Waste Canister Assembly [7].

Under HAC, the limiting damage occurs when the package is dropped radially. If the drop is radial, it is assumed that the shielded canisters will shift to one side, as shown in Figure 2 and Figure 3. The dose rate location is 1-m from the crushed outer surface of the package.

The MCNP model geometry is shown in Figure 4 for both the NS30 and NS15. Sample MCNP input files are provided in Section 5.2.

The gamma point-kernel models are simplified and neglect attenuation in the polyethylene, although distance credit is taken for the polyethylene. Also, the outer steel layer in the gamma models is 1.635-in thick rather than the 1.625-in thick used in the neutron models. The actual value is 1.635-in, so using 1.625-in for the neutron models is conservative and is consistent with the baseline 72-B SAR neutron analysis.

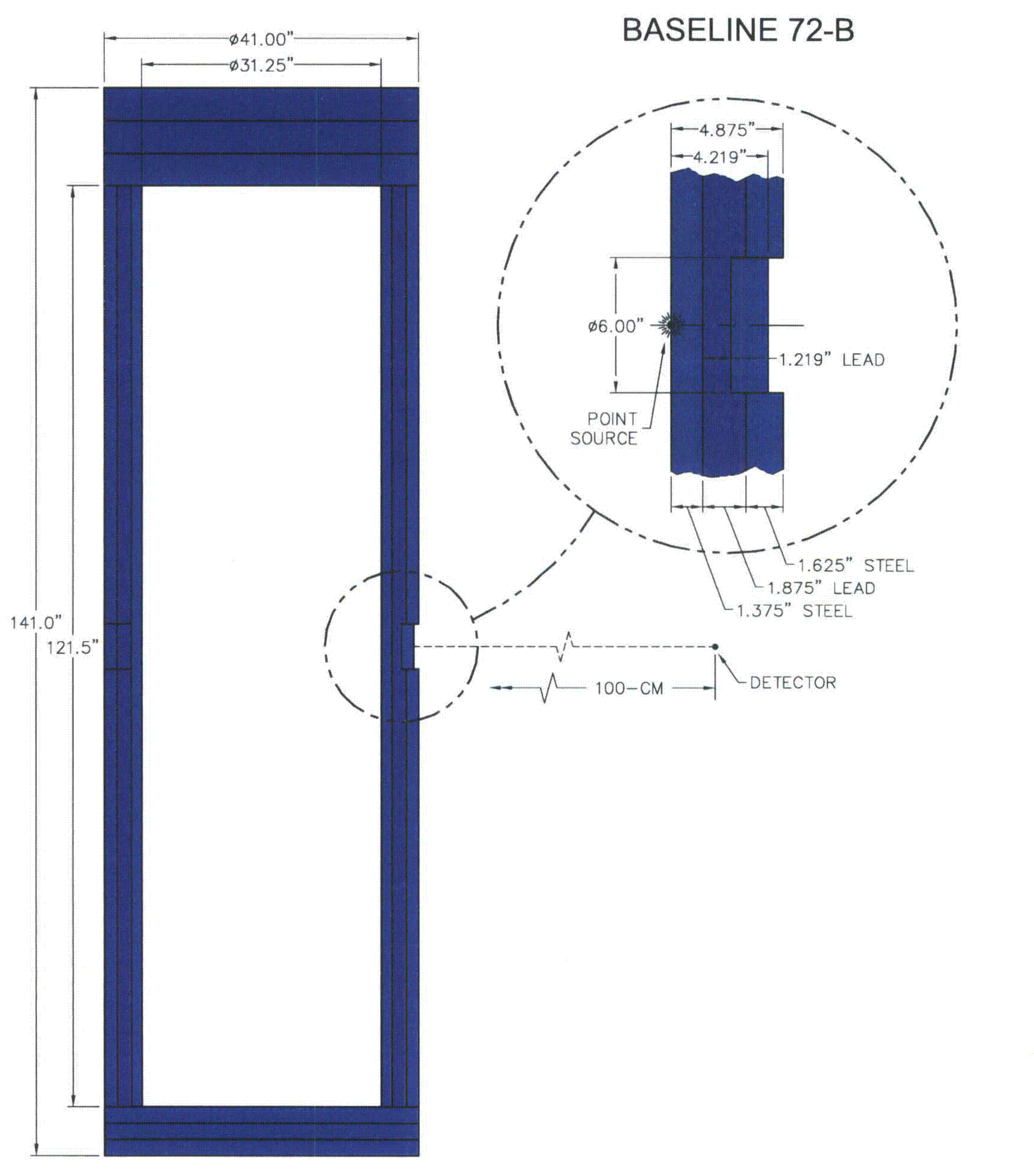

The point source is at the axial midpoint of the puncture bar damage and next to the inner radius. The detector is at 100 cm from package at the source elevation.

Figure 1 – 72-B Geometry (baseline SAR)

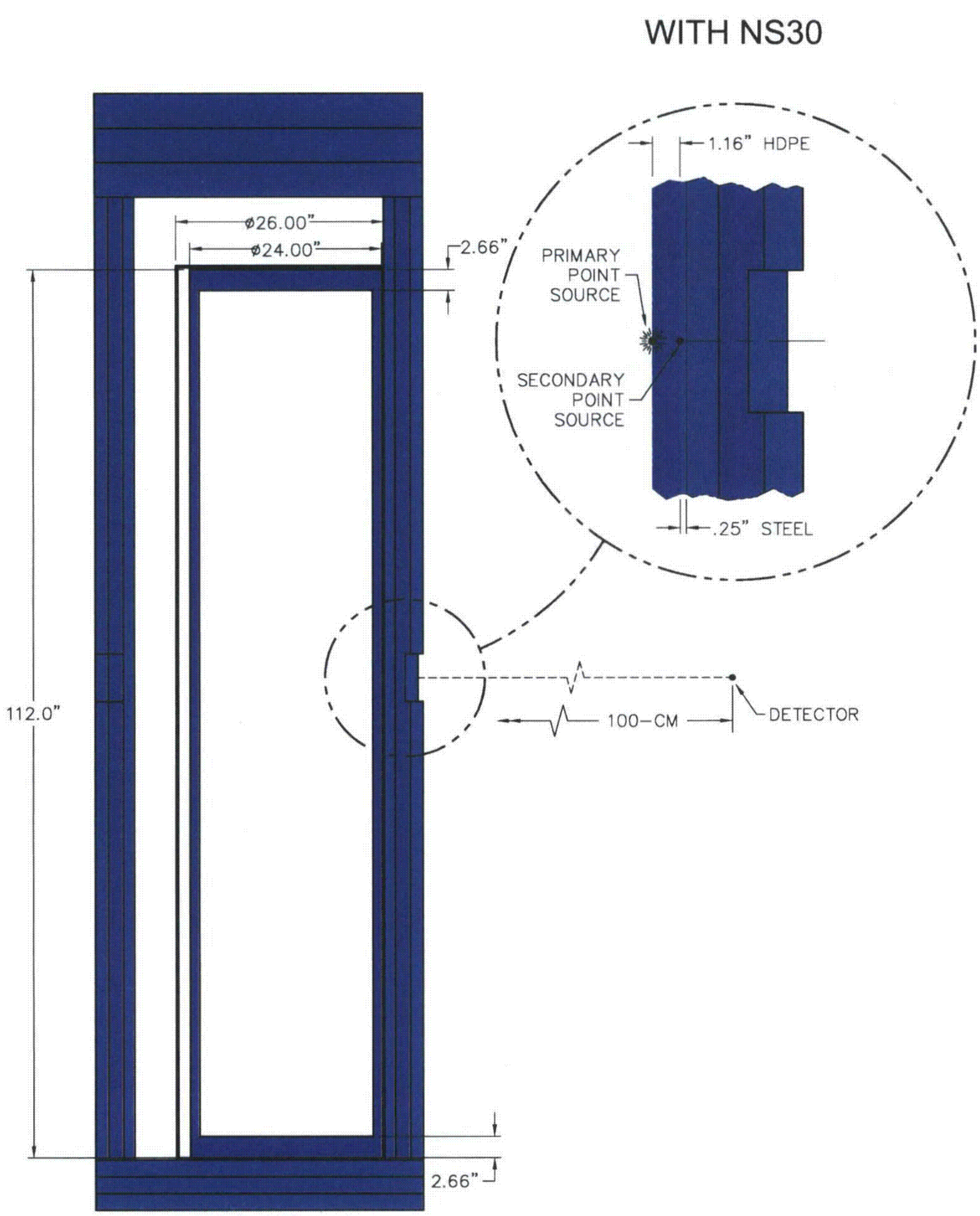

The primary point source (98% of total) is at the axial midpoint of the puncture bar damage and next to the inner radius of the HDPE body pipe. The secondary point source (2% of total) is at the axial midpoint of the puncture bar damage and next to the inner radius of the canister shell. The detector is at 100 cm from package at the source elevation.

Figure 2 – NS30 Geometry

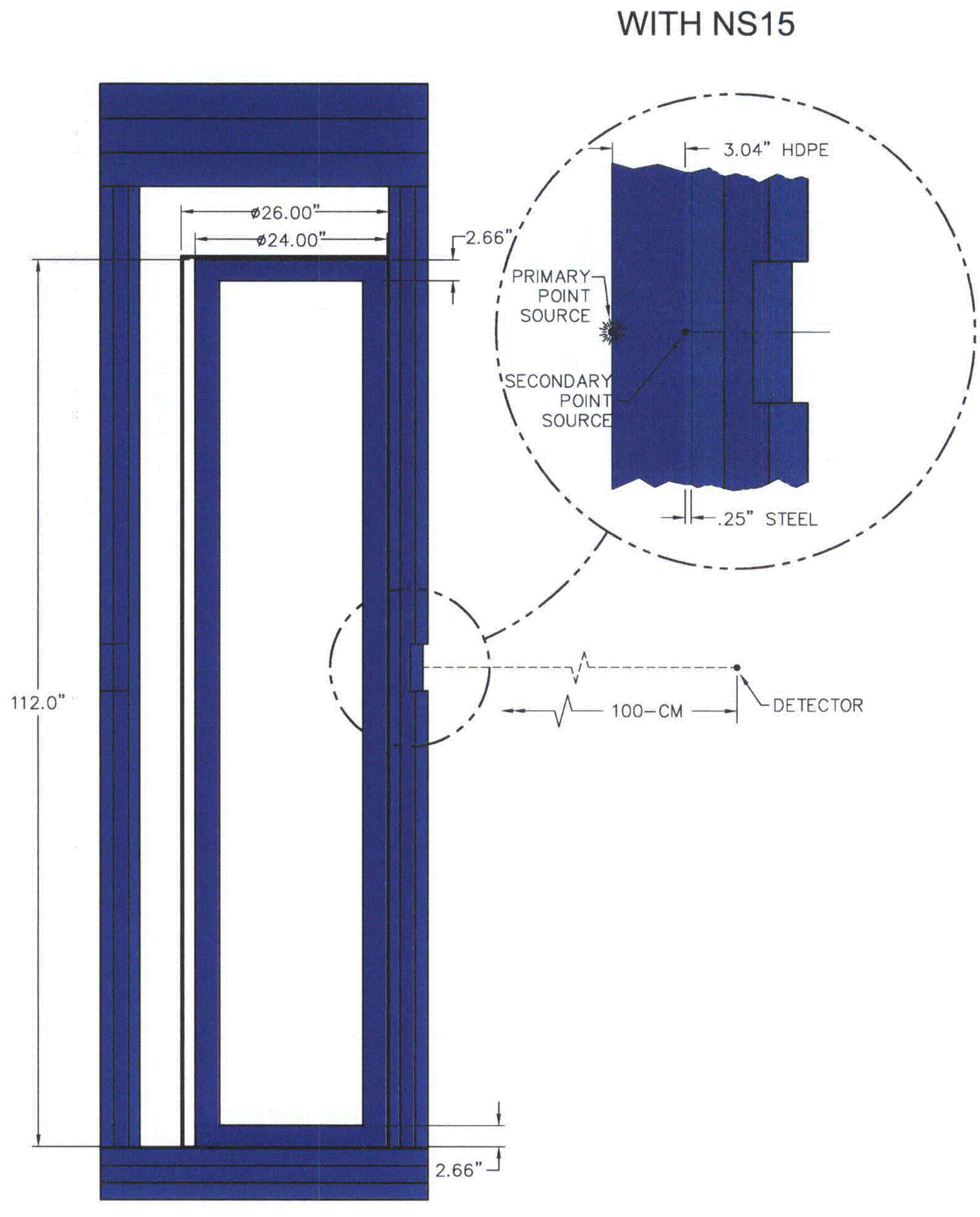

The primary point source (98% of total) is at the axial midpoint of the puncture bar damage and next to the inner radius of the HDPE body pipe. The secondary point source (2% of total) is at the axial midpoint of the puncture bar damage and next to the inner radius of the canister shell. The detector is at 100 cm from package at the source elevation.

Figure 3 – NS15 Geometry

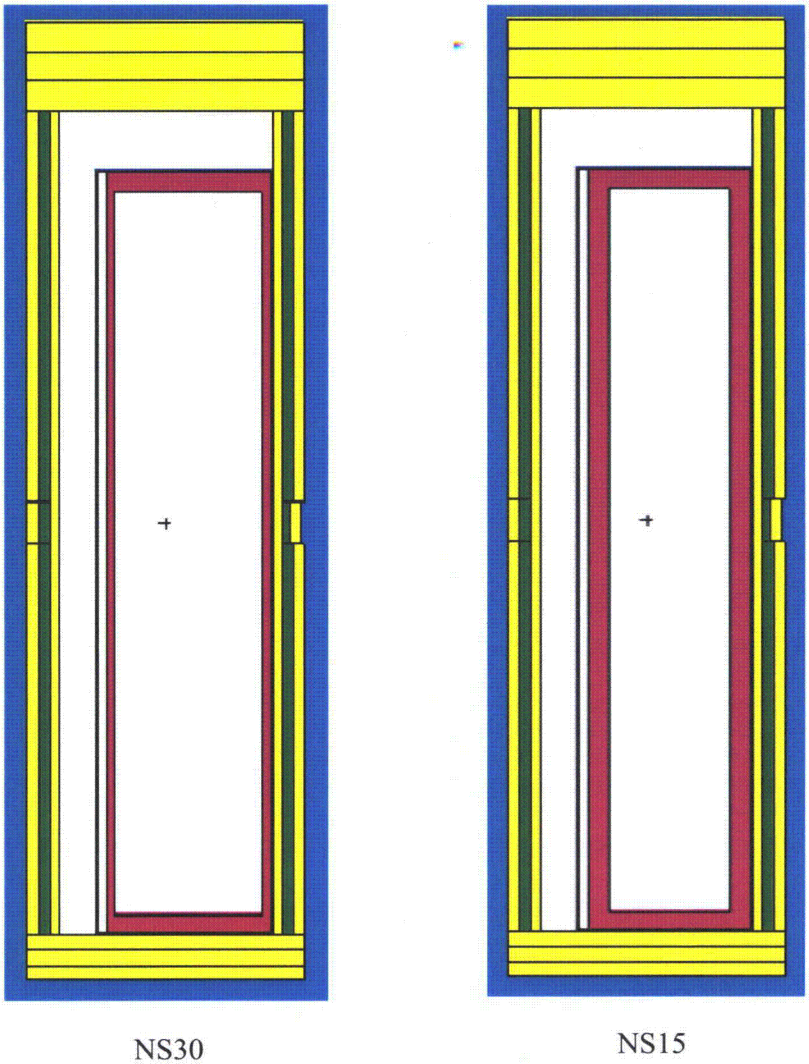

Figure 4 – MCNP Models

3.2 Material Properties

The shield regional densities for all shield materials are summarized in Table 6. Materials used in the analysis include lead, carbon steel, stainless steel, and high-density polyethylene. The metallic compositions and densities are used in both the point-kernel and MCNP analyses, although the polyethylene is used only in the MCNP analysis. The composition and densities are selected to be consistent with the RH-TRU 72B SAR [1]. Lead is modeled with a density of 11.35 g/cm^3. Carbon steel is modeled as pure iron with a density of 7.8526 g/cm^3. Stainless steel is modeled with a density of 8.0128 g/cm^3.

The polyethylene pipe is a high-density polyethylene (CH_2) material with a density of at least 0.94 g/cm^3 (per ASTM D3350 [11], cell classification #345444C, or better). The polyethylene is input to MCNP using a simple H:C atom ratio of 2:1. The S(α,β) card POLY.60T is also used to simulate hydrogen bound to carbon.

Table 6 – Summary of Shield Regional Densities

	Carbon Steel		Type 304 Stainless Steel		Lead	
Element	**Percent**	**Partial Density (g/cc)**	**Percent**	**Partial Density (g/cc)**	**Percent**	**Partial Density (g/cc)**
Silicon	—	—	1%	0.0801	—	—
Chromium	—	—	19%	1.5224	—	—
Manganese	—	—	2%	0.1603	—	—
Iron	100%	7.8526	68%	5.4487	—	—
Nickel	—	—	10%	0.8013	—	—
Lead	—	—	—	—	100%	11.3500
Total	*100%*	*7.8526*	*100%*	*8.0128*	*100%*	*11.3500*

4.0 Results

4.1 Neutron Results

The neutron activity limits are provided in Table 7 and Table 8, respectively, for the NS30 and NS15 shielded canisters. The MCNP statistical uncertainty is ≤ 1.0% in all cases, indicating a well-converged solution. The two point sources in the model have a combined source strength of 1 n/s. Therefore, the dose rate reported in Column B of Table 7 and Table 8 is very small. This dose rate is the combined neutron and secondary gamma dose rate. The secondary gamma dose rate is negligible because the gammas that are produced are shielded by the 72-B wall.

To determine the radioisotope mass to achieve a 1-m dose rate of 1000 mrem/hr, the limiting dose rate is divided by the dose rate for a 1 n/s source (including the subcritical neutron multiplication factor of 2.7), and by the total neutron source strength for 1 g of material. This mass (which is a total mass for both sources) is provided in Column C of Table 7 and Table 8. To convert to a total neutron activity limit for the package, this total mass is multiplied by the specific activity. The final result is provided in Column E of Table 7 and Table 8.

4.2 Gamma Results

The gamma activity limits are determined by application of the point-kernel model as implemented in MathCAD Version 13.1. The MathCAD application considers both point sources, although the final results are reported for the combined source. The results are reported in Table 9. For convenience, this table includes all isotopes, including non-gamma emitters, which are assigned an allowable activity of 1.000E99 Ci.

An example NS30 calculation is provided in Section 5.3 for Co-60.

4.3 Combined Results

For isotopes that are both gamma and neutron emitters, the total activity limit is determined by combining the gamma and neutron results using the following equation: $1/[(1/A_G)+(1/A_N)]$. The limits are reported in Table 10.

The sum of dose rate partial fractions for any combination of the radionuclides must be less than or equal to unity, or:

$$\sum_{i=1}^{n} \frac{a_i}{A_{GN_i}} \leq 1$$

where, for a particular payload mix, a_i is the actual curie content of radionuclide "i" and A_{GNi} is the limiting curie content of radionuclide "i" given in Table 10.

For example, 38.35 curies of ^{60}Co, 586.7 curies of ^{95}Zr, and 2609 curies of ^{242}Pu each result in a limiting HAC dose rate of 1000 mrem/hr at a distance of 1-m from the package surface for an NS30 shielded canister. The sum of the partial fractions for a payload containing 10.0 curies of ^{60}Co, 200.0 curies of ^{95}Zr, and 1000.0 curies of ^{242}Pu in an NS30 shielded canister is:

$$\frac{a_{60_{Co}}}{A_{GN_{60_{Co}}}} + \frac{a_{95_{Zr}}}{A_{GN_{95_{Zr}}}} + \frac{a_{242_{Pu}}}{A_{GN_{242_{Pu}}}} = \frac{10}{38.35} + \frac{200}{586.7} + \frac{1000}{2609} = 0.26 + 0.34 + 0.38 = 0.98 \leq 1.00$$

Thus, the combination of isotopes for the above example will not exceed the HAC limiting dose rate.

Table 7 – Neutron Activity Calculations, NS30

	A	B		C = 1000/(2.7*A*B)	D	E = C*D
Radio-nuclide	Source Strength (n/s/g) [2]	Dose Rate from 1 n/s source (mrem/hr)	σ	Total Mass for 1000 mrem/hr at 1-m (g)	Specific Activity (Ci/g) [1]	Activity 1000 mrem/hr at 1-m, (Ci), A_N
^{230}Th	9.13E+00	3.76E-07	0.26%	1.08E+08	2.10E-02	2.27E+06
^{232}Th	2.28E-05	3.58E-07	0.27%	4.54E+13	1.10E-07	4.99E+06
^{231}Pa	2.64E+01	3.79E-07	0.26%	3.70E+07	4.70E-02	1.74E+06
^{232}U	1.50E+04	3.83E-07	0.26%	6.44E+04	2.20E+01	1.42E+06
^{233}U	4.83E+00	3.76E-07	0.26%	2.04E+08	9.70E-03	1.98E+06
^{234}U	3.03E+00	3.76E-07	0.26%	3.25E+08	6.20E-03	2.02E+06
^{235}U	1.02E-03	3.53E-07	0.27%	1.03E+12	2.20E-06	2.26E+06
^{236}U	2.94E-02	3.61E-07	0.27%	3.49E+10	6.50E-05	2.27E+06
^{238}U	1.37E-02	2.95E-07	0.30%	9.17E+10	3.40E-07	3.12E+04
^{237}Np	3.43E-01	3.76E-07	0.26%	2.87E+09	7.10E-04	2.04E+06
^{236}Pu	5.33E+05	3.91E-07	0.26%	1.78E+03	5.30E+02	9.41E+05
^{238}Pu	1.62E+04	3.78E-07	0.27%	6.05E+04	1.70E+01	1.03E+06
^{239}Pu	3.86E+01	3.80E-07	0.26%	2.52E+07	6.20E-02	1.57E+06
^{240}Pu	1.17E+03	3.24E-07	0.29%	9.77E+05	2.30E-01	2.25E+05
^{241}Pu	1.35E+00	3.75E-07	0.26%	7.31E+08	1.00E+02	7.31E+10
^{242}Pu	1.72E+03	3.22E-07	0.29%	6.69E+05	3.90E-03	2.61E+03
^{244}Pu	1.90E+03	3.02E-07	0.29%	6.45E+05	1.80E-05	1.16E+01
^{241}Am	2.71E+03	3.87E-07	0.26%	3.53E+05	3.40E+00	1.20E+06
^{242m}Am	1.65E+02	3.42E-07	0.28%	6.56E+06	1.00E+01	6.56E+07
^{243}Am	1.40E+02	3.81E-07	0.26%	6.94E+06	2.00E-01	1.39E+06
^{240}Cm	9.48E+07	3.70E-07	0.28%	1.06E+01	2.00E+04	2.11E+05
^{242}Cm	2.48E+07	3.44E-07	0.28%	4.34E+01	3.30E+03	1.43E+05
^{243}Cm	4.10E+05	3.50E-07	0.29%	2.58E+03	5.20E+01	1.34E+05
^{244}Cm	1.09E+07	3.34E-07	0.30%	1.02E+02	8.10E+01	8.25E+03
^{245}Cm	3.82E+03	3.38E-07	0.29%	2.87E+05	1.72E-01	4.94E+04
^{246}Cm	9.68E+06	3.31E-07	0.30%	1.15E+02	3.10E-01	3.58E+01
^{248}Cm	4.03E+07	3.19E-07	0.29%	2.88E+01	4.20E-03	1.21E-01
^{250}Cm	1.25E+10	2.97E-07	0.30%	9.96E-02	1.50E-01	1.49E-02
^{249}Bk	1.65E+05	3.05E-07	0.30%	7.35E+03	1.60E+03	1.18E+07
^{249}Cf	6.26E+03	3.82E-07	0.27%	1.55E+05	4.10E+00	6.35E+05
^{250}Cf	1.08E+10	3.63E-07	0.28%	9.45E-02	1.10E+02	1.04E+01
^{251}Cf	1.52E+03	3.95E-07	0.26%	6.16E+05	1.60E+00	9.86E+05
^{252}Cf	2.05E+12	3.69E-07	0.28%	4.89E-04	5.40E+02	2.64E-01
^{254}Cf	1.05E+15	3.72E-07	0.27%	9.49E-07	8.50E+03	8.07E-03
^{253}Es	3.13E+08	3.73E-07	0.28%	3.17E+00	2.50E+04	7.93E+04
^{254}Es	9.43E+06	3.80E-07	0.27%	1.03E+02	1.90E+03	1.97E+05
^{254m}Es	1.94E+13	3.67E-07	0.28%	5.20E-05	3.10E+05	1.61E+01

Table 8 – Neutron Activity Calculations, NS15

	A	B		C = 1000/(2.7*A*B)	D	E = C*D
Radio-nuclide	Source Strength (n/s/g) [2]	Dose Rate from 1 n/s source (mrem/hr)	σ	Total Mass for 1000 mrem/hr at 1-m (g)	Specific Activity (Ci/g) [1]	Activity 1000 mrem/hr at 1-m, (Ci), A_N
^{230}Th	9.13E+00	1.28E-07	0.47%	3.16E+08	2.10E-02	6.64E+06
^{232}Th	2.28E-05	1.13E-07	0.48%	1.43E+14	1.10E-07	1.58E+07
^{231}Pa	2.64E+01	1.32E-07	0.45%	1.07E+08	4.70E-02	5.01E+06
^{232}U	1.50E+04	1.36E-07	0.45%	1.81E+05	2.20E+01	3.98E+06
^{233}U	4.83E+00	1.29E-07	0.46%	5.92E+08	9.70E-03	5.75E+06
^{234}U	3.03E+00	1.28E-07	0.45%	9.53E+08	6.20E-03	5.91E+06
^{235}U	1.02E-03	1.19E-07	0.49%	3.04E+12	2.20E-06	6.69E+06
^{236}U	2.94E-02	1.21E-07	0.49%	1.04E+11	6.50E-05	6.75E+06
^{238}U	1.37E-02	9.77E-08	0.61%	2.77E+11	3.40E-07	9.41E+04
^{237}Np	3.43E-01	1.29E-07	0.46%	8.37E+09	7.10E-04	5.94E+06
^{236}Pu	5.33E+05	1.43E-07	0.45%	4.85E+03	5.30E+02	2.57E+06
^{238}Pu	1.62E+04	1.35E-07	0.45%	1.69E+05	1.70E+01	2.88E+06
^{239}Pu	3.86E+01	1.33E-07	0.45%	7.19E+07	6.20E-02	4.46E+06
^{240}Pu	1.17E+03	1.14E-07	0.50%	2.79E+06	2.30E-01	6.41E+05
^{241}Pu	1.35E+00	1.30E-07	0.46%	2.11E+09	1.00E+02	2.11E+11
^{242}Pu	1.72E+03	1.13E-07	0.52%	1.91E+06	3.90E-03	7.43E+03
^{244}Pu	1.90E+03	1.02E-07	0.54%	1.91E+06	1.80E-05	3.43E+01
^{241}Am	2.71E+03	1.39E-07	0.45%	9.83E+05	3.40E+00	3.34E+06
^{242m}Am	1.65E+02	1.23E-07	0.49%	1.83E+07	1.00E+01	1.83E+08
^{243}Am	1.40E+02	1.34E-07	0.45%	1.97E+07	2.00E-01	3.94E+06
^{240}Cm	9.48E+07	1.41E-07	0.46%	2.78E+01	2.00E+04	5.55E+05
^{242}Cm	2.48E+07	1.25E-07	0.48%	1.20E+02	3.30E+03	3.95E+05
^{243}Cm	4.10E+05	1.30E-07	0.49%	6.93E+03	5.20E+01	3.60E+05
^{244}Cm	1.09E+07	1.22E-07	0.49%	2.79E+02	8.10E+01	2.26E+04
^{245}Cm	3.82E+03	1.22E-07	0.49%	7.95E+05	1.72E-01	1.37E+05
^{246}Cm	9.68E+06	1.19E-07	0.52%	3.21E+02	3.10E-01	9.94E+01
^{248}Cm	4.03E+07	1.13E-07	0.53%	8.16E+01	4.20E-03	3.43E-01
^{250}Cm	1.25E+10	1.01E-07	0.53%	2.93E-01	1.50E-01	4.40E-02
^{249}Bk	1.65E+05	1.05E-07	0.53%	2.15E+04	1.60E+03	3.44E+07
^{249}Cf	6.26E+03	1.42E-07	0.44%	4.16E+05	4.10E+00	1.70E+06
^{250}Cf	1.08E+10	1.41E-07	0.47%	2.43E-01	1.10E+02	2.67E+01
^{251}Cf	1.52E+03	1.45E-07	0.44%	1.68E+06	1.60E+00	2.68E+06
^{252}Cf	2.05E+12	1.45E-07	0.48%	1.25E-03	5.40E+02	6.75E-01
^{254}Cf	1.05E+15	1.47E-07	0.47%	2.40E-06	8.50E+03	2.04E-02
^{253}Es	3.13E+08	1.46E-07	0.45%	8.10E+00	2.50E+04	2.02E+05
^{254}Es	9.43E+06	1.47E-07	0.45%	2.67E+02	1.90E+03	5.07E+05
^{254m}Es	1.94E+13	1.45E-07	0.47%	1.32E-04	3.10E+05	4.09E+01

Table 9 – Gamma Activity Calculations

Radionuclide Name	NS30 Gamma HAC @1-m	NS15 Gamma HAC @1-m
^{3}H	1.000E+99	1.000E+99
^{10}Be	1.000E+99	1.000E+99
^{14}C	1.000E+99	1.000E+99
^{22}Na	7.410E+01	8.026E+01
^{32}P	1.000E+99	1.000E+99
^{33}P	1.000E+99	1.000E+99
^{35}S	1.000E+99	1.000E+99
^{45}Ca	1.035E+89	1.121E+89
^{46}Sc	7.429E+01	8.047E+01
^{49}V	1.000E+99	1.000E+99
^{51}Cr	2.604E+08	2.821E+08
^{54}Mn	3.093E+02	3.350E+02
^{55}Fe	1.000E+99	1.000E+99
^{59}Fe	9.029E+01	9.780E+01
^{57}Co	5.521E+05	5.980E+05
^{58}Co	3.286E+02	3.559E+02
^{60}Co	3.835E+01	4.154E+01
^{59}Ni	1.000E+99	1.000E+99
^{63}Ni	1.000E+99	1.000E+99
^{64}Cu	1.321E+04	1.431E+04
^{65}Zn	2.151E+02	2.330E+02
^{73}As	2.977E+82	3.225E+82
^{79}Se	1.000E+99	1.000E+99
^{85}Kr	1.614E+06	1.748E+06
^{86}Rb	1.385E+03	1.501E+03
^{87}Rb	1.000E+99	1.000E+99
^{89}Sr	2.295E+06	2.486E+06
^{90}Sr	1.000E+99	1.000E+99
^{88}Y	2.616E+01	2.833E+01
^{90}Y	1.563E+09	1.693E+09
^{90m}Y	1.574E+04	1.705E+04
^{91}Y	3.369E+04	3.649E+04
^{88}Zr	2.320E+05	2.513E+05
^{90}Zr	1.000E+99	1.000E+99
^{90m}Zr	1.000E+99	1.000E+99
^{93}Zr	5.574E+86	6.038E+86
^{95}Zr	5.867E+02	6.355E+02
^{93m}Nb	5.438E+86	5.890E+86
^{94}Nb	1.986E+02	2.151E+02
^{95}Nb	4.819E+02	5.220E+02
^{95m}Nb	1.600E+06	1.733E+06
^{99}Tc	4.777E+86	5.174E+86
^{99m}Tc	2.281E+13	2.471E+13
^{103}Ru	7.537E+03	8.164E+03
^{106}Ru	1.000E+99	1.000E+99
^{103m}Rh	4.566E+84	4.946E+84
^{106}Rh	2.294E+03	2.485E+03
^{107}Pd	1.000E+99	1.000E+99
^{108}Ag	6.243E+04	6.762E+04
^{108m}Ag	5.330E+02	5.774E+02
^{109m}Ag	8.391E+82	9.089E+82
^{110}Ag	2.075E+04	2.247E+04
^{110m}Ag	6.633E+01	7.184E+01
^{109}Cd	8.391E+82	9.089E+82
^{113m}Cd	1.194E+15	1.293E+15
^{115m}Cd	4.145E+03	4.490E+03
^{114}In	4.990E+04	5.405E+04
^{114m}In	1.762E+04	1.908E+04
^{115m}In	9.785E+06	1.060E+07
^{119m}Sn	1.926E+82	2.086E+82
^{121m}Sn	1.678E+83	1.818E+83
^{123}Sn	1.844E+04	1.998E+04
^{126}Sn	4.870E+81	5.274E+81
^{124}Sb	5.266E+01	5.704E+01
^{125}Sb	4.385E+03	4.750E+03
^{126}Sb	2.007E+02	2.174E+02
^{126m}Sb	4.830E+02	5.232E+02
^{123}Te	1.000E+99	1.000E+99
^{123m}Te	2.997E+18	3.246E+18
^{125m}Te	6.599E+47	7.148E+47
^{127}Te	8.607E+06	9.322E+06
^{127m}Te	8.364E+06	9.059E+06
^{129}Te	1.295E+04	1.403E+04
^{129m}Te	1.784E+04	1.932E+04
^{125}I	4.648E+82	5.034E+82
^{129}I	4.134E+82	4.478E+82

Radionuclide Name	NS30 Gamma HAC @1-m	NS15 Gamma HAC @1-m
^{131}I	1.252E+04	1.356E+04
^{134}Cs	2.573E+02	2.786E+02
^{135}Cs	1.000E+99	1.000E+99
^{137}Cs	1.335E+03	1.446E+03
^{133}Ba	2.071E+06	2.243E+06
^{137}Ba	1.000E+99	1.000E+99
^{137m}Ba	1.260E+03	1.365E+03
^{141}Ce	1.072E+39	1.161E+39
^{142}Ce	1.000E+99	1.000E+99
^{144}Ce	7.053E+51	7.639E+51
^{143}Pr	4.865E+10	5.270E+10
^{144}Pr	2.518E+03	2.728E+03
^{144m}Pr	7.758E+04	8.403E+04
^{146}Pm	9.887E+02	1.071E+03
^{147}Pm	1.230E+27	1.333E+27
^{148}Pm	1.853E+02	2.007E+02
^{148m}Pm	2.712E+02	2.937E+02
^{146}Sm	1.000E+99	1.000E+99
^{147}Sm	1.000E+99	1.000E+99
^{151}Sm	9.888E+84	1.071E+85
^{150}Eu	2.894E+02	3.135E+02
^{152}Eu	1.209E+02	1.309E+02
^{154}Eu	1.166E+02	1.263E+02
^{155}Eu	2.181E+41	2.363E+41
^{152}Gd	1.000E+99	1.000E+99
^{153}Gd	7.414E+29	8.030E+29
^{160}Tb	1.451E+02	1.572E+02
^{166m}Ho	2.699E+02	2.924E+02
^{168}Tm	3.229E+02	3.497E+02
^{182}Ta	9.435E+01	1.022E+02
^{198}Au	3.235E+04	3.504E+04
^{207}Tl	8.879E+04	9.618E+04
^{208}Tl	1.702E+01	1.843E+01
^{209}Tl	4.020E+01	4.354E+01
^{209}Pb	1.000E+99	1.000E+99
^{210}Pb	7.305E+82	7.913E+82
^{211}Pb	6.723E+03	7.282E+03
^{212}Pb	6.384E+07	6.915E+07
^{214}Pb	2.070E+04	2.242E+04

Radionuclide Name	NS30 Gamma HAC @1-m	NS15 Gamma HAC @1-m
^{207}Bi	1.170E+02	1.267E+02
^{210}Bi	1.000E+99	1.000E+99
^{211}Bi	2.575E+07	2.789E+07
^{212}Bi	1.412E+03	1.529E+03
^{213}Bi	1.986E+04	2.152E+04
^{214}Bi	5.869E+01	6.357E+01
^{209}Po	4.941E+04	5.352E+04
^{210}Po	2.967E+07	3.214E+07
^{211}Po	3.830E+04	4.149E+04
^{212}Po	1.000E+99	1.000E+99
^{213}Po	9.015E+06	9.765E+06
^{214}Po	1.000E+99	1.000E+99
^{215}Po	1.193E+08	1.292E+08
^{216}Po	1.874E+07	2.030E+07
^{218}Po	1.000E+99	1.000E+99
^{211}At	3.463E+05	3.751E+05
^{217}At	1.761E+07	1.908E+07
^{219}Rn	1.073E+06	1.162E+06
^{220}Rn	3.551E+06	3.846E+06
^{222}Rn	9.805E+06	1.062E+07
^{221}Fr	7.038E+07	7.623E+07
^{223}Fr	4.316E+04	4.675E+04
^{223}Ra	7.889E+05	8.545E+05
^{224}Ra	2.376E+07	2.573E+07
^{225}Ra	1.035E+82	1.121E+82
^{226}Ra	3.748E+08	4.060E+08
^{228}Ra	1.622E+83	1.757E+83
^{225}Ac	3.079E+06	3.335E+06
^{227}Ac	2.345E+18	2.540E+18
^{228}Ac	1.821E+02	1.973E+02
^{227}Th	1.695E+06	1.836E+06
^{228}Th	1.396E+09	1.512E+09
^{229}Th	1.878E+12	2.034E+12
^{230}Th	5.670E+10	6.141E+10
^{231}Th	1.029E+12	1.115E+12
^{232}Th	1.429E+47	1.548E+47
^{234}Th	5.999E+72	6.498E+72
^{231}Pa	1.237E+07	1.340E+07
^{233}Pa	3.281E+06	3.554E+06

Radionuclide Name	NS30 Gamma HAC @1-m	NS15 Gamma HAC @1-m
^{234}Pa	1.442E+02	1.562E+02
^{234m}Pa	8.910E+03	9.651E+03
^{232}U	6.159E+09	6.671E+09
^{233}U	5.671E+10	6.143E+10
^{234}U	1.084E+10	1.174E+10
^{235}U	5.308E+08	5.749E+08
^{236}U	1.000E+74	1.083E+74
^{237}U	3.699E+08	4.006E+08
^{238}U	3.976E+73	4.306E+73
^{239}U	3.271E+04	3.543E+04
^{240}U	7.511E+11	8.135E+11
^{237}Np	3.704E+14	4.012E+14
^{238}Np	2.327E+02	2.521E+02
^{239}Np	5.248E+07	5.684E+07
^{240}Np	2.642E+02	2.862E+02
^{240m}Np	8.578E+02	9.291E+02
^{236}Pu	4.185E+08	4.533E+08
^{238}Pu	1.194E+09	1.293E+09
^{239}Pu	8.150E+08	8.828E+08
^{240}Pu	6.255E+09	6.775E+09
^{241}Pu	6.033E+37	6.535E+37
^{242}Pu	2.064E+36	2.236E+36
^{243}Pu	6.709E+07	7.266E+07
^{244}Pu	1.000E+99	1.000E+99
^{241}Am	1.243E+08	1.347E+08
^{242}Am	2.250E+85	2.437E+85
^{242m}Am	1.418E+33	1.536E+33
^{243}Am	7.953E+07	8.614E+07
^{245}Am	1.164E+11	1.261E+11
^{240}Cm	1.000E+99	1.000E+99
^{242}Cm	3.960E+08	4.289E+08
^{243}Cm	1.996E+10	2.162E+10
^{244}Cm	3.328E+08	3.604E+08
^{245}Cm	4.843E+23	5.246E+23
^{246}Cm	1.000E+99	1.000E+99
^{247}Cm	1.867E+05	2.022E+05
^{248}Cm	1.000E+99	1.000E+99
^{250}Cm	1.000E+99	1.000E+99
^{247}Bk	6.863E+11	7.434E+11

Radionuclide Name	NS30 Gamma HAC @1-m	NS15 Gamma HAC @1-m
^{249}Bk	8.999E+13	9.747E+13
^{250}Bk	1.628E+02	1.763E+02
^{249}Cf	4.234E+05	4.586E+05
^{250}Cf	2.219E+85	2.404E+85
^{251}Cf	8.846E+10	9.581E+10
^{252}Cf	4.591E+37	4.972E+37
^{254}Cf	1.000E+99	1.000E+99
^{252}Es	1.744E+03	1.889E+03
^{253}Es	1.408E+08	1.525E+08
^{254}Es	6.055E+08	6.558E+08
^{254m}Es	1.554E+03	1.684E+03

Table 10 – Summary of HAC Activity Limits

Radio-nuclide	Gamma Emitter	Neutron Emitter	NS30 HAC @ 1-m Maximum Allowable Activity (Ci), A_{GN}	NS15 HAC @ 1-m Maximum Allowable Activity (Ci), A_{GN}
^{3}H			unlimited	unlimited
^{10}Be			unlimited	unlimited
^{14}C			unlimited	unlimited
^{22}Na	×		7.410E+01	8.026E+01
^{32}P			unlimited	unlimited
^{33}P			unlimited	unlimited
^{35}S			unlimited	unlimited
^{45}Ca	×		unlimited	unlimited
^{46}Sc	×		7.429E+01	8.047E+01
^{49}V			unlimited	unlimited
^{51}Cr	×		unlimited	unlimited
^{54}Mn	×		3.093E+02	3.350E+02
^{55}Fe			unlimited	unlimited
^{59}Fe	×		9.029E+01	9.780E+01
^{57}Co	×		5.521E+05	5.980E+05
^{58}Co	×		3.286E+02	3.559E+02
^{60}Co	×		3.835E+01	4.154E+01
^{59}Ni			unlimited	unlimited
^{63}Ni			unlimited	unlimited
^{64}Cu	×		1.321E+04	1.431E+04
^{65}Zn	×		2.151E+02	2.330E+02
^{73}As	×		unlimited	unlimited
^{79}Se			unlimited	unlimited
^{85}Kr	×		1.614E+06	1.748E+06
^{86}Rb	×		1.385E+03	1.501E+03
^{87}Rb			unlimited	unlimited
^{89}Sr	×		2.295E+06	2.486E+06
^{90}Sr			unlimited	unlimited
^{88}Y	×		2.616E+01	2.833E+01
^{90}Y	×		unlimited	unlimited
^{90m}Y	×		1.574E+04	1.705E+04
^{91}Y	×		3.369E+04	3.649E+04
^{88}Zr	×		2.320E+05	2.513E+05
^{90}Zr			unlimited	unlimited
^{90m}Zr			unlimited	unlimited
^{93}Zr	×		unlimited	unlimited
^{95}Zr	×		5.867E+02	6.355E+02
^{93m}Nb	×		unlimited	unlimited
^{94}Nb	×		1.986E+02	2.151E+02
^{95}Nb	×		4.819E+02	5.220E+02
^{95m}Nb	×		1.600E+06	1.733E+06
^{99}Tc	×		unlimited	unlimited
^{99m}Tc	×		unlimited	unlimited
^{103}Ru	×		7.537E+03	8.164E+03
^{106}Ru			unlimited	unlimited
^{103m}Rh	×		unlimited	unlimited
^{106}Rh	×		2.294E+03	2.485E+03
^{107}Pd			unlimited	unlimited
^{108}Ag	×		6.243E+04	6.762E+04
^{108m}Ag	×		5.330E+02	5.774E+02
^{109m}Ag	×		unlimited	unlimited
^{110}Ag	×		2.075E+04	2.247E+04
^{110m}Ag	×		6.633E+01	7.184E+01
^{109}Cd	×		unlimited	unlimited
^{113m}Cd	×		unlimited	unlimited
^{115m}Cd	×		4.145E+03	4.490E+03
^{114}In	×		4.990E+04	5.405E+04
^{114m}In	×		1.762E+04	1.908E+04
^{115m}In	×		9.785E+06	1.060E+07
^{119m}Sn	×		unlimited	unlimited
^{121m}Sn	×		unlimited	unlimited
^{123}Sn	×		1.844E+04	1.998E+04
^{126}Sn	×		unlimited	unlimited
^{124}Sb	×		5.266E+01	5.704E+01
^{125}Sb	×		4.385E+03	4.750E+03
^{126}Sb	×		2.007E+02	2.174E+02
^{126m}Sb	×		4.830E+02	5.232E+02
^{123}Te			unlimited	unlimited
^{123m}Te	×		unlimited	unlimited
^{125m}Te	×		unlimited	unlimited

Radio-nuclide	Gamma Emitter	Neutron Emitter	NS30 HAC @ 1-m Maximum Allowable Activity (Ci), A_{GN}	NS15 HAC @ 1-m Maximum Allowable Activity (Ci), A_{GN}
^{127}Te	×		8.607E+06	9.322E+06
^{127m}Te	×		8.364E+06	9.059E+06
^{129}Te	×		1.295E+04	1.403E+04
^{129m}Te	×		1.784E+04	1.932E+04
^{125}I	×		unlimited	unlimited
^{129}I	×		unlimited	unlimited
^{131}I	×		1.252E+04	1.356E+04
^{134}Cs	×		2.573E+02	2.786E+02
^{135}Cs			unlimited	unlimited
^{137}Cs	×		1.335E+03	1.446E+03
^{133}Ba	×		2.071E+06	2.243E+06
^{137}Ba			unlimited	unlimited
^{137m}Ba	×		1.260E+03	1.365E+03
^{141}Ce	×		unlimited	unlimited
^{142}Ce			unlimited	unlimited
^{144}Ce	×		unlimited	unlimited
^{143}Pr	×		unlimited	unlimited
^{144}Pr	×		2.518E+03	2.728E+03
^{144m}Pr	×		7.758E+04	8.403E+04
^{146}Pm	×		9.887E+02	1.071E+03
^{147}Pm	×		unlimited	unlimited
^{148}Pm	×		1.853E+02	2.007E+02
^{148m}Pm	×		2.712E+02	2.937E+02
^{146}Sm			unlimited	unlimited
^{147}Sm			unlimited	unlimited
^{151}Sm	×		unlimited	unlimited
^{150}Eu	×		2.894E+02	3.135E+02
^{152}Eu	×		1.209E+02	1.309E+02
^{154}Eu	×		1.166E+02	1.263E+02
^{155}Eu	×		unlimited	unlimited
^{152}Gd			unlimited	unlimited
^{153}Gd	×		unlimited	unlimited
^{160}Tb	×		1.451E+02	1.572E+02
^{166m}Ho	×		2.699E+02	2.924E+02
^{168}Tm	×		3.229E+02	3.497E+02
^{182}Ta	×		9.435E+01	1.022E+02
^{198}Au	×		3.235E+04	3.504E+04

Radio-nuclide	Gamma Emitter	Neutron Emitter	NS30 HAC @ 1-m Maximum Allowable Activity (Ci), A_{GN}	NS15 HAC @ 1-m Maximum Allowable Activity (Ci), A_{GN}
^{207}Tl	×		8.879E+04	9.618E+04
^{208}Tl	×		1.702E+01	1.843E+01
^{209}Tl	×		4.020E+01	4.354E+01
^{209}Pb			unlimited	unlimited
^{210}Pb	×		unlimited	unlimited
^{211}Pb	×		6.723E+03	7.282E+03
^{212}Pb	×		6.384E+07	6.915E+07
^{214}Pb	×		2.070E+04	2.242E+04
^{207}Bi	×		1.170E+02	1.267E+02
^{210}Bi			unlimited	unlimited
^{211}Bi	×		2.575E+07	2.789E+07
^{212}Bi	×		1.412E+03	1.529E+03
^{213}Bi	×		1.986E+04	2.152E+04
^{214}Bi	×		5.869E+01	6.357E+01
^{209}Po	×		4.941E+04	5.352E+04
^{210}Po	×		2.967E+07	3.214E+07
^{211}Po	×		3.830E+04	4.149E+04
^{212}Po			unlimited	unlimited
^{213}Po	×		9.015E+06	9.765E+06
^{214}Po			unlimited	unlimited
^{215}Po	×		unlimited	unlimited
^{216}Po	×		1.874E+07	2.030E+07
^{218}Po			unlimited	unlimited
^{211}At	×		3.463E+05	3.751E+05
^{217}At	×		1.761E+07	1.908E+07
^{219}Rn	×		1.073E+06	1.162E+06
^{220}Rn	×		3.551E+06	3.846E+06
^{222}Rn	×		9.805E+06	1.062E+07
^{221}Fr	×		7.038E+07	7.623E+07
^{223}Fr	×		4.316E+04	4.675E+04
^{223}Ra	×		7.889E+05	8.545E+05
^{224}Ra	×		2.376E+07	2.573E+07
^{225}Ra	×		unlimited	unlimited
^{226}Ra	×		unlimited	unlimited
^{228}Ra	×		unlimited	unlimited
^{225}Ac	×		3.079E+06	3.335E+06
^{227}Ac	×		unlimited	unlimited

Radio-nuclide	Gamma Emitter	Neutron Emitter	NS30 HAC @ 1-m Maximum Allowable Activity (Ci), A_{GN}	NS15 HAC @ 1-m Maximum Allowable Activity (Ci), A_{GN}
^{228}Ac	×		1.821E+02	1.973E+02
^{227}Th	×		1.695E+06	1.836E+06
^{228}Th	×		unlimited	unlimited
^{229}Th	×		unlimited	unlimited
^{230}Th	×	×	2.268E+06	6.635E+06
^{231}Th	×		unlimited	unlimited
^{232}Th	×	×	4.995E+06	1.577E+07
^{234}Th	×		unlimited	unlimited
^{231}Pa	×	×	1.526E+06	3.644E+06
^{233}Pa	×		3.281E+06	3.554E+06
^{234}Pa	×		1.442E+02	1.562E+02
^{234m}Pa	×		8.910E+03	9.651E+03
^{232}U	×	×	1.417E+06	3.981E+06
^{233}U	×	×	1.978E+06	5.745E+06
^{234}U	×	×	2.017E+06	5.904E+06
^{235}U	×	×	2.250E+06	6.613E+06
^{236}U	×	×	2.266E+06	6.748E+06
^{237}U	×		unlimited	unlimited
^{238}U	×	×	3.118E+04	9.407E+04
^{239}U	×		3.271E+04	3.543E+04
^{240}U	×		unlimited	unlimited
^{237}Np	×	×	2.037E+06	5.942E+06
^{238}Np	×		2.327E+02	2.521E+02
^{239}Np	×		5.248E+07	5.684E+07
^{240}Np	×		2.642E+02	2.862E+02
^{240m}Np	×		8.578E+02	9.291E+02
^{236}Pu	×	×	9.390E+05	2.558E+06
^{238}Pu	×	×	1.027E+06	2.869E+06
^{239}Pu	×	×	1.562E+06	4.437E+06
^{240}Pu	×	×	2.247E+05	6.406E+05
^{241}Pu	×	×	unlimited	unlimited
^{242}Pu	×	×	2.609E+03	7.434E+03
^{243}Pu	×		6.709E+07	7.266E+07
^{244}Pu		×	1.161E+01	3.433E+01
^{241}Am	×	×	1.188E+06	3.260E+06
^{242}Am	×		unlimited	unlimited
^{242m}Am	×	×	6.559E+07	unlimited

Radio-nuclide	Gamma Emitter	Neutron Emitter	NS30 HAC @ 1-m Maximum Allowable Activity (Ci), A_{GN}	NS15 HAC @ 1-m Maximum Allowable Activity (Ci), A_{GN}
^{243}Am	×	×	1.365E+06	3.768E+06
^{245}Am	×		unlimited	unlimited
^{240}Cm		×	2.111E+05	5.552E+05
^{242}Cm	×	×	1.431E+05	3.947E+05
^{243}Cm	×	×	1.343E+05	3.602E+05
^{244}Cm	×	×	8.250E+03	2.262E+04
^{245}Cm	×	×	4.935E+04	1.368E+05
^{246}Cm		×	3.579E+01	9.941E+01
^{247}Cm	×		1.867E+05	2.022E+05
^{248}Cm		×	1.209E-01	3.427E-01
^{250}Cm		×	1.494E-02	4.400E-02
^{247}Bk	×		unlimited	unlimited
^{249}Bk	×	×	1.176E+07	3.436E+07
^{250}Bk	×		1.628E+02	1.763E+02
^{249}Cf	×	×	2.541E+05	3.614E+05
^{250}Cf	×	×	1.040E+01	2.675E+01
^{251}Cf	×	×	9.861E+05	2.684E+06
^{252}Cf	×	×	2.643E-01	6.745E-01
^{254}Cf		×	8.066E-03	2.044E-02
^{252}Es	×		1.744E+03	1.889E+03
^{253}Es	×	×	7.928E+04	2.022E+05
^{254}Es	×	×	1.965E+05	5.065E+05
^{254m}Es	×	×	1.594E+01	3.995E+01

5.0 Appendices

5.1 References

1. *RH-TRU 72-B Safety Analyis Report*, Rev. 4, June 2006.
2. *Neutron Source Rates for TRU Waste*, ED-042, Rev. 2, November 2000, Packaging Technology, Inc., Tacoma, Washington.
3. MCNP5, "*MCNP – A General Monte Carlo N-Particle Transport Code, Version 5; Volume II: User's Guide*," LA-CP-03-0245, Los Alamos National Laboratory, April 2003. MCNP5 is distributed by the Radiation Safety Information Computational Center (www-rsicc.ornl.gov), Release C00730MNYCP00 (Version 1.40, Windows PC).
4. *MCNP5 Testing and Acceptance Report, v1.30 and v1.40, ADANC491TC,* AFS-TR-VV-001, Rev. 1, September 2009.
5. ANSI/ANS-6.1.1-1977, American National Standard Neutron and Gamma-Ray Flux-to-Dose-Rate Factors.
6. Drawing X-106-503-SNP, Rev. 0, *RH-TRU Waste Canister Assembly, NS30 and NS15 Neutron Shielded Design* (included in 72-B SAR).
7. Drawing X-106-502-SNP, Rev. 2, *RH-TRU Waste Canister Assembly, Removable Lid Design* (included in 72-B SAR).
8. R.R. Kinsey, et al., *The NUDAT/PCNUDAT Program for Nuclear Data, paper submitted to the 9th International Symposium of Capture Gamma-Ray Spectroscopy and Related Topics*, Budapest, Hungary, October 1996; data extracted from the NUDAT database, version September 7, 2000, CD-ROM.
9. T. Rockwell III, et al, *Reactor Shielding Design Manual*, TID-7004, First Edition, U.S. Atomic Energy Commission, Oak Ridge, Tennessee, March 1956, Chapter 1, Section 3.2, Equation 1.
10. ANSI/ANS 6.4.3-1991, *Gamma-Ray Attenuation Coefficients & Buildup Factors for Engineering Materials*, American Nuclear Society (ANS), La Grange Park, Illinois.
11. ASTM D3350, *Standard Specification for Polyethylene Plastics Pipe and Fittings Materials.*
12. Engineering Report 7953-R-027, *30-foot Free Drop Post-Test Summary Report for the NS30 Neutron Shielded Canister*, Revision 0, Petersen Incorporated, November 2009.

5.2 Sample MCNP Input Files

<u>Sample NS30 MCNP input file (NS30Am241)</u>

```
72-b Cask, dose rate at 100 cm
c
c      *****radial of cask, except along 6" puncture bar for lead and outer
11      3 -8.0128 -12 11 -24 23          imp:n=1 imp:p=1 $ inner radial steel
12      5  -11.35 -13 12 -24 23 (22:-21) imp:n=1 imp:p=1 $ lead
13      3 -8.0128 -14 13 -24 23 (22:-21) imp:n=1 imp:p=1 $ ss outer cask, outer
shell
```

```
c      *****radial of cask for 6" puncture bar for lead and outer
17      5  -11.35 -13 12 -22 21 -15          imp:n=1 imp:p=1 $ lead
18      3 -8.0128 -14 -22 21 -16 (15:13) imp:n=1 imp:p=1 $ ss outer cask, outer
shell
c      *****bottom of cask
21      3 -8.0128 -14 -23 25                 imp:n=1 imp:p=1 $ next to inside
22      3 -8.0128 -14 -25 27                 imp:n=1 imp:p=1 $ intermediate
23      3 -8.0128 -14 -27 29                 imp:n=1 imp:p=1 $ outer
c      *****top of cask
24      3 -8.0128 -14 -26 24                 imp:n=1 imp:p=1 $ next to inside
25      3 -8.0128 -14 -28 26                 imp:n=1 imp:p=1 $ intermediate
26      3 -8.0128 -14 -30 28                 imp:n=1 imp:p=1 $ outer
c      *****inside cask
30      0              51 -52 -70                 imp:n=1 imp:p=1 $ inside poly
31      1 -0.94        (-51:52:70) 50 -53 -71  imp:n=1 imp:p=1 $ poly
32      0              50 -53 71 -72              imp:n=1 imp:p=1 $ between poly/steel
33      2 -7.8526      (-50:53:72) 23 -54 -73  imp:n=1 imp:p=1 $ steel
34      0              (73:54) 23 -24 -11         imp:n=1 imp:p=1 $ between steel/cask
c      *****beyond cask
91      7  -0.00123 -8 -42 41 $ air to beyond detector
              ((14:-29:30):(16 -22 21)) imp:n=1 imp:p=1
92      7  -0.00123 -9 -44 43 (8:-41:42) imp:n=1 imp:p=1 $ air on beyond
999     0            (9:-43:44)            imp:n=0 imp:p=0 $ outside world

c       radial cask
11      cz 39.6875  $ inner radial of cask
12      cz 43.1800  $ inner steel
13      cz 47.9425  $ lead
14      cz 52.0700  $ outer steel
15      px 46.27626 $ lead at puncture bar
16      px 50.40376 $ outer steel at puncture bar
c       axial cask
21      pz -7.620   $ bottom of puncture bar
22      pz 7.620    $ top of puncture bar
23      pz -154.305 $ bottom inside of cask
24      pz 154.305  $ top inside of cask
25      pz -159.808 $ bottom first intermediate
26      pz 165.317  $ top first intermediate
27      pz -165.312 $ bottom second intermediate
28      pz 176.318  $ top second intermediate
29      pz -170.815 $ bottom outside of cask
30      pz 187.325  $ top outside of cask
c       air beyond cask
41      pz -320.815 $ 150 cm below
42      pz 337.325  $ 150 cm above
43      pz -670.815 $ 500 cm below
44      pz 687.325  $ 500 cm above
8       cz 202.070  $ 150 cm beyond
9       cz 552.070  $ 500 cm beyond
c
50      pz -153.67   $ bottom of poly
51      pz -146.9136 $ inner bottom of poly
52      pz  124.0536 $ inner top of poly
53      pz  130.81   $ top of poly
54      pz  131.445  $ top of steel
c
70      c/z 8.5525 0  27.5336  $ IR poly
71      c/z 8.5525 0  30.48    $ OR poly
72      c/z 6.6575 0  32.385   $ IR steel
```

```
73     c/z 6.6575 0  33.02    $ OR steel

mode   n p
cut:n  j j 0 0
nps    1000000
prdmp  j j 1 2
c
c     point unit source just inside shield, midway puncture bar
sdef   pos=d1 erg=d7 wgt=1.0
si1    L 36.0851 0 0   39.0335 0 0
sp1    98.0 2.0
sc7   AM241
si7   0.1 0.5     1.0     2.0     3.0     4.0     6.0     8.0
          10.0  15.0
sp7    0.00E+00  1.07E+02  1.43E+02  5.87E+02  1.18E+03
       6.31E+02  5.98E+01  2.91E-02  6.68E-03  1.75E-03
c
m1     6000.60c 1  1001.60c 2                         $ poly
mt1    poly.60t
m2     26000.55c 1.0                                  $ carbon steel
m3     25055.50c -0.02 15031.50c -0.01                $ SS-304
       28000.50c -0.10 24000.50c -0.19 26000.55c -0.68
m5     82000.50c -1.00                                $ lead
m7     8016.60c 0.220 7014.60c 0.780                  $ air
c
fc5     Neutron dose rate in mrem/hr at 1 meter from outer surface
f5:n    150.40376 0. 0. 20.
c       ANSI/ANS-6.1.1-1977 Neutron Flux to Dose Factors (mrem/hr)/(n/cm**2/s)

de5     2.5e-08    1.0e-07    1.0e-06    1.0e-05    1.0e-04
        1.0e-03    1.0e-02    1.0e-01    5.0e-01    1.0
        2.5        5.0        7.0        10.0       14.0
        20.0
df5     3.67e-03   3.67e-03   4.46e-03   4.54e-03   4.18e-03
        3.76e-03   3.56e-03   2.17e-02   9.26e-02   1.32e-01
        1.25e-01   1.56e-01   1.47e-01   1.47e-01   2.08e-01
        2.27e-01
c
fc15    Gamma dose rate in mrem/hr at 1 meter from outer surface
f15:p   150.40376 0. 0. 20.
c       ansi/ans-6.1.1-1977 flux-to-dose, photons (mrem/hr)/(p/cm**2/s)
de15    0.01   0.03   0.05   0.07   0.10   0.15   0.20   0.25   0.30
        0.35   0.40   0.45   0.50   0.55   0.60   0.65   0.70   0.80
        1.00   1.40   1.80   2.20   2.60   2.80   3.25   3.75   4.25
        4.75   5.00   5.25   5.75   6.25   6.75   7.50   9.00   11.0
        13.0   15.0
df15    3.96-3 5.82-4 2.90-4 2.58-4 2.83-4 3.79-4 5.01-4 6.31-4 7.59-4
        8.78-4 9.85-4 1.08-3 1.17-3 1.27-3 1.36-3 1.44-3 1.52-3 1.68-3
        1.98-3 2.51-3 2.99-3 3.42-3 3.82-3 4.01-3 4.41-3 4.83-3 5.23-3
        5.60-3 5.80-3 6.01-3 6.37-3 6.74-3 7.11-3 7.66-3 8.77-3 1.03-2
        1.18-2 1.33-2
```

Sample NS15 MCNP input file (NS15Cm240)

```
72-b Cask, dose rate at 100 cm
c
c     *****radial of cask, except along 6" puncture bar for lead and outer
11     3 -8.0128 -12 11 -24 23          imp:n=1 imp:p=1 $ inner radial steel
12     5  -11.35 -13 12 -24 23 (22:-21) imp:n=1 imp:p=1 $ lead
```

```
13      3 -8.0128 -14 13 -24 23 (22:-21) imp:n=1 imp:p=1 $ ss outer cask, outer
shell
c      *****radial of cask for 6" puncture bar for lead and outer
17      5  -11.35 -13 12 -22 21 -15       imp:n=1 imp:p=1 $ lead
18      3 -8.0128 -14 -22 21 -16 (15:13) imp:n=1 imp:p=1 $ ss outer cask, outer
shell
c      *****bottom of cask
21      3 -8.0128 -14 -23 25              imp:n=1 imp:p=1 $ next to inside
22      3 -8.0128 -14 -25 27              imp:n=1 imp:p=1 $ intermediate
23      3 -8.0128 -14 -27 29              imp:n=1 imp:p=1 $ outer
c      *****top of cask
24      3 -8.0128 -14 -26 24              imp:n=1 imp:p=1 $ next to inside
25      3 -8.0128 -14 -28 26              imp:n=1 imp:p=1 $ intermediate
26      3 -8.0128 -14 -30 28              imp:n=1 imp:p=1 $ outer
c      *****inside cask
30      0              51 -52 -70               imp:n=1 imp:p=1 $ inside poly
31      1 -0.94        (-51:52:70) 50 -53 -71  imp:n=1 imp:p=1 $ poly
32      0              50 -53 71 -72            imp:n=1 imp:p=1 $ between poly/steel
33      2 -7.8526      (-50:53:72) 23 -54 -73  imp:n=1 imp:p=1 $ steel
34      0              (73:54) 23 -24 -11       imp:n=1 imp:p=1 $ between steel/cask
c      *****beyond cask
91      7  -0.00123 -8 -42 41 $ air to beyond detector
              ((14:-29:30):(16 -22 21)) imp:n=1 imp:p=1
92      7  -0.00123 -9 -44 43 (8:-41:42) imp:n=1 imp:p=1 $ air on beyond
999     0             (9:-43:44)           imp:n=0 imp:p=0 $ outside world

c       radial cask
11      cz 39.6875  $ inner radial of cask
12      cz 43.1800  $ inner steel
13      cz 47.9425  $ lead
14      cz 52.0700  $ outer steel
15      px 46.27626 $ lead at puncture bar
16      px 50.40376 $ outer steel at puncture bar
c       axial cask
21      pz -7.620   $ bottom of puncture bar
22      pz 7.620    $ top of puncture bar
23      pz -154.305 $ bottom inside of cask
24      pz 154.305  $ top inside of cask
25      pz -159.808 $ bottom first intermediate
26      pz 165.317  $ top first intermediate
27      pz -165.312 $ bottom second intermediate
28      pz 176.318  $ top second intermediate
29      pz -170.815 $ bottom outside of cask
30      pz 187.325  $ top outside of cask
c       air beyond cask
41      pz -320.815 $ 150 cm below
42      pz 337.325  $ 150 cm above
43      pz -670.815 $ 500 cm below
44      pz 687.325  $ 500 cm above
8       cz 202.070  $ 150 cm beyond
9       cz 552.070  $ 500 cm beyond
c
50      pz -153.67    $ bottom of poly
51      pz -146.9136 $ inner bottom of poly
52      pz  124.0536 $ inner top of poly
53      pz  130.81    $ top of poly
54      pz  131.445   $ top of steel
c
70      c/z 8.5525 0  22.7584  $ IR poly
```

```
71      c/z 8.5525 0  30.48     $ OR poly
72      c/z 6.6575 0  32.385    $ IR steel
73      c/z 6.6575 0  33.02     $ OR steel

mode    n p
cut:n   j j 0 0
nps     1000000
prdmp   j j 1 2
c
c      point unit source just inside shield, midway puncture bar
sdef    pos=d1 erg=d7 wgt=1.0
si1     L 31.3099 0 0   39.0335 0 0
sp1     98.0 2.0
sc7    CM240
si7    0.1 0.5     1.0      2.0      3.0      4.0      6.0      8.0
           10.0  15.0
sp7     0.00E+00  7.82E+06  1.13E+07  2.36E+07  2.22E+07
        1.58E+07  1.07E+07  2.49E+06  6.94E+05  2.35E+05
c
m1      6000.60c 1  1001.60c 2                               $ poly
mt1     poly.60t
m2      26000.55c 1.0                                        $ carbon steel
m3      25055.50c -0.02 15031.50c -0.01                      $ SS-304
        28000.50c -0.10 24000.50c -0.19 26000.55c -0.68
m5      82000.50c -1.00                                      $ lead
m7      8016.60c 0.220 7014.60c 0.780                        $ air
c
fc5      Neutron dose rate in mrem/hr at 1 meter from outer surface
f5:n     150.40376 0. 0. 20.
c        ANSI/ANS-6.1.1-1977 Neutron Flux to Dose Factors (mrem/hr)/(n/cm**2/s)

de5      2.5e-08    1.0e-07    1.0e-06    1.0e-05    1.0e-04
         1.0e-03    1.0e-02    1.0e-01    5.0e-01    1.0
         2.5        5.0        7.0        10.0       14.0
         20.0
df5      3.67e-03   3.67e-03   4.46e-03   4.54e-03   4.18e-03
         3.76e-03   3.56e-03   2.17e-02   9.26e-02   1.32e-01
         1.25e-01   1.56e-01   1.47e-01   1.47e-01   2.08e-01
         2.27e-01
c
fc15     Gamma dose rate in mrem/hr at 1 meter from outer surface
f15:p    150.40376 0. 0. 20.
c        ansi/ans-6.1.1-1977 flux-to-dose, photons (mrem/hr)/(p/cm**2/s)
de15     0.01   0.03   0.05   0.07   0.10   0.15   0.20   0.25   0.30
         0.35   0.40   0.45   0.50   0.55   0.60   0.65   0.70   0.80
         1.00   1.40   1.80   2.20   2.60   2.80   3.25   3.75   4.25
         4.75   5.00   5.25   5.75   6.25   6.75   7.50   9.00   11.0
         13.0   15.0
df15     3.96-3 5.82-4 2.90-4 2.58-4 2.83-4 3.79-4 5.01-4 6.31-4 7.59-4
         8.78-4 9.85-4 1.08-3 1.17-3 1.27-3 1.36-3 1.44-3 1.52-3 1.68-3
         1.98-3 2.51-3 2.99-3 3.42-3 3.82-3 4.01-3 4.41-3 4.83-3 5.23-3
         5.60-3 5.80-3 6.01-3 6.37-3 6.74-3 7.11-3 7.66-3 8.77-3 1.03-2
         1.18-2 1.33-2
```

5.3 Example NS30 Gamma Calculation (Co-60)

An example NS30 gamma calculation is below. The NS15 gamma calculations are the same, although the distance to the detector for the primary (98%) gamma source is 46.8870 inches.

HAC at 1m Point Source Gamma Shielding Analysis for the NS30 Neutron Shielded Canister

Unit Definition:

Units not standard to MathCAD and additional constants are defined as follows:

$\gamma := Bq \cdot s$ $\quad \nu := \gamma$ $\quad Ci := 3.7 \cdot 10^{10} \cdot Bq$ $\quad eV := 1.60 \cdot 10^{-19} \cdot J$

$KeV := 1 \cdot 10^{3} \cdot eV$ $\quad MeV := 1 \cdot 10^{6} \cdot eV$ $\quad mrem := \frac{hr \cdot \gamma}{cm^2 \cdot s}$

Mass Attentuation Coefficients from ANSI/ANS 6.4.3-1991:

Tabular mass attenuation coefficients as a function of gamma energy for 1) silicon, 2) chromium, 3) manganese, 4) iron, 5) nickel, and 6) lead are imported and assigned to the following variables:

Ti := Mass_attenuation_coefficients.xls $\qquad i := 0 .. rows(Ti) - 1$

$Ei_i := Ti_{i,0} \cdot MeV$ $\qquad \mu1\rho_i := Ti_{i,1} \cdot \frac{cm^2}{g}$ $\quad \mu2\rho_i := Ti_{i,2} \cdot \frac{cm^2}{g}$ $\quad \mu3\rho_i := Ti_{i,3} \cdot \frac{cm^2}{g}$

$\mu4\rho_i := Ti_{i,4} \cdot \frac{cm^2}{g}$ $\quad \mu5\rho_i := Ti_{i,5} \cdot \frac{cm^2}{g}$ $\quad \mu6\rho_i := Ti_{i,6} \cdot \frac{cm^2}{g}$

Iron Exposure Build Up Factor Coefficients from ANSI/ANS 6.4.3-1991:

Tabular iron exposure build up factor coefficients as function of gamma energy are imported and assigned to the following variables:

Tj := Iron_buildup_coefficients.xls $\qquad j := 0 .. rows(Tj) - 1$

$Ej_j := Tj_{j,0} \cdot MeV$ $\qquad a_j := Tj_{j,1}$ $\quad b_j := Tj_{j,2}$ $\quad c_j := Tj_{j,3}$ $\quad d_j := Tj_{j,4}$ $\quad xk_j := Tj_{j,5}$

Flux to Dose Rate Conversion Factors from ANSI/ANS 6.1.1-1977:

Tabular flux to dose rate conversion factors as a function of gamma energy are imported and assigned to the following variables:

Tk := Flux_doserate_factors.xls $\qquad k := 0 .. rows(Tk) - 1$

$Ek_k := Tk_{k,0} \cdot MeV$ $\qquad Kk_k := Tk_{k,1}$

Shield Composition Definition:

The following table defines the thickness, density, and percent composition of the shielding materials. The percent composition is defined by 1) silicon, 2) chromium, 3) manganese, 4) iron, 5) nickel, and 6) lead.

$m := 0..5$

Tm :=

	Thickness	Density	%Silicon	%Chromium	%Manganese	%Iron	%Nickel	%Lead
	0	1	2	3	4	5	6	7
0	0.2500	7.8526	0.0000	0.0000	0.0000	100.0000	0.0000	0.0000
1	0.3750	8.0128	1.0000	19.0000	2.0000	68.0000	10.0000	0.0000
2	1.0000	8.0128	1.0000	19.0000	2.0000	68.0000	10.0000	0.0000
3	1.2190	11.3500	0.0000	0.0000	0.0000	0.0000	0.0000	100.0000
4	1.5000	8.0128	1.0000	19.0000	2.0000	68.0000	10.0000	0.0000
5	0.1350	8.0128	1.0000	19.0000	2.0000	68.0000	10.0000	0.0000
6								
7								

$t_m := Tm_{m,0} \cdot in$ $\quad p1_m := Tm_{m,2} \cdot \%$ $\quad p3_m := Tm_{m,4} \cdot \%$ $\quad p5_m := Tm_{m,6} \cdot \%$

$\rho m := Tm_{m,1} \cdot \frac{g}{cm^3}$ $\quad p2_m := Tm_{m,3} \cdot \%$ $\quad p4_m := Tm_{m,5} \cdot \%$ $\quad p6_m := Tm_{m,7} \cdot \%$

Detector Distance and Dose Limit Definition:

The dose limit is defined as $D := 1000 \cdot mrem \cdot hr^{-1}$ when measured at a distance of 1 meter from the surface of the package. The following table defines the horizontal and vertical distance from each point source to the detector and calculates the resulting radial distance. Also specified is the relative distribution of activity in each source.

$nn := 1$ $\quad n := 0..nn$

Tn :=

	Horizontal	Vertical	Distribution
	0	1	2
0	43.8490	0.0000	0.0200
1	45.0110	0.0000	0.9800
2	0.0000	0.0000	0.0000
3	0.0000	0.0000	0.0000
4	0.0000	0.0000	0.0000
5	0.0000	0.0000	0.0000
6	0.0000	0.0000	0.0000
7	0.0000	0.0000	0.0000
8	0.0000	0.0000	0.0000
9	0.0000	0.0000	0.0000
10	0.0000	0.0000	0.0000
11	0.0000	0.0000	0.0000
12	0.0000	0.0000	0.0000
13	0.0000	0.0000	0.0000

$R_n := \sqrt{(Tn_{n,0})^2 + (Tn_{n,1})^2} \cdot in$ $\quad D_{rel_n} := Tn_{n,2}$

Radionuclide Gamma Energy and Intensity:

For the specified radionuclide, the gamma energies and gamma intensities are imported and assigned to the following variables:

Tl := Radionuclide_data.xls   index := 16

```
ll := | i ← 0
      | while Tl[i,0] ≠ index
      |   i ← i + 1
      | ll ← Tl[i,1] − 1
```

$l := 0..ll$

```
E := | i ← 0
     | while Tl[i,0] ≠ index
     |   i ← i + 1
     | ll ← Tl[i,1] − 1
     | for j ∈ 0..ll
     |   E[j] ← | 100 if Tl[i+j,2] < 100
     |          | Tl[i+j,2] otherwise
     | E·KeV
```

```
I := | i ← 0
     | while Tl[i,0] ≠ index
     |   i ← i + 1
     | ll ← Tl[i,1] − 1
     | for j ∈ 0..ll
     |   I[j] ← Tl[i+j,3]
     | I·%
```

Free Mean Path Calculations:

The following equations utilize mass attenuation coefficients as a function of gamma energy and the shield composition definition to calculate the number of mean free paths for each of the gamma energies and shield materials:

$$\mu_{m,l} := \left(\text{linterp}\left(Ei, \mu1_\rho, E_l\right)\cdot\rho_m\cdot p1_m\right) + \left(\text{linterp}\left(Ei, \mu2_\rho, E_l\right)\cdot\rho_m\cdot p2_m\right) + \left(\text{linterp}\left(Ei, \mu3_\rho, E_l\right)\cdot\rho_m\cdot p3_m\right) \dots$$
$$+ \left(\text{linterp}\left(Ei, \mu4_\rho, E_l\right)\cdot\rho_m\cdot p4_m\right) + \left(\text{linterp}\left(Ei, \mu5_\rho, E_l\right)\cdot\rho_m\cdot p5_m\right) + \left(\text{linterp}\left(Ei, \mu6_\rho, E_l\right)\cdot\rho_m\cdot p6_m\right)$$

$$x_{m,l} := \mu_{m,l}\cdot t_m$$

$$x_{total_l} := \sum x^{\langle l \rangle}$$

Build Up Factor Calculations:

The following G-P geometric progression equations (ANSI/ANS 6.4.3-1991) is utilized along with iron buildup factor coefficients and the number of mean free paths to calculate a buildup factor for each of the gamma energies:

$$Kx_l := \text{linterp}(Ej, c, E_l) \cdot (x_{total_l})^{\text{linterp}(Ej, a, E_l)} + \text{linterp}(Ej, d, E_l) \cdot \frac{\tanh\left[\left(\frac{x_{total_l}}{\text{linterp}(Ej, x_k, E_l)} - 2\right)\right] - \tanh(-2)}{1 - \tanh(-2)}$$

$$B_l := \begin{cases} 1 + (\text{linterp}(Ej, b, E_l) - 1) \cdot \left[\frac{(Kx_l)^{x_{total_l}} - 1}{Kx_l - 1}\right] & \text{if } Kx_l \neq 1 \\ 1 + (\text{linterp}(Ej, b, E_l) - 1) \cdot x_{total_l} & \text{if } Kx_l = 1 \end{cases}$$

Maximum Activity Calculations:

The following equations calculate the total gamma dose resulting from 1 Ci of the specified radionuclide, then ratio the total dose to calculate the activity required to meet the limiting dose rate. The limiting activity is then utilized to calculate the individual gamma dose contributions from each point source. The gamma dose calculations utilize Rockwell's methodology.

$$K_l := \text{linterp}(Ek, Kk, E_l)$$

$$D_{ratiocomp_{l,n}} := \left[\frac{D_{rel_n} \cdot Ci \cdot I_l \cdot B_l \cdot K_l}{4 \cdot \pi \cdot (R_n)^2}\right] \cdot e^{-x_{total_l}}$$

$$D_{ratiototal_n} := \sum D_{ratiocomp}^{\langle n \rangle}$$

$$D_{ratiolimit} := \sum D_{ratiototal}$$

$$A_{limit_n} := \begin{cases} D_{rel_n} \cdot Ci \cdot \frac{D}{D_{ratiolimit}} & \text{if } D_{ratiolimit} \neq 0 \\ D_{rel_n} \cdot Ci \cdot 10^{99} & \text{otherwise} \end{cases}$$

$$D_{limitcomp_{l,n}} := \left[\frac{A_{limit_n} \cdot I_l \cdot B_l \cdot K_l}{4 \cdot \pi \cdot (R_n)^2}\right] \cdot e^{-x_{total_l}}$$

$$D_{limittotal_n} := \sum D_{limitcomp}^{\langle n \rangle} \qquad D_{limit} := \sum D_{limittotal} \qquad A_{total} := \sum A_{limit}$$

Summary of Results:

The gamma energies and intensities for radionuclide $\text{index} = 16$ are as follows:

$$E^T = \begin{pmatrix} 346.9300 & 826.2800 & 1.1732\times10^3 & 1.3325\times10^3 & 2.1588\times10^3 & 2.5050\times10^3 \end{pmatrix}\text{KeV}$$

$$I^T = \begin{pmatrix} 7.6\times10^{-3} & 7.6\times10^{-3} & 99.974 & 99.986 & 1.11\times10^{-3} & 2\times10^{-6} \end{pmatrix}\%$$

The attenuation coefficients and the number of mean free paths for each of the gamma energies and shield materials are

$$\mu^T = \begin{pmatrix} 0.781 & 0.797 & 0.797 & 3.427 & 0.797 & 0.797 \\ 0.514 & 0.525 & 0.525 & 0.937 & 0.525 & 0.525 \\ 0.438 & 0.447 & 0.447 & 0.708 & 0.447 & 0.447 \\ 0.411 & 0.419 & 0.419 & 0.645 & 0.419 & 0.419 \\ 0.326 & 0.333 & 0.333 & 0.509 & 0.333 & 0.333 \\ 0.308 & 0.315 & 0.315 & 0.496 & 0.315 & 0.315 \end{pmatrix}\frac{1}{\text{cm}} \text{ and}$$

$$x^T = \begin{pmatrix} 0.496 & 0.759 & 2.024 & 10.61 & 3.037 & 0.273 \\ 0.327 & 0.5 & 1.335 & 2.901 & 2.002 & 0.18 \\ 0.278 & 0.426 & 1.136 & 2.192 & 1.705 & 0.153 \\ 0.261 & 0.399 & 1.065 & 1.997 & 1.598 & 0.144 \\ 0.207 & 0.317 & 0.845 & 1.577 & 1.267 & 0.114 \\ 0.196 & 0.3 & 0.799 & 1.535 & 1.199 & 0.108 \end{pmatrix},$$

such that the total mean free path for each gamma energy is

$$x_{total}^T = (17.199 \;\; 7.245 \;\; 5.891 \;\; 5.464 \;\; 4.326 \;\; 4.137).$$

The buildup factors and flux-to-dose rate conversion factors for each of the gamma energies are

$$B^T = (34.464 \;\; 11.227 \;\; 7.678 \;\; 6.703 \;\; 4.466 \;\; 4.09) \text{ and}$$

$$K^T = \begin{pmatrix} 8.707\times10^{-4} & 1.719\times10^{-3} & 2.21\times10^{-3} & 2.421\times10^{-3} & 3.376\times10^{-3} & 3.725\times10^{-3} \end{pmatrix}.$$

The distances from each of the point-sources to the detector location are

$$R^T = (43.85 \;\; 45.01)\,\text{in},$$

such that the individual gamma dose contributions from each gamma energy and point sources are

$$D_{limitcomp}^T = \begin{pmatrix} 1.408\times10^{-8} & 1.906\times10^{-4} & 8.536 & 12.515 & 4.028\times10^{-4} & 8.859\times10^{-7} \\ 6.548\times10^{-7} & 8.864\times10^{-3} & 396.941 & 581.98 & 0.019 & 4.12\times10^{-5} \end{pmatrix}\frac{\text{mrem}}{\text{hr}}.$$

Therefore, the total limiting dose of $D_{limit} = 1000\frac{\text{mrem}}{\text{hr}}$ is obtained with an individual point source activity of $A_{limit} = \begin{pmatrix} 0.767 \\ 37.583 \end{pmatrix}\text{Ci}$ for each of the $m + 1 = 2$ source(s), with a total source activity of $A_{total} = 38.35\,\text{Ci}$.

5.4 Computer Run Record

	COMPUTER RUN RECORD
Computer Run Number	See Input File Names
Analysis Software	MCNP5 v1.40
Hardware Description	Windows XP/Xeon Processor QA verification for MCNP5 v1.40 has been performed for this hardware platform [4]. Models were executed on computer ADANC491TC.
Disk Storage Description	Compact Disc

```
MCNP5 Input/Output Files
11/04/2009  03:02 PM         5,685 NS15Am241.i
11/04/2009  03:03 PM         5,693 NS15Am242m.i
11/04/2009  03:03 PM         5,685 NS15Am243.i
11/04/2009  03:03 PM         5,686 NS15Bk249.i
11/04/2009  03:03 PM         5,686 NS15Cf249.i
11/04/2009  03:04 PM         5,686 NS15Cf250.i
11/04/2009  03:04 PM         5,685 NS15Cf251.i
11/04/2009  03:04 PM         5,686 NS15Cf252.i
11/04/2009  03:04 PM         5,686 NS15Cf254.i
11/04/2009  03:04 PM         5,685 NS15Cm240.i
11/04/2009  03:04 PM         5,685 NS15Cm242.i
11/04/2009  03:05 PM         5,685 NS15Cm243.i
11/04/2009  03:05 PM         5,685 NS15Cm244.i
11/04/2009  03:05 PM         5,678 NS15Cm245.i
11/04/2009  03:06 PM         5,685 NS15Cm246.i
11/04/2009  03:06 PM         5,685 NS15Cm248.i
11/04/2009  03:07 PM         5,686 NS15Cm250.i
11/04/2009  03:07 PM         5,686 NS15Es253.i
11/04/2009  03:07 PM         5,686 NS15Es254.i
11/04/2009  03:07 PM         5,687 NS15Es254m.i
11/04/2009  03:07 PM         5,685 NS15Np237.i
11/04/2009  03:07 PM         5,629 NS15Pa231.i
11/04/2009  03:07 PM         5,685 NS15Pu236.i
11/04/2009  03:08 PM         5,685 NS15Pu238.i
11/04/2009  03:08 PM         5,685 NS15Pu239.i
11/04/2009  03:08 PM         5,685 NS15Pu240.i
11/04/2009  03:08 PM         5,685 NS15Pu241.i
11/04/2009  03:08 PM         5,685 NS15Pu242.i
11/04/2009  03:08 PM         5,685 NS15Pu244.i
11/04/2009  03:09 PM         5,618 NS15Th230.i
11/04/2009  03:09 PM         5,624 NS15Th232.i
11/04/2009  03:09 PM         5,614 NS15U232.i
11/04/2009  03:09 PM         5,619 NS15U233.i
11/04/2009  03:09 PM         5,618 NS15U234.i
11/04/2009  03:09 PM         5,618 NS15U235.i
11/04/2009  03:09 PM         5,685 NS15U236.i
11/04/2009  03:10 PM         5,685 NS15U238.i
```

```
11/04/2009  02:51 PM              5,617 NS30Am241.i
11/04/2009  02:52 PM              5,626 NS30Am242m.i
11/04/2009  02:52 PM              5,620 NS30Am243.i
11/04/2009  02:53 PM              5,619 NS30Bk249.i
11/04/2009  02:53 PM              5,619 NS30Cf249.i
11/04/2009  02:53 PM              5,620 NS30Cf250.i
11/04/2009  02:54 PM              5,619 NS30Cf251.i
11/04/2009  02:54 PM              5,619 NS30Cf252.i
11/04/2009  02:54 PM              5,620 NS30Cf254.i
11/04/2009  02:54 PM              5,618 NS30Cm240.i
11/04/2009  02:54 PM              5,619 NS30Cm242.i
11/04/2009  02:54 PM              5,618 NS30Cm243.i
11/04/2009  02:55 PM              5,618 NS30Cm244.i
11/04/2009  02:55 PM              5,611 NS30Cm245.i
11/04/2009  02:55 PM              5,618 NS30Cm246.i
11/04/2009  02:55 PM              5,618 NS30Cm248.i
11/04/2009  02:55 PM              5,619 NS30Cm250.i
11/04/2009  02:55 PM              5,619 NS30Es253.i
11/04/2009  02:56 PM              5,619 NS30Es254.i
11/04/2009  02:56 PM              5,620 NS30Es254m.i
11/04/2009  02:56 PM              5,618 NS30Np237.i
11/04/2009  02:56 PM              5,628 NS30Pa231.i
11/04/2009  02:56 PM              5,618 NS30Pu236.i
11/04/2009  02:56 PM              5,619 NS30Pu238.i
11/04/2009  02:57 PM              5,411 NS30Pu239.i
11/04/2009  02:57 PM              5,618 NS30Pu240.i
11/04/2009  02:57 PM              5,618 NS30Pu241.i
11/04/2009  02:57 PM              5,618 NS30Pu242.i
11/04/2009  02:57 PM              5,619 NS30Pu244.i
11/04/2009  02:57 PM              5,618 NS30Th230.i
11/04/2009  02:58 PM              5,623 NS30Th232.i
11/04/2009  02:58 PM              5,613 NS30U232.i
11/04/2009  02:58 PM              5,617 NS30U233.i
11/04/2009  02:58 PM              5,618 NS30U234.i
11/04/2009  02:58 PM              5,618 NS30U235.i
11/04/2009  02:58 PM              5,617 NS30U236.i
11/04/2009  02:59 PM              5,617 NS30U238.i

11/04/2009  04:24 PM             71,500 NS15Am241.o
11/04/2009  04:34 PM             72,016 NS15Am242m.o
11/04/2009  04:44 PM             65,507 NS15Am243.o
11/04/2009  04:54 PM             65,015 NS15Bk249.o
11/04/2009  05:03 PM             63,271 NS15Cf249.o
11/04/2009  05:13 PM             65,259 NS15Cf250.o
11/04/2009  05:23 PM             73,334 NS15Cf251.o
11/04/2009  05:32 PM             70,283 NS15Cf252.o
11/04/2009  05:42 PM             63,840 NS15Cf254.o
11/04/2009  05:52 PM             65,090 NS15Cm240.o
11/04/2009  06:01 PM             64,868 NS15Cm242.o
11/04/2009  06:11 PM             64,523 NS15Cm243.o
11/04/2009  06:21 PM             70,206 NS15Cm244.o
11/04/2009  06:31 PM             64,925 NS15Cm245.o
11/04/2009  06:40 PM             64,165 NS15Cm246.o
11/04/2009  06:50 PM             70,788 NS15Cm248.o
11/04/2009  07:00 PM             69,323 NS15Cm250.o
11/04/2009  07:10 PM             65,608 NS15Es253.o
11/04/2009  07:19 PM             64,679 NS15Es254.o
11/04/2009  07:29 PM             63,236 NS15Es254m.o
11/04/2009  07:38 PM             70,272 NS15Np237.o
```

```
11/04/2009  07:48 PM            70,230 NS15Pa231.o
11/04/2009  07:57 PM            71,214 NS15Pu236.o
11/04/2009  08:07 PM            62,907 NS15Pu238.o
11/04/2009  08:16 PM            69,402 NS15Pu239.o
11/04/2009  08:26 PM            69,949 NS15Pu240.o
11/04/2009  08:35 PM            63,875 NS15Pu241.o
11/04/2009  08:45 PM            69,424 NS15Pu242.o
11/04/2009  08:54 PM            69,894 NS15Pu244.o
11/04/2009  09:04 PM            64,844 NS15Th230.o
11/04/2009  09:13 PM            68,888 NS15Th232.o
11/04/2009  09:23 PM            72,262 NS15U232.o
11/04/2009  09:32 PM            63,115 NS15U233.o
11/04/2009  09:42 PM            70,929 NS15U234.o
11/04/2009  09:51 PM            64,578 NS15U235.o
11/04/2009  10:01 PM            72,609 NS15U236.o
11/04/2009  10:11 PM            70,296 NS15U238.o
11/04/2009  02:59 PM            69,187 NS30Am241.o
11/04/2009  03:07 PM            64,332 NS30Am242m.o
11/04/2009  03:14 PM            66,626 NS30Am243.o
11/04/2009  03:21 PM            67,748 NS30Bk249.o
11/04/2009  03:28 PM            67,467 NS30Cf249.o
11/04/2009  03:35 PM            69,514 NS30Cf250.o
11/04/2009  03:43 PM            69,657 NS30Cf251.o
11/04/2009  03:50 PM            67,392 NS30Cf252.o
11/04/2009  03:57 PM            67,467 NS30Cf254.o
11/04/2009  04:04 PM            69,901 NS30Cm240.o
11/04/2009  04:12 PM            70,663 NS30Cm242.o
11/04/2009  04:19 PM            68,719 NS30Cm243.o
11/04/2009  04:27 PM            69,389 NS30Cm244.o
11/04/2009  04:34 PM            70,373 NS30Cm245.o
11/04/2009  04:41 PM            61,283 NS30Cm246.o
11/04/2009  04:49 PM            63,894 NS30Cm248.o
11/04/2009  04:56 PM            68,642 NS30Cm250.o
11/04/2009  05:04 PM            71,140 NS30Es253.o
11/04/2009  05:11 PM            63,146 NS30Es254.o
11/04/2009  05:18 PM            56,149 NS30Es254m.o
11/04/2009  05:25 PM            60,018 NS30Np237.o
11/04/2009  05:33 PM            60,165 NS30Pa231.o
11/04/2009  05:40 PM            60,903 NS30Pu236.o
11/04/2009  05:47 PM            68,429 NS30Pu238.o
11/04/2009  05:54 PM            69,121 NS30Pu239.o
11/04/2009  06:02 PM            69,180 NS30Pu240.o
11/04/2009  06:09 PM            60,868 NS30Pu241.o
11/04/2009  06:16 PM            67,133 NS30Pu242.o
11/04/2009  06:24 PM            67,825 NS30Pu244.o
11/04/2009  06:31 PM            62,801 NS30Th230.o
11/04/2009  06:38 PM            70,250 NS30Th232.o
11/04/2009  06:45 PM            68,504 NS30U232.o
11/04/2009  06:52 PM            69,712 NS30U233.o
11/04/2009  07:00 PM            68,972 NS30U234.o
11/04/2009  07:07 PM            68,407 NS30U235.o
11/04/2009  07:14 PM            67,972 NS30U236.o
11/04/2009  07:21 PM            68,128 NS30U238.o
```

	COMPUTER RUN RECORD
Analysis Software	EXCEL and MathCADv13.1
Disk Storage Description	Compact Disc

The following EXCEL spreadsheets are utilized in the analysis.
NSCAN_SHIELDCALC_HAC_13.1.XLS is embedded with a MathCADv13.1 application that computes the gamma activities. The spreadsheet is constructed to automatically loop through each of the gamma emitting isotopes. This spreadsheet also summarizes the results of the neutron activity calculations and combines the results. The remaining EXCEL spreadsheets are used as input to the gamma point-kernel analysis as implemented in MathCAD.

```
nscan_shieldcalc_hac_13.1.xls
flux_doserate_factors.xls
iron_buildup_coefficients.xls
mass_attenuation_coefficients.xls
radionuclide_data.xls
```